AFRL-HE-WP-TR-1998-0012

UNITED STATES AIR FORCE
RESEARCH LABORATORY

EFFECTS OF SCENE MODULATION
IMAGE BLUR AND NOISE UPON HUMAN
TARGET ACQUISITION PERFORMANCE

19980805 095

Denise L. Aleva
Gilbert G. Kuperman

CREW SYSTEM INTERFACE DIVISION
HUMAN EFFECTIVENESS DIRECTORATE
WRIGHT-PATTERSON AFB OH 45433-7022

JUNE 1997

INTERIM REPORT FOR THE PERIOD JULY 1996 TO AUGUST 1996

DTIC QUALITY INSPECTED 1

NOTICES

Please do not request copies of this report from the Air Force Research Laboratory. Additional copies may be purchased from:

> National Technical Information Service
> 5285 Port Royal Road
> Springfield, Virginia 22161

Federal Government agencies registered with the Defense Technical Information Center should direct requests for copies of this report to:

> Defense Technical Information Center
> 8725 John J. Kingman Road, Suite 0944
> Ft. Belvoir, Virginia 22060-6218
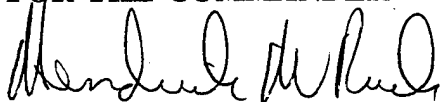
TECHNICAL REVIEW AND APPROVAL

AFRL-HE-WP-TR-1998-0012

This report has been reviewed by the Office of Public Affairs (PA) and is releasable to the National Technical Information Service (NTIS). At NTIS, it will be available to the general public, including foreign nations.

This technical report has been reviewed and is approved for publication.

FOR THE COMMANDER

HENDRICK W. RUCK, PhD
Chief, Crew System Interface Division
Air Force Research Laboratory

1. AGENCY USE ONLY *(Leave blank)*	2. REPORT DATE June 1997	3. REPORT TYPE AND DATES COVERED INTERIM (July 1996 - August 1996)

4. TITLE AND SUBTITLE
Effects of Scene Modulation Image Blur and
Noise Upon Human Target Acquisition
Performance (U)

6. AUTHOR(S)
Denise L. Aleva
Gilbert G. Kuperman

5. FUNDING NUMBERS
C F41624-94-D-6000
PE 62202F
PR 7184
TA 10
WU 44

7. PERFORMING ORGANIZATION NAME(S) AND ADDRESS(ES)

8. PERFORMING ORGANIZATION REPORT NUMBER

9. SPONSORING/MONITORING AGENCY NAME(S) AND ADDRESS(ES)
Air Force Research Laboratory
Crew System Interface Division
Human Effectiveness Directorate
Air Force Materiel Command
Wright-Patterson AFB OH 45433-7022

10. SPONSORING/MONITORING AGENCY REPORT NUMBER

AFRL-HE-WP-TR-1998-0012

11. SUPPLEMENTARY NOTES

12a. DISTRIBUTION/AVAILABILITY STATEMENT

Approved for public release; distribution is unlimited

12b. DISTRIBUTION CODE

13. ABSTRACT *(Maximum 200 words)*

Today's target acquisition systems are often composed of electro-optical imaging systems as well as the human observer. This system may be composed of detectors, transmission and storage devices and a display.

Errors are inherent in any transmission or display system. They are an unavoidable result of the physical limitations of the system. A classic dilemma in image transmission and display is that we must compromise between the conflicting constraints of dynamic range and noise.

Three target acquisition experiments were conducted using simulated infrared imagery of eight military vehicles. The first, a target detection study, required subjects to declare whether or not a military vehicle was present in an image. The two succeeding studies were recognition studies which required the subject to determine whether the vehicle present in an image belonged to one of four classes.

Scene modulation, image blur and noise were found to interact in their effects upon operator target acquisition performance. Image blur and noise were less detrimental to target acquisition performance when scene modulation was high. Conversely, the same performance could be achieved at lower modulations if image blur and noise were reduced. These results suggest possible system design trade-offs.

14. SUBJECT TERMS
Target acquisition, human visual performance

15. NUMBER OF PAGES
106

16. PRICE CODE

17. SECURITY CLASSIFICATION OF REPORT Unclassified	18. SECURITY CLASSIFICATION OF THIS PAGE Unclassified	19. SECURITY CLASSIFICATION OF ABSTRACT Unclassified	20. LIMITATION OF ABSTRACT Unlimited

This Page Intentionally Left Blank

ACKNOWLEDGMENTS

TABLE OF CONTENTS

LIST OF ILLUSTRATIONS

FIGURE

LIST OF TABLES

TABLE

CHAPTER 1

INTRODUCTION

Today's target acquisition systems are often composed of electro-optical imaging systems as well as the human observer. Instead of viewing a scene directly with his own eyes, the observer often views an image of the actual scene which has been produced by an electro-optical system. This system may be composed of detectors, transmission and storage devices and a display.

Errors are inherent in any transmission or display system. They are an unavoidable result of the physical limitations of the system. A classic dilemma in image transmission and display is that we must compromise between the conflicting constraints of dynamic range and noise. The most important problem in image display is the limited dynamic range of typical displays. High fidelity images such as those seen by the human eye in the real world obtain dynamic ranges far in excess of 1000:1 or even 10000:1 (Stockham, 1975), whereas displays have typical dynamic ranges of 300:1. Other problems that may be introduced in any transmission and display system are image blur and noise.

Acquisition refers to a series of visual processes, which range from the first awareness of some local difference in energy at a specific point in the visual field through a progressive awareness of the detail structure of an object (Overington, 1976). Detection refers to the awareness of existence of local difference energy. Recognition refers to the awareness that an object is of a particular class. Identification refers to the ability to specify that an object is a particular one of a class.

To achieve maximum target acquisition performance from these man-machine systems, the output of the electro-optical system must be designed with the capabilities and limitations of the human visual system in mind.

> "So it is that one might expect the most modern efforts in image transmission, display and processing to be strongly influenced by a knowledge of the human observer characteristics. The implication of this statement is that the image processing scientist must be well versed not only in the physics of optics, the electrophysics of sensing, the electronics and chemistry of transmission, and the analog and digital disciplines of processing, but also in the psychophysics, biophysics and psychology of vision" (Stockham, 1975).

The purpose of this research effort was to gain a better understanding of the scene modulation, image resolution and signal-to-noise requirements of the human visual system in performing the target acquisition task. The interactions of these variables are examined

1

experimentally to quantify their combined effects upon target acquisition performance. The results hold significant implications for trade-offs in target acquisition system design. Further, theory of signal detection is applied to the experimental results to quantify operator target acquisition requirements independently of operator decision criterion.

The next section of this report presents a background review of light and photometric quantities, a description of the human visual system, description of a systems approach to visual perception, a discussion of factors believed to affect target acquisition performance (detection and recognition) and a discussion of theory of signal detection as applied to visual target acquisition. Chapter 3 describes the studies performed under the current research effort: a detection experiment, and two recognition experiments. Chapter 4 presents a summarization of the results of the three studies. Chapter 5 presents a discussion of the results of the current research effort and ideas for future directions.

CHAPTER 2
BACKGROUND REVIEW

Light

Everything we see is dependent upon light. Light is part of the continuous spectrum of electromagnetic radiation. An electromagnetic wave carries energy. The energy distribution of the wave passing through a spatial plane: $c(x,y,t,\lambda)$ is called spectral irradiance per (area x wavelength) or irradiance per wavelength. The x and y are spatial variables, t is time and λ is wavelength. The λ is related to frequency by: $\lambda = c / f$ where c is the speed of an electromagnetic wave ($3x10^8$m/sec). The unit associated with $c(x,y,t,\lambda)$ is energy per (area x time x wavelength) and is joules/(m³ sec). Integrating $c(x,y,t,\lambda)$ with respect to λ gives irradiance in unit of joules/(m²sec) or watts/m². Integrating $c(x,y,t,\lambda)$ with respect to all four variables gives the total energy (joules) passing through a spatial plane.

Light is distinguished from other electromagnetic waves by the fact that the eye is sensitive to it. The eye is sensitive to electromagnetic waves over a narrow range of wavelengths -λ = 350 nm to 750 nm (1 nm = 10^{-9} meter).

Quantities associated with c(λ), such as radiant flux and irradiance, are radiometric units. These are physical quantities which can be measured and defined independent of a human observer. Contributions that $c(\lambda_1)$ and $c(\lambda_2)$ make to the human perception of brightness are generally quite different for $\lambda_1 \neq \lambda_2$ even when $c(\lambda_1)$ and $c(\lambda_2)$ are equal. The perceived brightness is dependent upon λ. Of course, if λ is not within the visible range, it will not contribute at all to the perception of brightness. Light that consists of only one spectral component is called monochromatic.

The basic photometric quantity is luminance, adopted in 1948 by the Commission Internationale de l'Ecliarage (C.I.E.), an international body concerned with standards for light and color. A relative luminous efficiency function, v(λ), was determined by having observers equate brightness of lights of various wavelengths to a fixed standard, c'(λ), at 555 nm. The relative luminous efficiency function, denoted by $v(\lambda)$, describes the ratio of energy required for light at other wavelengths to match the brightness of light at 555 nm. The typical observer has maximum brightness sensitivity at 555 nm. Therefore, c(λ)/c'(λ) is always less than or equal to unity. The C.I.E. function is roughly bell shaped with a maximum value of 1 at 555 nm (Lin, 1990).

The basic unit of luminance is the lumen (lm). The luminance per area l of a light with c(λ) can be defined by $l = k \int_{\lambda=0}^{x} c(\lambda)v(\lambda)d\lambda$. Neither luminance nor luminance per area measures the human perception of brightness. That is, a light of 2 lumens/m² will not

appear to the observer to be twice as bright as a light of 1 lumen/m². However, luminance per area is related to the perception of brightness more closely than an integral of c(λ), and in typical viewing conditions, a light with larger luminance per area is perceived to be brighter than a light with smaller luminance per area (Lin, 1990).

Human perception of light with c(λ) (fixed spatial point and fixed time) can be described in terms of brightness, hue and saturation. Brightness refers to the perceived intensity or strength of the light. Hue is defined as the attribute of color which allows us to distinguish red from blue. Light with approximately equal amounts of c(λ) across the visible range appears white. Monochromatic light appears colored and its color depends on λ. Saturation refers to the purity or vividness of the color. The perceived saturation of a color is related to the effective width of c(λ). Monochromatic light has very narrow spectral content and looks very vivid and pure. Therefore, it is said to be highly saturated. As the spectral content of c(λ) widens, the color is perceived to be less vivid and pure and is said to be less saturated (Lin, 1990).

Human Visual System

The human visual system consists of the eye that transforms light to neural signals and the related parts of the brain that process the neural signals and extract information.

The eye is approximately spherical with a diameter of about 2 cm. It is a device that gathers light and focuses it onto its rear surface. If we examine a horizontal cross section of eye from the outside inward (Figure 1), we find the following elements. The cornea faces outside world. It is a tough transparent membrane whose function is to refract or bend light. It acts like the convex lens of a camera and accounts for about two thirds of the light bending necessary for focusing. The aqueous humor is clear free-flowing liquid behind the cornea. The iris is the colored part of eye. It controls amount of light entering the eye by changing the size of the pupil, a small round hole in its center. Pupil diameter adjusts between 1.5 mm and 8 mm depending on the amount of external light.

The lens consists of many transparent fibers encased in a transparent elastic membrane. The lens is bi-convex in shape with a refractive index of 1.4. It is surrounded by media having similar refractive indices. Less light bending occurs at the lens than at the cornea. (The cornea has a refractive index of 1.8 but faces air.) The function of the lens is to provide that bending required to accurately focus light on a screen at back of eye called the retina. While a camera changes the distance between lens and screen to focus objects at different distances, the eye changes the shape of the lens while the distance between lens and retina remains constant. This process of changing the shape of the lens is called accommodation and takes place almost instantly.
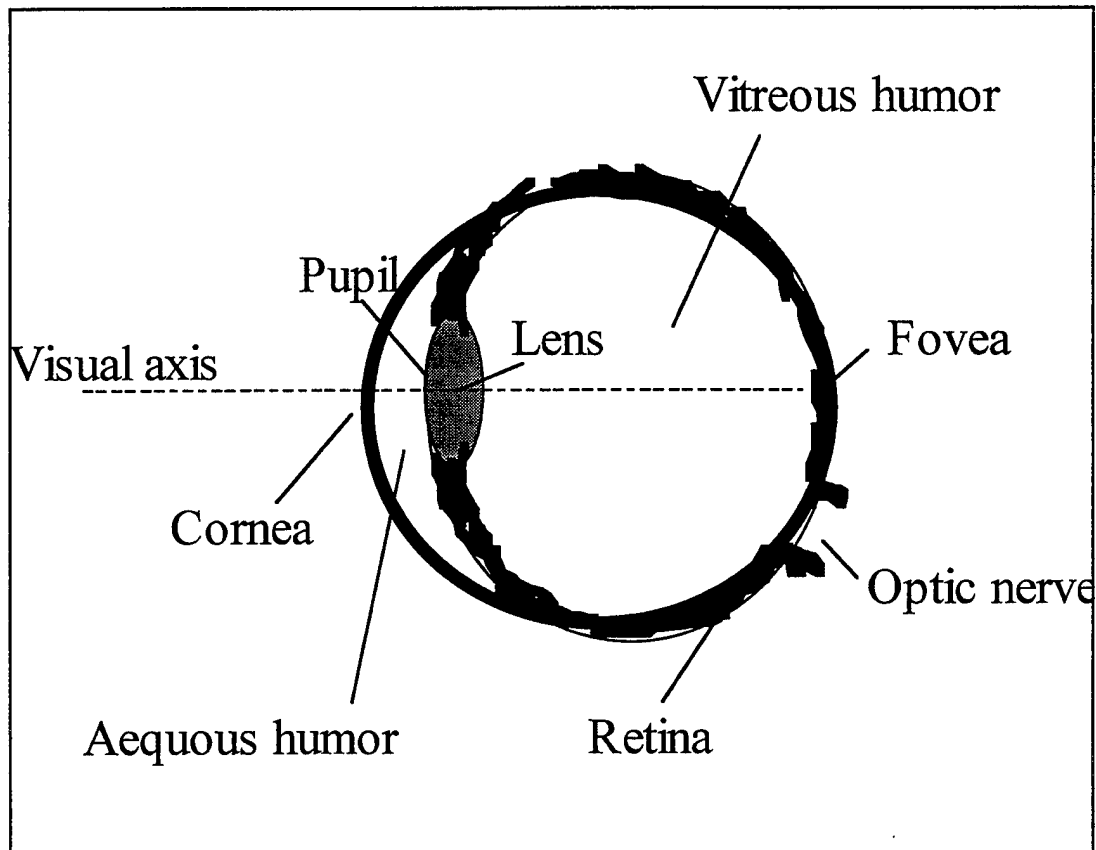
Figure 1. Horizontal cross section of the eye.

The vitreous humor, a transparent jelly-like substance, is behind the lens. It is optically matched to keep light focused by lens on the same course. It fills the space between the lens and the retina and gives support to the shape of the eye. The retina is the screen on which light is focused and light-receptive cells convert light to neural signals. Two types of light receptor cells are found in the retina, called rods and cones. The cones are primarily for day color vision (photopic) and are less sensitive to light than rods. There are about seven million cones in the retina. The three types of cones are sensitive to either red, green or blue light. The rods are more sensitive to light and are primarily for night vision (scotopic). There are about 120 million rods in the retina. Since rods are responsible for night vision and cones do not respond to low light levels, we do not see color at night. Rods and cones are not distributed evenly about the retina. Most of the cones are concentrated in the fovea, a small round area directly behind the pupil of the eye. When we look straight ahead at an object, the object is focused on the fovea. There are no rods in this region. Therefore, it is the region for most accurate vision in bright light. The rods are concentrated away from the fovea. Objects focused in the fovea are, therefore, not visible in dim light. In dim light, we see objects most clearly in the periphery.

A complex electro-chemical reaction takes place when light impinges on cones and rods. Light is converted to neural impulses which are transmitted to the brain via the optic nerve fibers. While there are approximately 130 million rods and cones, there are only about one million nerve fibers. The nerve fibers are shared by the rods and cones. However, they are not shared equally. Some cones in the fovea have one nerve each. Rods always share nerve fibers.

After the optic nerve bundles leave the two eyes they meet at the optic chiasm. Here each bundle splits into two sections and one section from each eye joins with a section from the other eye. This crossing of the nerve bundles from the two eyes is partly responsible for our stereoscopic vision which allows us to see a three-dimensional world. The two newly formed bundles go to the left and right lateral geniculate bodies. Here new fibers continue to the visual cortex where visual processing takes place.

The visual cortex is a mass of gray matter forming two hemispheres at the back of the brain. Little is known about how neural signals are processed in the visual cortex.

Visual Perception

When a scene is viewed by a human observer, the spatial information contained in that scene must undergo three stages of processing. The first stage is optical processing and involves the formation of a picture of the scene on the retina. The second stage is neural processing and starts at the retina where the image is detected by a mosaic of photoreceptors. Signals are transmitted through the neural network of the ganglion cells to the geniculate fibers and then to neurons of the visual cortex. The third stage is psychophysical. This is the final perception of the picture (Cornsweet, 1970).

The perceived picture cannot be directly measured. Therefore we cannot easily describe it as some numerical function of the original scene. We can only assume a hypothetical perceived picture which consists of numerical brightness as a function of position (Saleh, 1982).

A systems approach can be applied to the study of transmission of information by defining a system whose input is the original picture and whose output is the hypothetical perceived picture. Hall and Hall (1977) describe the simplest model as one of three cascaded systems. The first is a linear system which represents the optics of the eye. The second is a logarithmic point nonlinearity which represents the response of the photoreceptors. The third is a linear system which represents neural processing.

The overall system described above is nonlinear. Researchers have avoided this complication by using visual stimuli having low contrast. The system is also space variant; that is, the response of the system to an impulse depends upon the location of the impulse. Davidson (1968), however, argues that the system is approximately locally invariant over regions within which structural inhomogeneity is effectively self-homogenizing. These issues are important because a system which is linear and space-

invariant can be completely characterized by its response to sinusoidal stimuli. The response of the system to any complex stimulus can then be characterized as the superposition of the responses to each of the sinusoidal Fourier components of the stimulus.

The response of a linear, space-invariant system to a sinusoidal stimulus is also sinusoidal. However, the amplitude is generally attenuated and the phase shifted. The attenuation as a function of frequency defines the modulation transfer function (MTF). The phase shift as a function of frequency defines the phase transfer function. The two taken together, determine the transfer function of the system.

The transfer function of a linear system is usually determined by measuring the attenuation and phase shift of sinusoidal stimuli of different frequencies. To apply this technique to the visual system, sinusoidal spatial gratings

$$I(x.y) = I_0\{1 + m\cos[2\pi f_0 (x\cos\theta - y\sin\theta) + \varphi]\}$$

of contrast m, frequency f_0, and orientation θ are displayed to the observer (Saleh, 1982). However, in the human visual system, there is no way to directly measure the amplitude or the contrast of the perceived sinusoidal function.

Our ability to perceive the details of a visual scene is determined by the relative size and contrast of the detail present. Schade (1956), who was the first to use Fourier methods to study vision, measured the contrast sensitivity function (CSF). He did this by reducing the contrast of a sine wave grating displayed on an oscilloscope until the viewer no longer saw the grating but rather, saw a uniform field. The mean value of the grating was kept fixed as the contrast was reduced. The reciprocal of the level at which the grating was no longer perceived was then the contrast sensitivity. This procedure was repeated at a number of different spatial frequencies, thus producing the contrast sensitivity function ($C(f)$).

To determine the relationship between the CSF and the MTF of the linearized visual system, a mechanism of threshold detection must be postulated. The simplest mechanism is that of comparing the perceived small contrast to a fixed threshold level δ. When δ is exceeded, the pattern is declared to be detected. The measured contrast threshold of the original pattern $[C(f)]^{-1}$ should, when reduced by the MTF, $H(f)$, of the visual system be equal to the threshold level δ. Therefore, $[C(f)]^{-1} H(f) = \delta$ or $H(f) = \delta C(f)$. The MTF is proportional to the CSF (Saleh, 1982).

Campbell and Green (1965) separated the optical and neural contributions of the CSF by creating sinusoidal patterns directly on the retina. They found that the optics of the eye acts as a low-pass spatial filter while the retina brain system acts as a bandpass filter attenuating both very low and very high spatial frequencies. The spatial frequencies of maximum sensitivity were found to be between 3.0 and 4.5 cycles per degree of arc subtended in the viewer's field of vision. The sensitivity also depends upon orientation of the grating. Sensitivity is greatest for $\theta = 0$ or 90 degrees and least for $\theta = 45$ degrees.

Factors Affecting Target Acquisition

Detection

Available energy affects detection; we must have a sufficient amount of the right form of energy. The human visual system is sensitive to only a very limited portion of the electromagnetic spectrum--wavelengths from 400 to 700 nm with peak sensitivity at about 550 nm. The band of sensitivity corresponds roughly with the peak of radiation from the sun, which is at about 500 nm. The visual system, then, tends to be optimized for natural illumination. Cones and rods enable the human visual system to cope with a tremendous range of luminance levels met in natural viewing from 10^{-6} cd/m^2 to 5000 cd/m^2. Most cones are in the fovea, which covers a circular portion of the visual field subtending between 10 and 20 mrad diameter.

Stimulus characteristics affect our ability to detect. These include size, shape and form, contrast against surroundings, texture, edge sharpness, interaction with surroundings.

It has been found that the eye can usually just detect a black disc of angular subtense about 0.15 mrad against a plain background in good light. Similarly it was found possible to detect the presence of twin points of light as twin points when they were separated by about 0.15 mrad, again in good light.

As the size of an object is increased while all other conditions are held constant, it almost invariably becomes easier to see. The contrast required to see a simple circular stimulus having angular subtense at the eye on the order of a milliradian or less is governed by Ricco's Law: $\varepsilon\alpha^2$ =constant, where α is the angular diameter of the stimulus and ε is the contrast defined by $(B/B'-1)$ where B and B' are the luminances of the stimulus and immediate background, respectively. As size is increased above about 3 mrad diameter, the deviation from Ricco's Law becomes more and more marked until when looking at stimuli with diameters in excess of 30-60 mrad, further increase in size has little further effect on the value of ε.

The contrast required to see an object is also a function of field luminances, with higher contrast being required if the background luminance is low. Blackwell (1946) has plotted threshold contrast curves as a function of luminance for disc stimuli of various sizes. At low luminance levels, these curves show a discontinuity where the cones cease to function and rods take over. These threshold curves hold true only if the eye has become adapted to the background illumination level. The process of adaptation can take many minutes depending upon the difference in luminance levels before and after adaptation.

Experimenters have looked at effects of shape. Lamar (1948) studied the effects of object aspect ratio, using rectangular stimuli with aspect ratios ranging from 2:1 to 200:1. Contrast threshold was found to decrease with increased object area at all aspect ratios.

However, thresholds were found to be largely independent of aspect ratios up to about 7:1, after which thresholds began to be considerably higher for objects of same area but greater aspect ratio. Guth and McNelis (1969) studied threshold functions for various complex targets such as parallel bars, Landolt rings, letters and dot patterns. They found that detection was approximately independent of shape for high luminance. Although luminance trends tended to be shape dependent, trends for circular stimuli were a good mean.

Effects of edge sharpness were examined by Ogle (1961). Thresholds for various sizes of out-of-focus aerial images of disc stimuli were utilized. The results of this work have shown that there is a massive effect of blur on thresholds for very small objects. This is presumably due to the extensive spreading of energy in the retinal image. There was also significant threshold degradations due to blurring for large objects.

Contrast sensitivity and orientation have been found to affect detection. Campbell et al (1966) found visual response to be maximal to vertical edges with a secondary maximum to horizontal edges and pronounced minima for patterns inclined at approximately 45 degrees to the vertical.

Effective exposure time, the total time available for inspection of any particular part of a stimulus, will affect detection performance. Search may be necessary due to uncertainty as to where a stimulus is in the visual field or it may be an imposed detail search within a local area of a visual scene, or even within local parts of a complex stimulus. In each case the search strategy will yield progressive bits of data on which to build a brain 'picture' of the fine details of the scene being studied, but at the expense of available time to study any one elemental area. Scene structure may include similar objects to the stimulus, thus producing conflicting input data. This may upset adaptation level at which the local visual inspection is taking place or may introduce local veiling glare effects. Other factors include retinal position, motion, color, state of eye focus, positive versus negative contrast, training and motivation. All these factors can have effects on performance, most of which are ill-defined.

Recognition

In our everyday life, we are usually required to do more than just detect the presence of an object. More often, we must be able to recognize that an object is one of a particular class. Less is understood about how the visual system performs recognition. It is not obvious exactly what structure it is necessary to see in order to effect recognition in a given situation. Nor is it obvious how to relate the detectability of certain local structure to the detection thresholds of isolated simple shapes.

Suprathreshold vision is more complex than threshold vision as it involves the appearance of viewed pictures rather than the question of whether or not a stimulus is detected (Saleh, 1982). Measurements of the suprathreshold MTF, performed by matching sinusoidal gratings of different spatial frequencies (Springer, 1978; Kulilowski, 1976), yield a suprathreshold that is much flatter, not falling off at high and low

9

frequencies. Springer (1978) suggests that neural processing compensates for optical degradation, thus achieving a deblurring of the image.

Furchner, Thomas and Campbell (1977) and Campbell, Howell and Johnstone (1978) found that under certain conditions of low frequency and low contrast, a square wave pattern could not be distinguished from a similar square wave pattern without the fundamental. Campbell *et al.* (1978) suggest that the visual system responds "as though hardwired to detect square gratings and edges by means of quasi-Fourier analysis."

Recognition ability must depend, at least to some extent, upon such factors as the number of possible stimuli, complexity of form, previous experience, orientation of the retinal image and association with the particular field of view in addition to the factors found to influence detection.

Helson and Fehrer (1932) found, for simple shape recognition including rectangles, discs and triangles, rectangles are easiest to recognize with triangles generally being next easiest.

Results of several studies (Bitterman, Krauskopf and Hochberg, 1954; Engstrand and Moeller, 1962) show recognition threshold to vary directly with "compactness." This term is used to describe forms of low aspect ratio and simple contour characterized by a low perimeter to area ratio (P/A ratio). Fox (1957) found that while form does affect recognition threshold, neither perimeter, area nor P/A were good predictors. Casperson (1950) used 30 geometric shapes, five each of various forms of rectangles, ellipses, triangles, diamonds, crosses and stars of various sizes. He found no common behavior for the different forms. While area was a good predictor of threshold for all triangles, it was a very poor predictor for stars and crosses. The maximum dimension or perimeter was found to be a good predictor for stars but very poor for ellipses and diamonds. There seems to be no simple measure of form which can be used as a universal predictor of recognition threshold. Attneave (1954) postulated that it might be the local parts of the profile of an object which allowed its recognition. He produced a series of outline shapes with irregular contours, and, allowing each of several observers ten dots with which to define the figure, produced a statistical impression of the importance of various local parts of the profile. There appeared to be a strong concentration of importance in the regions of maximum rate of change of contour direction, with very little importance to straight regions of contour.

Experience, expectancy and familiarity are very important factors in recognition. Experienced observers can discriminate fine details of familiar objects very quickly and accurately. Unfamiliar or unexpected objects are not as easily discriminated as the familiar or expected.

The availability of lasers and high-capacity digital computers has made it feasible to apply spatial filtering techniques to the problem of picture analysis. The practical problems that arise in making an object recognition device are of direct relevance to solving the problem of how we recognize familiar objects in complex scenes. Conversely,

pattern recognition engineers are very interested in the visual system, for here is a device that actually works very well (Campbell, 1974).

Overington (1976) discusses contributory factors to the recognition decision. First there is the object which has certain characteristics which differentiate it from its surroundings and other objects. This is not a simple difference of luminance on adjacent receptors as with detection, but a difference of local luminance structure from that which would be expected for an alternative confusable object. Expectation implies a required input from the memory. It is only by experience that we can learn what visually discriminates one object from another. As with detection, the differential effects must be differences in the retinal image, not in the original object. The whole of the understanding of the visual process is tied up with an understanding of ability to detect details (Overington, 1976). Ginsburg (1971) has shown that we require only a quite narrow range of low spatial frequency information to recognize many objects.

Johnson (1957) presented the first frequency domain approach to predicting the ability of observers to perform target detection and recognition tasks. Johnson compared the level of decision making he could extract from an image (i.e., detection, recognition, identification) to the frequencies he could resolve in a US Air Force standard tri-bar chart which was scaled to the image. He determined the number of resolved line pairs required per foot of target dimension to perform a given task for a number of different targets. For example, detection of a tank requires 0.75 cycles per minimum dimension, recognition required 3.5 cycles and identification requires 7 cycles. All target views were broadside. Johnson stipulated that the bar pattern used must have the same contrast as the internal contrast of the actual target.

Moser (1972) found that the Johnson Criteria did not work well for Naval vessels at some aspect angles. Moser experimented with breaking the ships' images into two-dimensional blocks of various resolutions. He determined that approximately 66 blocks were required to recognize whether the ship was a combatant or noncombatant. Approximately 400 blocks were required before the class of warship could be identified. While Johnson's Criteria was related to the minimum dimension of the target, Moser's was related to the average area.

Johnson and Lawson (1974) established the Target Transform Probability Function as an improvement to the original Johnson Criteria. The Target Transform Probability Function relates the probability of performing a given visual task to the ratio of the number of cycles one can resolve across the minimum dimension of the target to the standard number given in the original Johnson Criteria.

The Night Vision and Electronics Systems Directorate adopted the Johnson Criteria and the Target Transform Probability Function as their standard for predicting operational performance in 1974. This standard is still in use today. The approach for calculating target detectability, recognizability and identifiability has not changed significantly in more than 20 years (Shumaker, 1995).

11

O' Neill (1974) showed that ship images having the same number of resolved lines across their minimum dimension had different levels of discernability under different video signal to noise conditions. That is, with increased video signal to noise ratio, fewer lines were required across the target in order to accomplish the same level of detection, recognition or identification.

Snyder (1983) evaluated the effects of image blur and noise on hardcopy and softcopy image quality scaling and information extraction. Five levels of blur and five levels of noise were employed. They found that both blur and noise resulted in reduced judgments of image quality and information extraction capability. They also found that increases in either noise or blur tended to mask the influence of the other variable on perceived quality. For information extraction, they found the effect of noise to be somewhat less at the greatest blur levels.

Theory of Signal Detection

While the previous discussion has focused on fluctuations in target acquisition performance due to input, it seems unreasonable to assume that there are no fluctuations due to the visual system itself, particularly at the decision level of the brain. More than sensory information is involved in target detection and recognition. The process of perceiving is not merely one of passively reflecting events in the environment, but one to which perceiver himself makes a substantial contribution. The observer relates his sense data to information he has previously acquired, and to his goals, in a manner specified by statistical decision theory (Swets, Tanner and Birdsall, 1964).

An operator's performance in a target detection or recognition task may be a function of (1) properties of the target and imagery such as image resolution, modulation, blur, etc.; and (2) the operator's decision rule (e.g., presumed to be related to the payoff for correctly identifying a target and the consequences associated with false alarms.) Performance measures such as probability of hits and probability of false alarms do not allow one to unambiguously interpret the results; that is, the contribution to the response measures associated with stimulus characteristics and response bias are not separable. For example, an operator may achieve a high probability of hits, but achieve this result by calling everything a target (e.g., a high probability of false alarms).

The theory of signal detection (TSD) provides a means by which one can obtain two independent measures that relate to operator sensitivity and response bias, respectively (Green and Swets, 1966). The measure of sensitivity, referred to as d', is generally affected by sensory/perceptual factors such as image resolution and target-to-background relationship. The other parameter, Beta, is a measure of response bias which is affected by such variables as the consequences of misses and false alarms, rules of engagement, a priori knowledge, expectations and training. The value of Beta is an index of the operator's response criterion.

The theory proposes that d' is equal to the difference between the means of the signal and noise (SN) and noise (N) distributions (u_{SN}-u_N) expressed in standard deviation units of the N distribution (Figure 2). Because the location of the SN distribution with respect to that of the N distribution is entirely a function of the stimulus intensity and properties of the sensory system, d' is a pure index of stimulus detectability which is independent of the operator's criterion (Beta).

In signal detection analysis, the corresponding Z scores from a normal distribution for the proportions of hits and false alarms are used to calculate d', which is the measure of target detectability or operator sensitivity (Gescheider, 1976). A Z score represents the number of standard deviation units that a particular hit rate or false alarm rate is from the mean of a standard (zero mean, unit standard deviation) normal distribution. The equation used to calculate d' is: d' = Z(Hits) - Z (False Alarms). A d' of 0 is equivalent to chance performance, while a d' of 3 represents near perfect performance.

Beta, on the other hand, is the ratio of the ordinate of the SN distribution at the criterion to the ordinate of the N distribution at the criterion, as follows: $\beta = \dfrac{f_{SN(X)}}{f_{N(X)}}$.

A low value of Beta represents a lax criterion where the operator will be liberal about reporting "signals," while a high value of Beta represents a strict criterion where the operator will be conservative about reporting "signals."

In TSD studies, both parameters affecting perceptual sensitivity and parameters affecting decision criterion may be manipulated. This allows the determination of receiver operating characteristic (ROC) curves (Gesheider, 1976). An ROC shows the relationship between false alarm and hit rates (Figure 3).

13
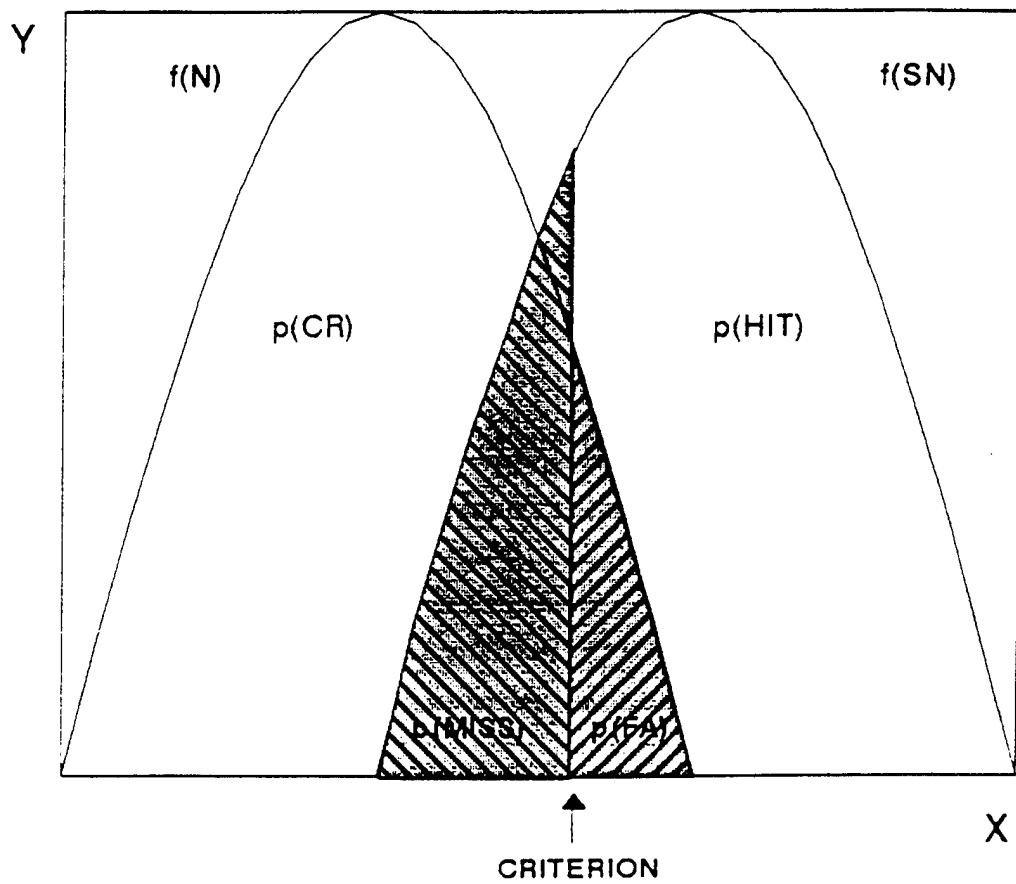
Figure 2. Relationship of p(Hit), p(FA), p(Miss), and p(CR) to noise (N) and signal plus noise (SN) distributions.
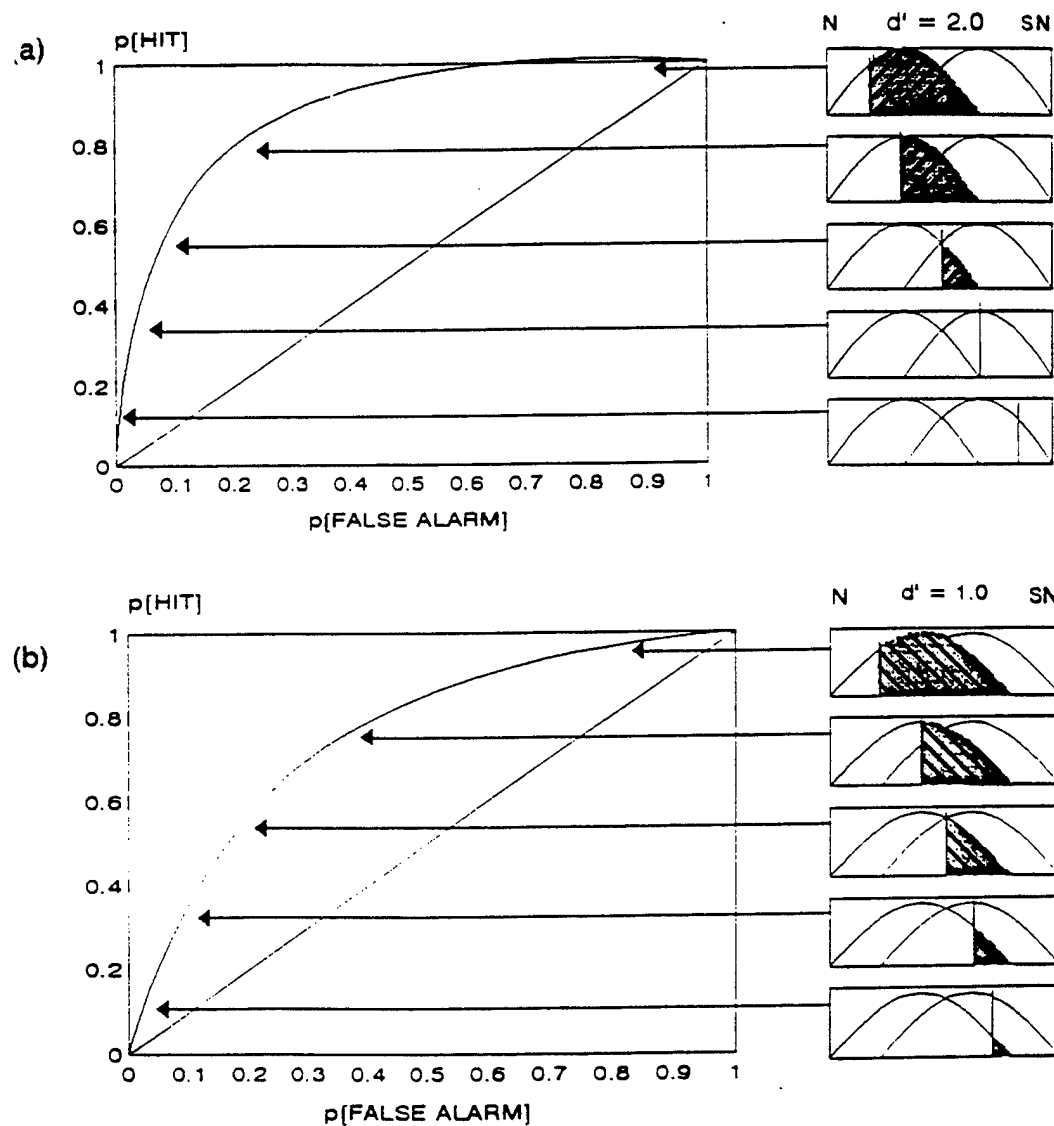
Figure 3. Illustration of the manner in which ROC curves are predicted from TSD. (a) depicts a situation in which signal strength is sufficient to result in only a slight overlap of the N and SN distributions, while (b) depicts a situation in which signal strength is weak, resulting in considerable overlap.

CHAPTER 3
EXPERIMENTS

Three target acquisition experiments were conducted using simulated infrared imagery of eight military vehicles. The first, a target detection study, required subjects to declare whether or not a military vehicle was present in an image. The two succeeding studies were recognition studies which required the subject to determine whether the vehicle present in an image belonged to one of four classes. The purpose of all three target acquisition studies was to evaluate the possible trade-offs between scene modulation, image blur and noise in their effects upon target acquisition. Further, the theory of signal detection was applied to take into account operator false alarm rate, thus separating perceptual sensitivity from operator decision criteria.

Detection Experiment

Variables of interest in the detection study were target internal contrast, target range, scene modulation and blur. The primary purpose of the detection study was to determine whether target internal contrast was a significant factor in target acquisition. Also, the detection study was used to estimate the appropriate levels of target range, scene modulation and blur to be used in subsequent recognition studies.

Method

Subjects: The subjects were ten trained observers. All were Air Force or on-site contractor personnel who had volunteered to participate in the study. All subjects exhibited 6/6 (20/20) or better Snellen acuity and were found to exhibit normal contrast sensitivity as tested by the Vector Vision Model CSV-1000 contrast sensitivity tester.

Apparatus: This research was conducted in the Visual Image Processing, Enhancement and Reconstruction (VIPER) Laboratory at the Armstrong Laboratory's Human Engineering Division located at Wright-Patterson Air Force Base, Ohio. A diagram of the VIPER facility is shown in Figure 4.

An International Imaging Systems (I^2S) Image Array Processor hosted on a PDP 11-34 or PDP 11-70 was used for image preparation and calibration as well as for image presentation and data collection. Images were presented on a 35.56 cm (14 inches) diagonal, Electrohome Model 38-V19NDA-BP monochrome monitor having a P-43 green phosphor. The display resolution is 512^2 pixels.

The display brightness and contrast were adjusted by displaying a 64 step gray scale and adjusting the brightness and contrast for subjectively equal differentiation between all adjacent steps of the gray scale. The luminance output of the display as a function of image intensity value (0-255) was measured using a Topcon Model BM-7 luminance colorimeter calibrated according to manufacturer's instructions using a Hoffman LS-65B/HO Standard Source. The calibration limit for luminance accuracy of the Topcon
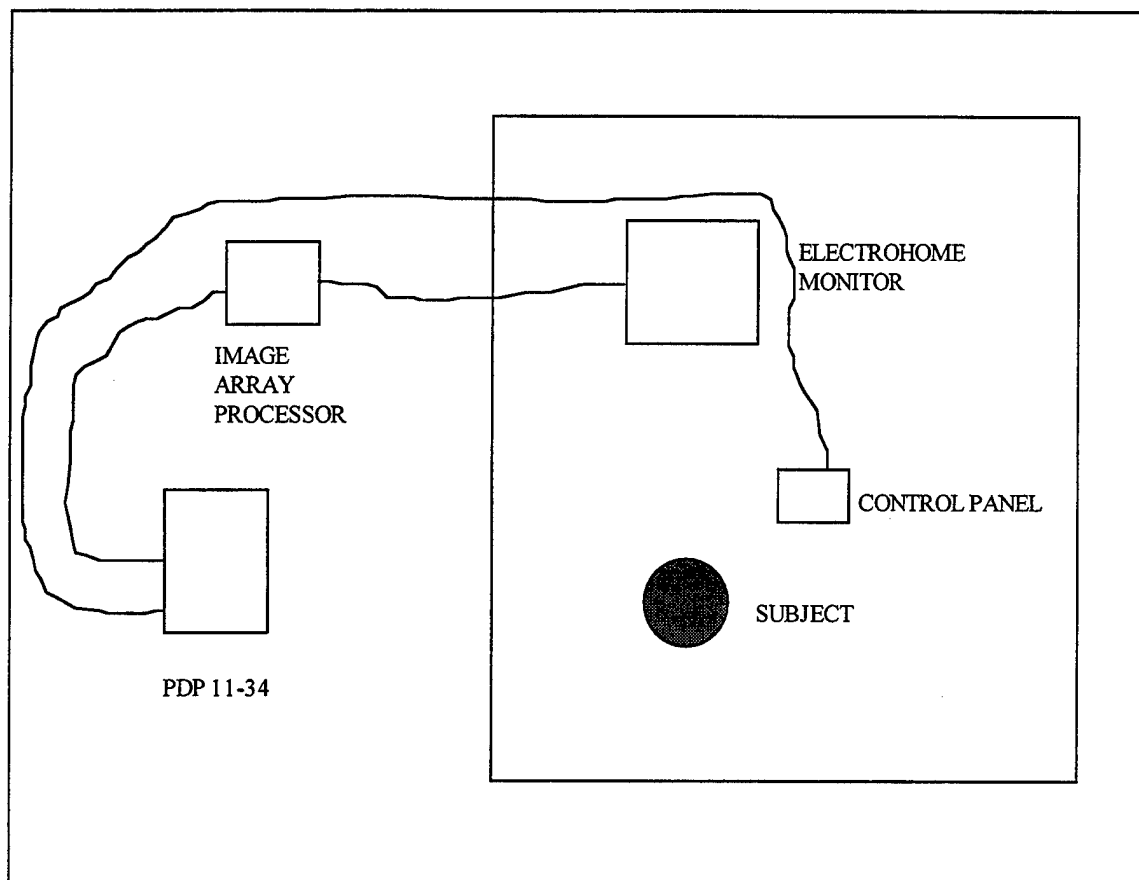
Figure 4. The VIPER facility

is specified by the manufacturer at +/- 4 percent. The display luminance transfer function is given in Figure 5. A custom-built response box which incorporates push buttons and a trackball was used for collection of subject responses.

Stimuli: The stimuli were acquired from a training imagery database established at the Terrain Board facility at the Night Vision and Electronic Sensors Directorate (NV&ESD). NV&ESD established the imagery database for the purpose of training and testing automatic target recognizers (ATRs). The images were generated by systematically varying target aspects, target contrasts (i.e., SNRs), range (i.e., pixels-on-target), target signatures, target types, backgrounds and depression angles while controlling other target and background characteristics. The target models were imaged on a terrain board. The set up was designed to simulate imagery produced by a state-of-the-art infrared sensor.

The format of the digitized imagery is 640 horizontal pixels by 480 vertical pixels with 8 bits per pixel. Ground truth files which accompany the imagery contain target type(s), x and y pixel location(s), target contrast(s), target aspect(s) and the image identification number. The imagery was stored in the Automatic Target Recognizer Working Group (ATRWG) Raster Format (ARF) and the ground truth files in Automa.
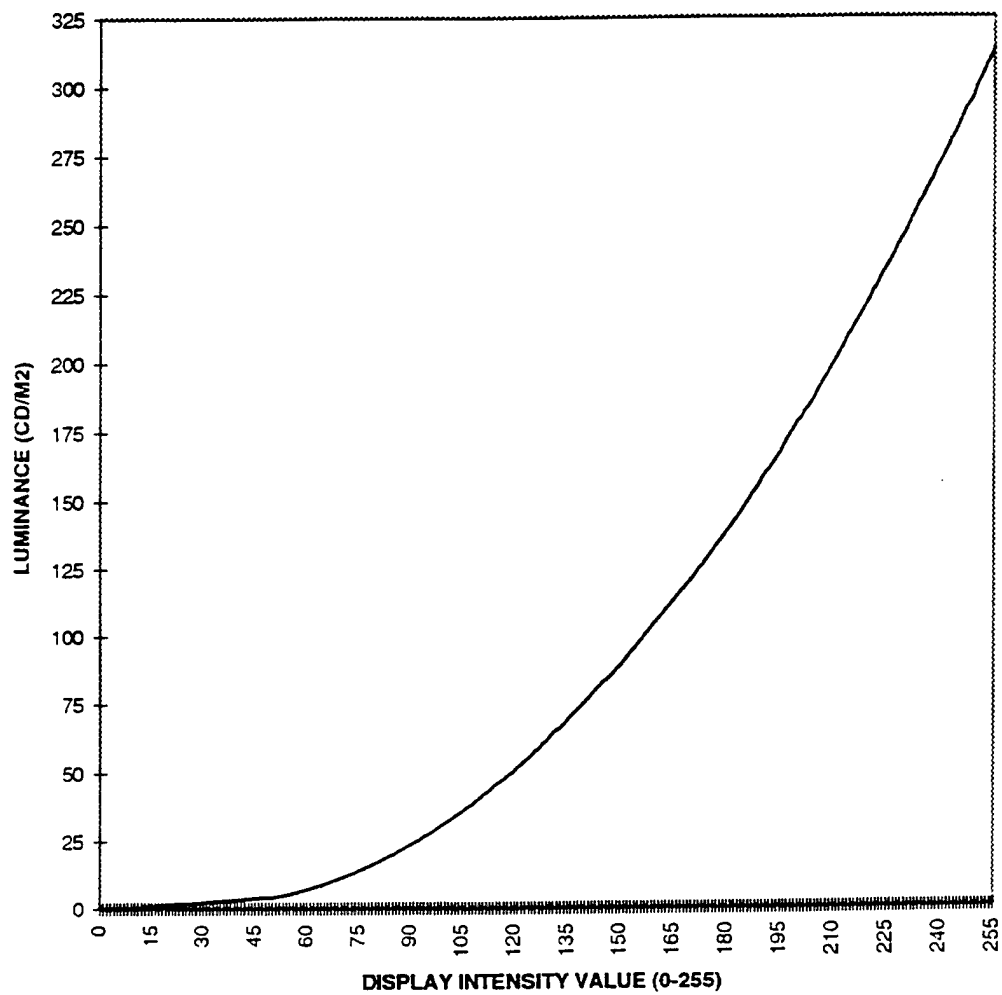
Figure 5. Display luminance transfer function.

The Training Imagery Set 2 (TRIM2) was selected for this research effort. This training set consisted of 12 targets in six classes. The targets were imaged at 21 different aspect angles ranging from 0 degrees to 355 degrees. Two paint treatments were used to achieve conditions of target internal contrast and no target internal contrast. The targets were imaged at four simulated ranges (1500, 2500, 3500 and 4500 meters) at a depression angle of two degrees. The targets were imaged against three levels of background clutter. The total number of images in the TRIM2 imagery set was 2,244.

For this research effort, eight targets were selected in four classes. These were the M-1 and M-60 Tanks, the M-113 and M-2 Armored Personnel Carriers (APCs) the M-35 and HMMWV Wheeled Vehicles and the M-163 and M-730 Air Defense Units (Artillery). The 45 degree aspect angle and the medium clutter level were selected for all targets. For this pilot study, all four ranges and both contrast conditions were used for each target for a total of 64 target images. Figures 6 thru 9 show the eight targets at each of the four ranges for the internal contrast condition.

Each of the 640 by 480 pixel images contained from eight to ten individual targets from a single class. Therefore individual target chips were extracted from the target images. These chips were 128^{10} pixels for the 1500 and 2500 meter ranges and 64^2 pixels for the 3500 and 4500 meter ranges. Table 1 gives the number of pixels across the horizontal target dimension and the angular subtense subtended by the target at the observers eye (given the 76.2 cm viewing distance) for each target and each range. A single pixel subtended .03 degrees, resulting in 16.67 cycles per degree of visual angle. The ground-resolved distance per pixel was approximately 8.5 cm, 18.5 cm, 26 cm and 33.5 cm for the 1500, 2500, 3500 and 4500 target ranges, respectively.

In addition to the 64 target image chips, 64 background image chips were also extracted. These chips were of areas of the terrain board which were near the target area and similar in appearance to the target area but contained no targets. For each "target" image chip, then, there was a corresponding "no target" image chip of the same size possible levels of image blur (image resolution). This was achieved by applying a gaussian filter to the image. Each image received three conditions of blur; these conditions were no blur, blur by gaussian filter of radius 8, and blur by gaussian filter of radius 12. This resulted in 192 "target" images and 192 "no target" images. The theoretical effects of the blur conditions can be seen in Figure 10. The figure shows the results of applying the blur conditions to a line one pixel wide. The blur was achieved by first taking the Fourier transform of both the image and the gaussian filter. The height of the resultant gaussian was then rescaled to unity to avoid decreasing the modulation of the image. This gaussian was then multiplied by the Fourier transform of the image and the inverse Fourier transform taken of their product. The sharp edge is "smeared" over 16 pixels when filtered by the gaussian of radius 8. It is "smeared" over 24 pixels when filtered by the gaussian of radius 12. At half the maximum luminance, the blur extends over 8 pixels and 12 pixels for the filters of radii 8 and 12, respectively.
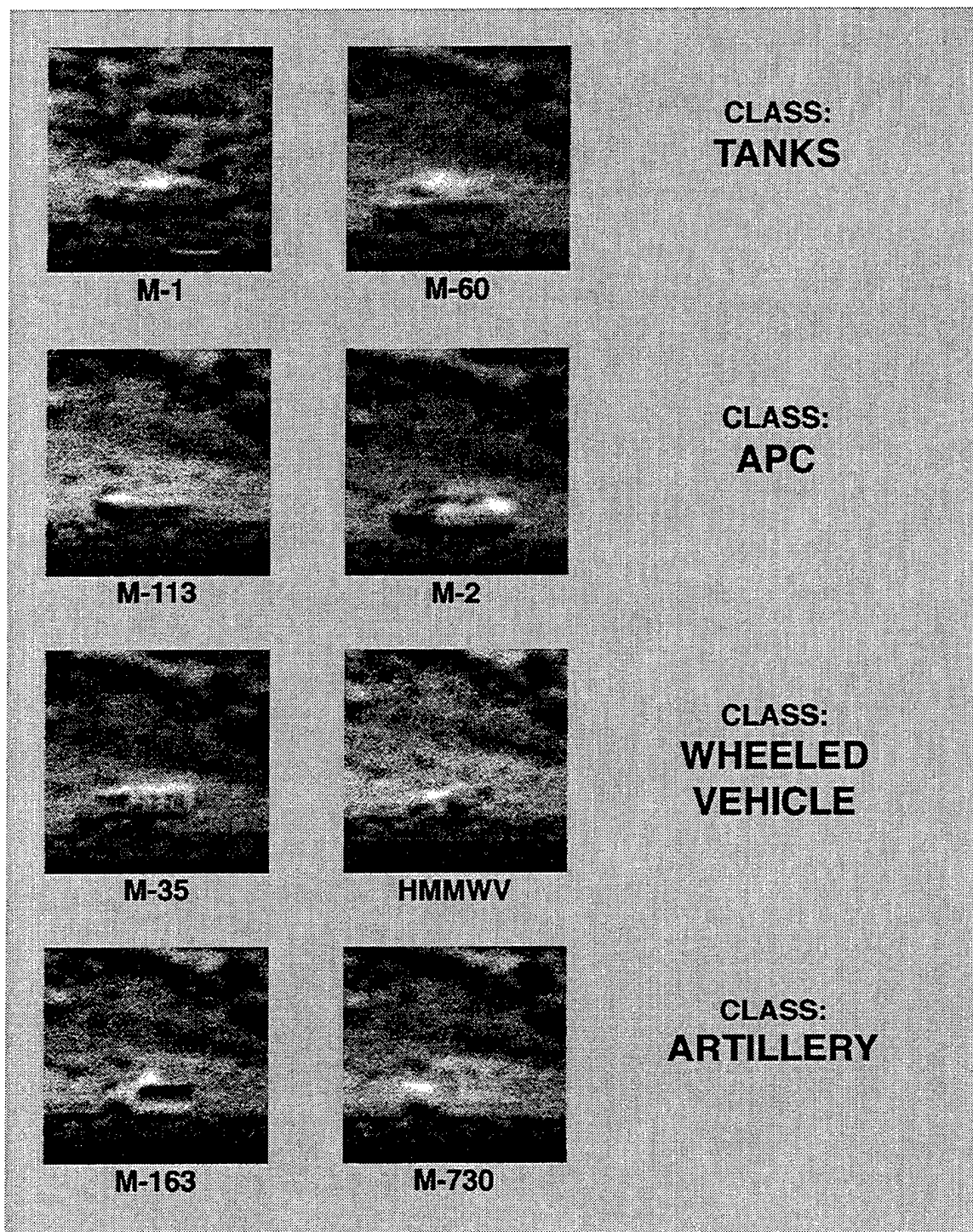
Figure 6. Targets chips extracted from the TRIM2 simulated infrared imagery set; target range = 1500 meters.
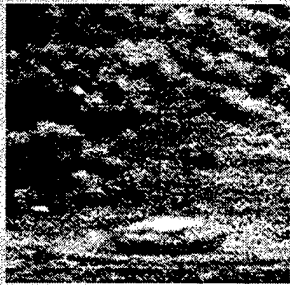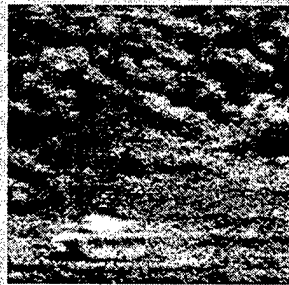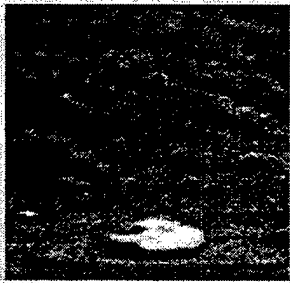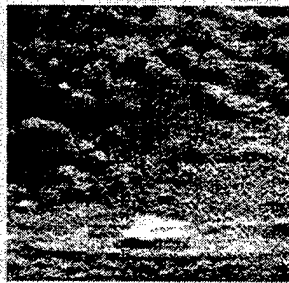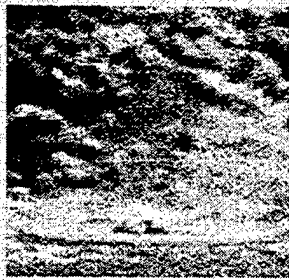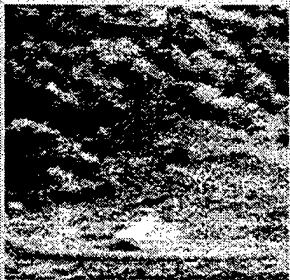
Figure 7. Target chips extracted from the TRIM2 simulated infrared imagery set;
range = 2500 meters.

CLASS: **TANKS**

M-1 M-60

CLASS: **APC**

M-113 M-2

CLASS: **WHEELED VEHICLE**

M-35 HMMWV

CLASS: **ARTILLERY**

M-163 M-730
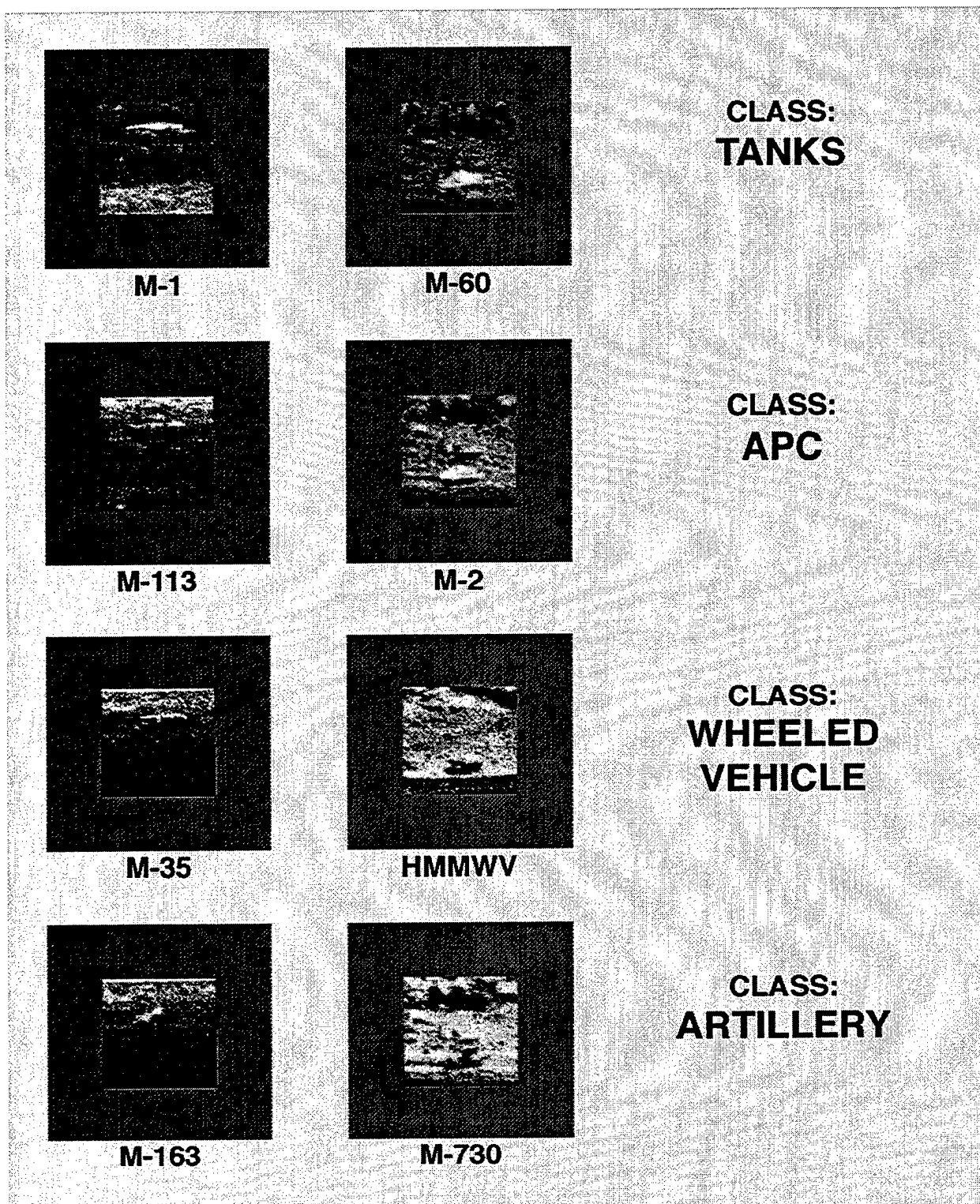
Figure 8. Target chips extracted from the TRIM2 simulated infrared imagery set; range = 3500 meters.
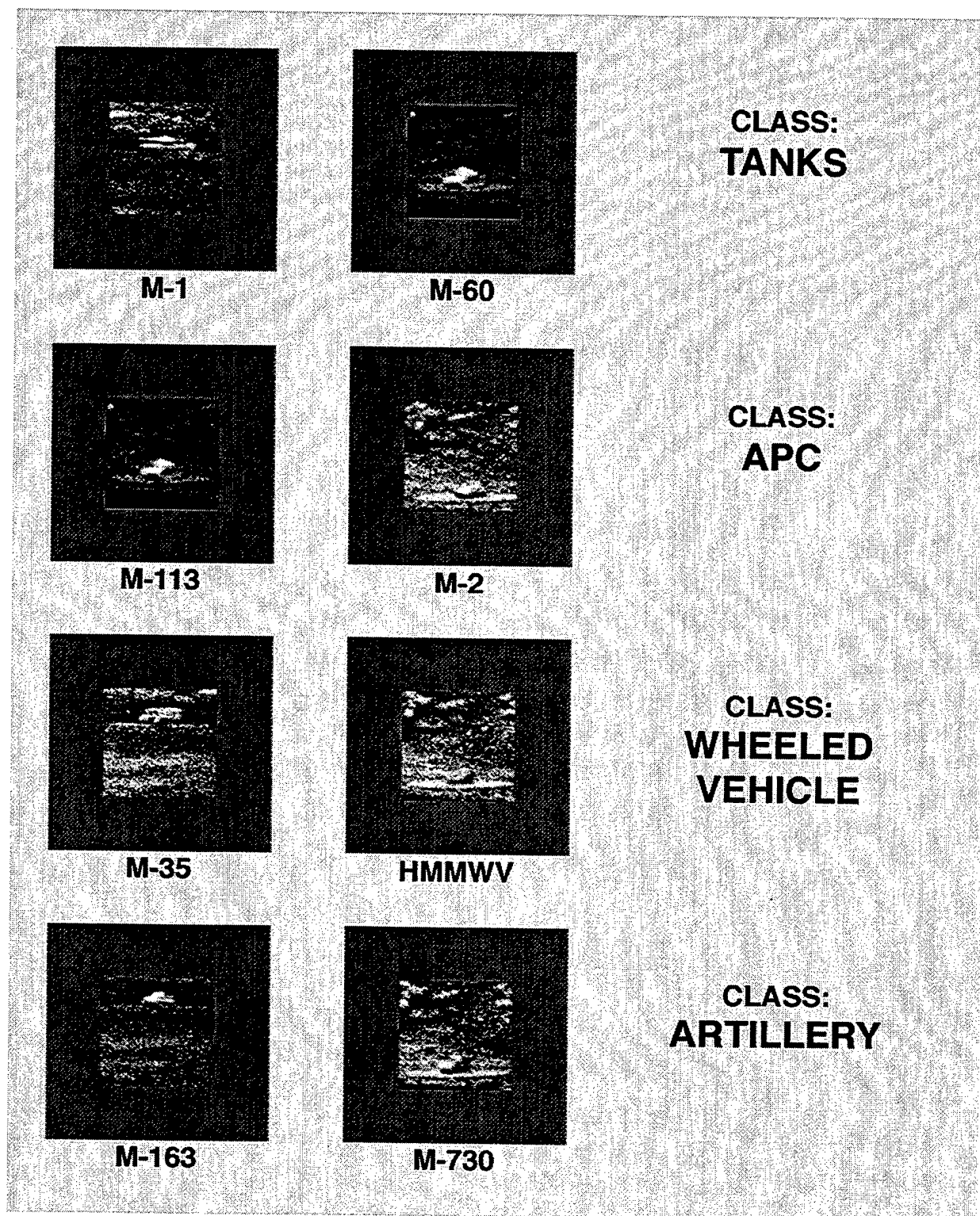
Figure 9. Target chips extracted from the TRIM2 simulated infrared imagery set; range = 4500 meters.

Table 1
Number of pixels across target horizontal dimension and target angular subtense (degrees) at each target range.

TARGET at 1500m	NO. PIXELS	VISUAL ANGLE
M-1	85	2.55
M-60	90	2.70
M-113	71	2.13
M-2	86	2.58
M-35	78	2.34
HMMWV	64	1.92
M-163	72	2.16
M-730	59	1.77
TARGET at 2500m	NO. PIXELS	VISUAL ANGLE
M-1	53	1.59
M-60	49	1.47
M-113	42	1.26
M-2	44	1.32
M-35	39	1.17
HMMWV	29	0.87
M-163	33	0.99
M-730	35	1.05
TARGET at 3500m	NO. PIXELS	VISUAL ANGLE
M-1	35	1.05
M-60	30	0.90
M-113	22	0.66
M-2	31	0.93
M-35	29	0.87
HMMWV	19	0.57
M-163	28	0.84
M-730	23	0.69
TARGET at 4500m	NO. PIXELS	VISUAL ANGLE
M-1	32	0.96
M-60	24	0.72
M-113	17	0.51
M-2	25	0.75
M-35	23	0.69
HMMWV	15	0.45
M-163	24	0.72
M-730	20	0.60

At the time of presentation, each of the resultant 384 images was further processed to achieve one of three levels of image modulation (dynamic range). The three levels of modulation were 0.1, 0.3 and 0.85 as defined by the formula for Michelson Contrast,

$$C_M = \frac{L_{max} - L_{min}}{L_{max} + L_{min}}$$

where L_{min} represents the minimum luminance value and L_{max} represents the maximum luminance value.

The display transfer function was used to create a look-up table for control of image modulation. At all three modulations, the mean luminance of the images was held constant at 104 cd/m². The luminance ranges were 86-113 for modulation of 0.1, 73-131 for modulation of .3, and 17-186 for modulation of 0.85. Selection of the 104 cd/m² mean luminance and the maximum modulation of 0.85 allowed for all images to be displayed within the display intensity value range of 70-200. Below the intensity value of 70, there is little increase in display luminance per unit increase in intensity value. Above intensity value 200, display luminance increases more sharply with each unit increase of intensity value (see Figure 5). Figures 11 through 14 show the internal contrast images of the M1 tank at all combinations of blur and modulation for each of the four target ranges.

Procedure: Image presentation was grouped by contrast modulation, resulting in three blocks (three levels of modulation) of 384 images each. Half of the images in each block were "target" images and the other half were "no target" images. Each data collection session consisted of one block, resulting in three data collection sessions for each subject. Each subject completed one or two (morning and afternoon) sessions per day on consecutive days (except weekends) until all three sessions had been completed.

Prior to beginning the first session, the subjects were tested for visual acuity and contrast sensitivity. They were shown pictures of all of the targets at all ranges. They were not shown degraded images (blur, reduced modulation). The subjects were also given a one-page set of written instructions to read. The pictures and the written instructions are presented in Appendix A. They were also asked to sign a consent form for their participation in the study. A copy of the consent form is found in Appendix B.

The subject was seated in the VIPER subject booth approximately 76 centimeters (30 inches) from the display. While no head restraint was used, subjects were reminded at the beginning of each session to keep their head and chair touching the back wall of the booth in order to maintain the 76 centimeter viewing distance.
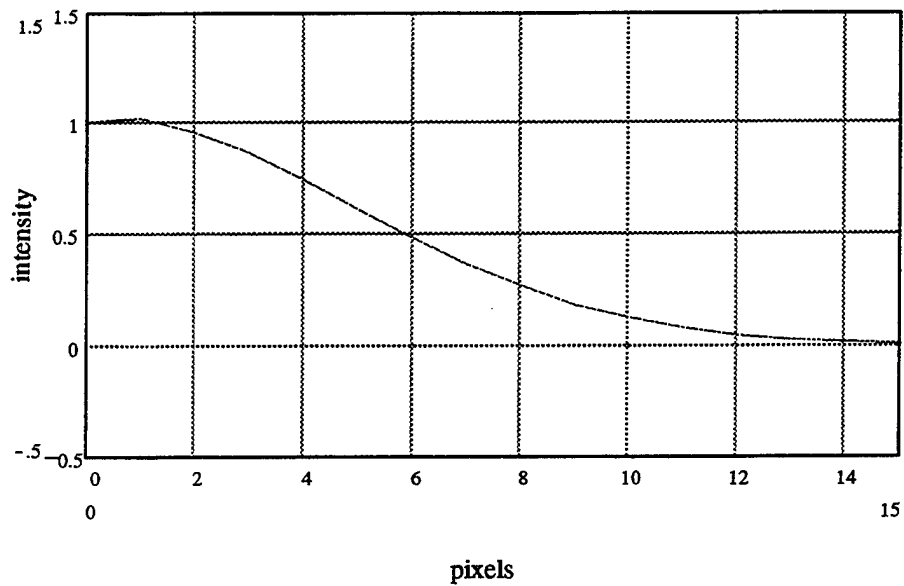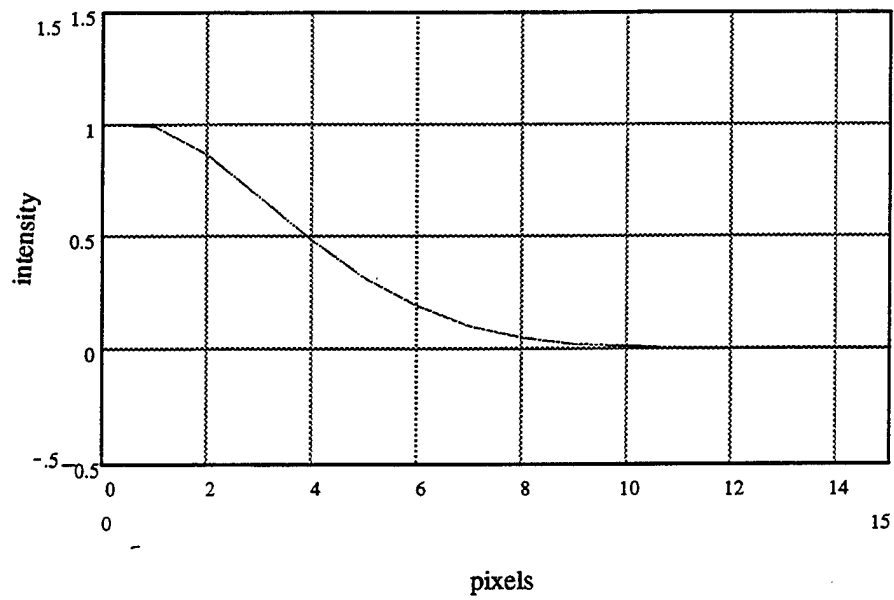
Figure 10. Effects of blur upon an edge. The top figure shows the effects of filtering a line one pixel wide of maximum intensity with a gaussian of radius 8 pixels. The lower figure shows the effects of filtering the same line with a gaussian of radius 12.
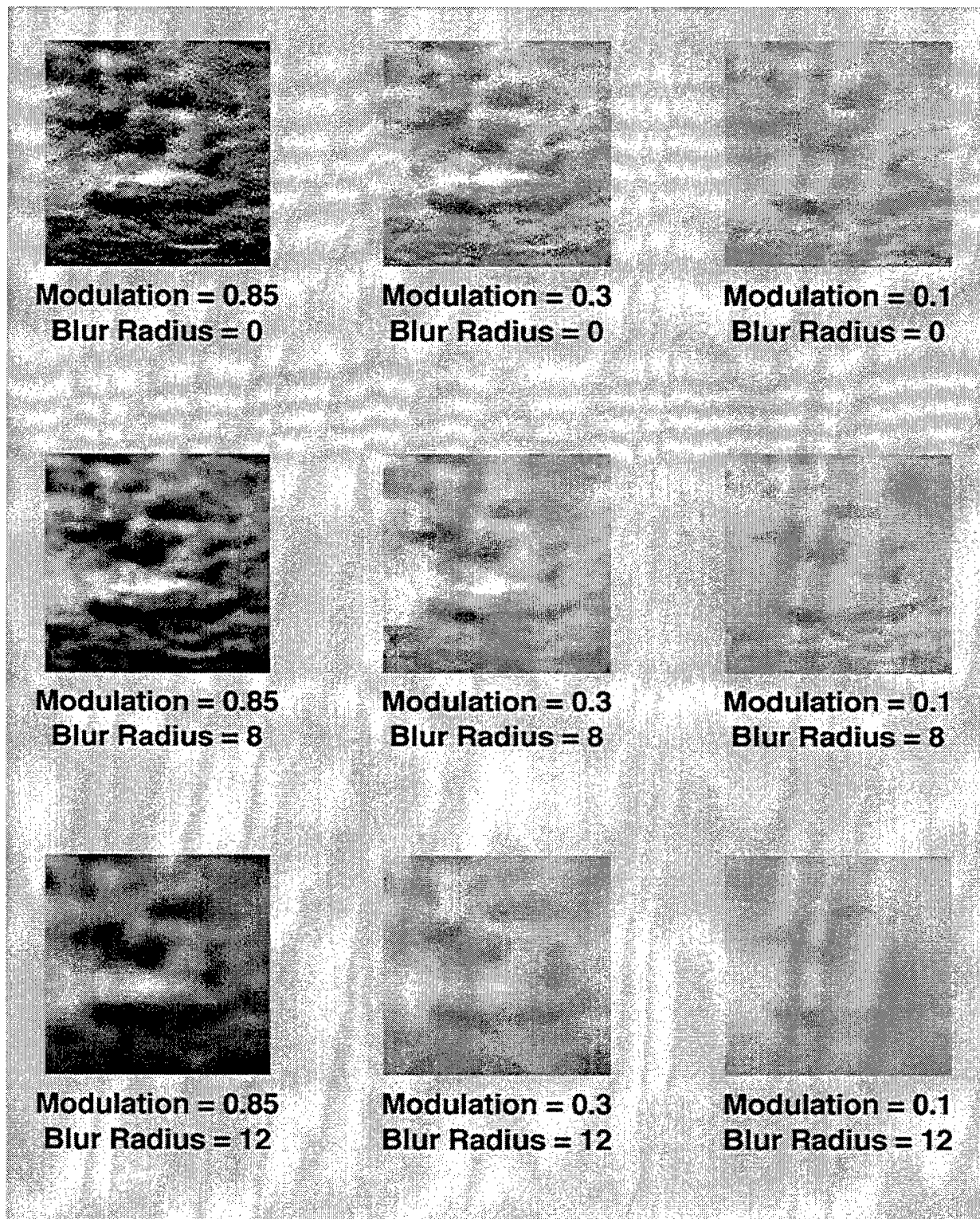
Figure 11. M-1 tank at all combinations of modulation and blur; range = 1500 meters.
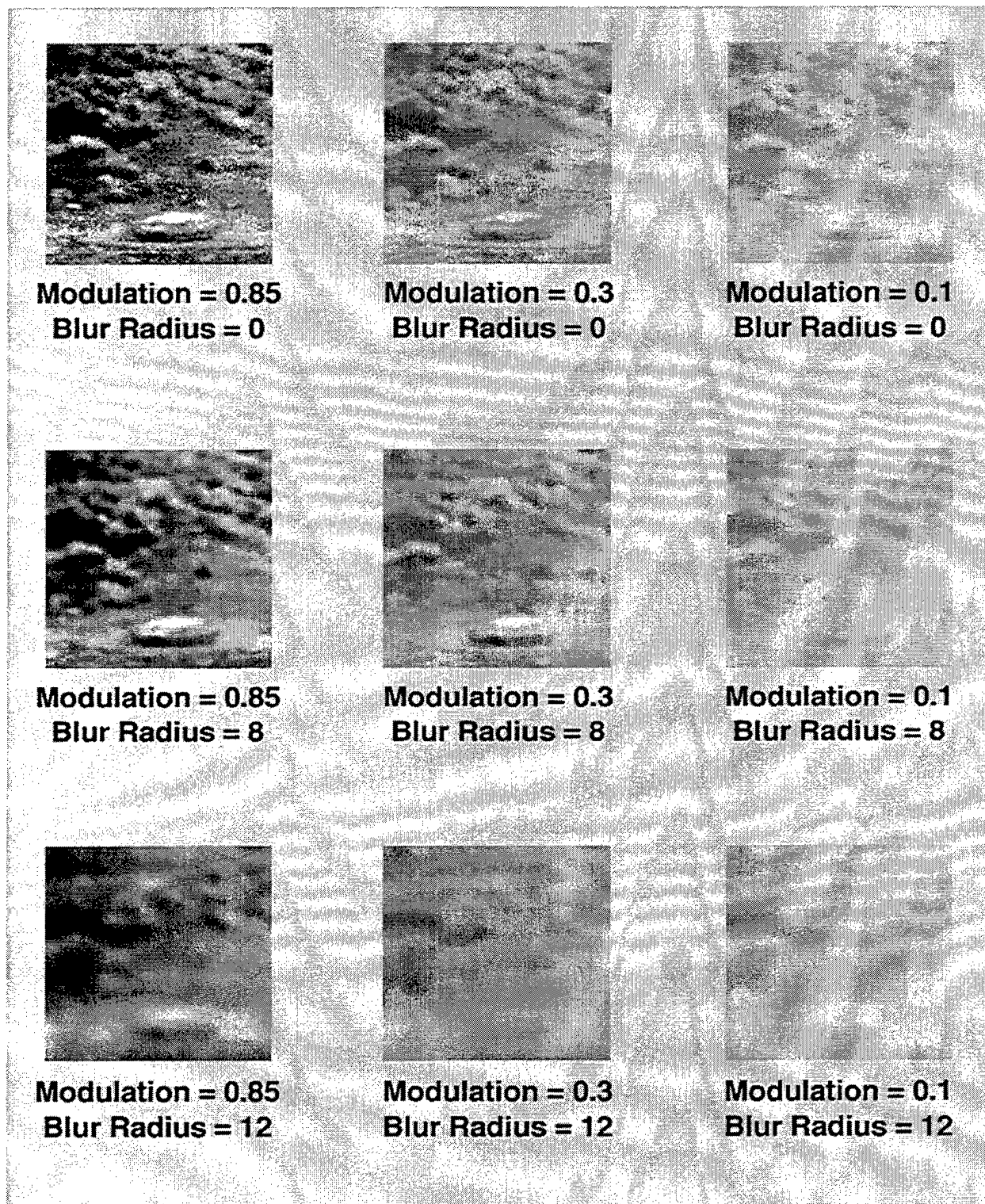
Figure 12. M-1 tank at all combinations of modulation and blur. Range = 2500 meters; no noise.

Modulation = 0.85
Blur Radius = 0

Modulation = 0.3
Blur Radius = 0

Modulation = 0.1
Blur Radius = 0

Modulation = 0.85
Blur Radius = 8

Modulation = 0.3
Blur Radius = 8

Modulation = 0.1
Blur Radius = 8

Modulation = 0.85
Blur Radius = 12

Modulation = 0.3
Blur Radius = 12

Modulation = 0.1
Blur Radius = 12
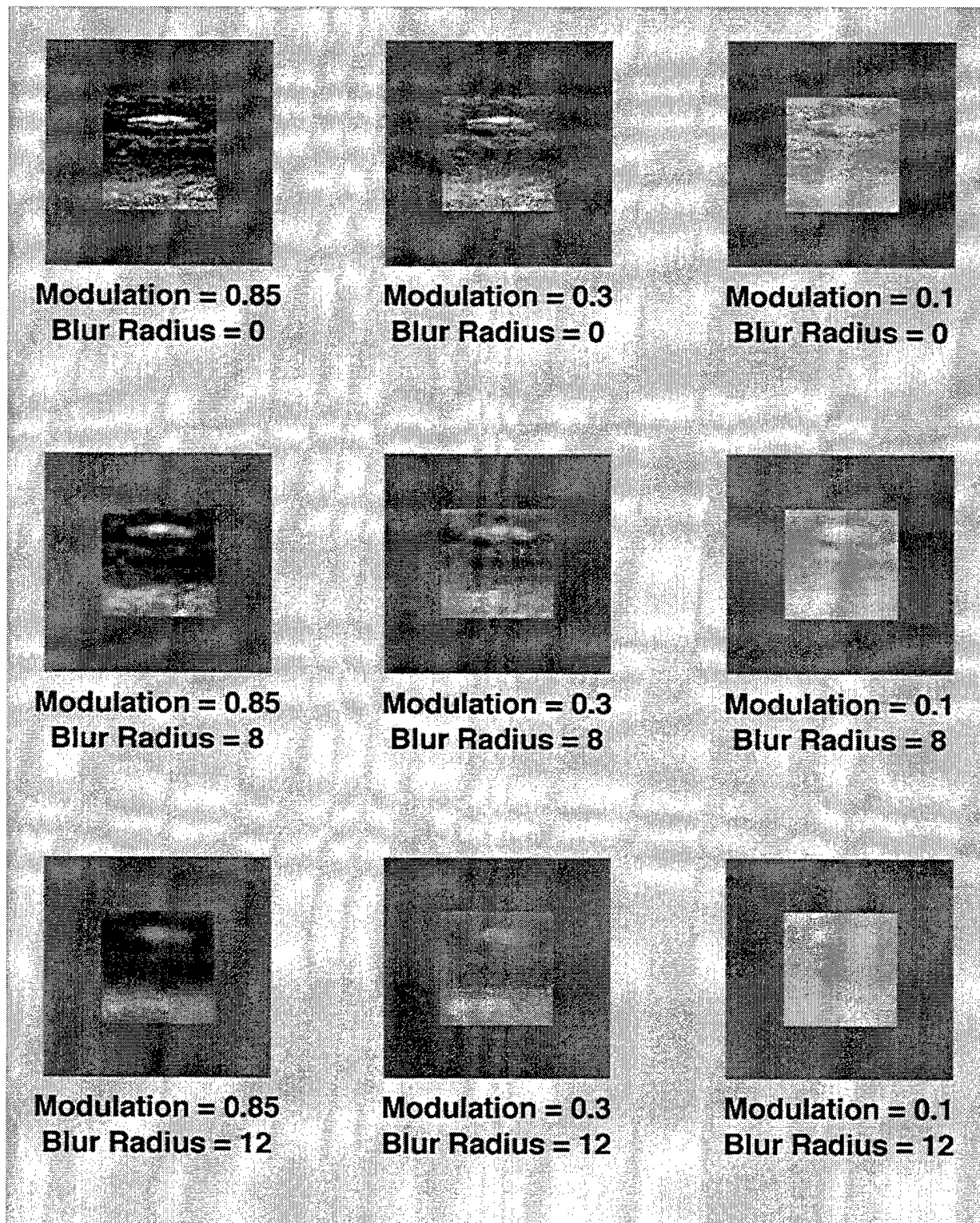
Figure 13. M-1 tank at all combinations of modulation and blur; range = 3500 meters.
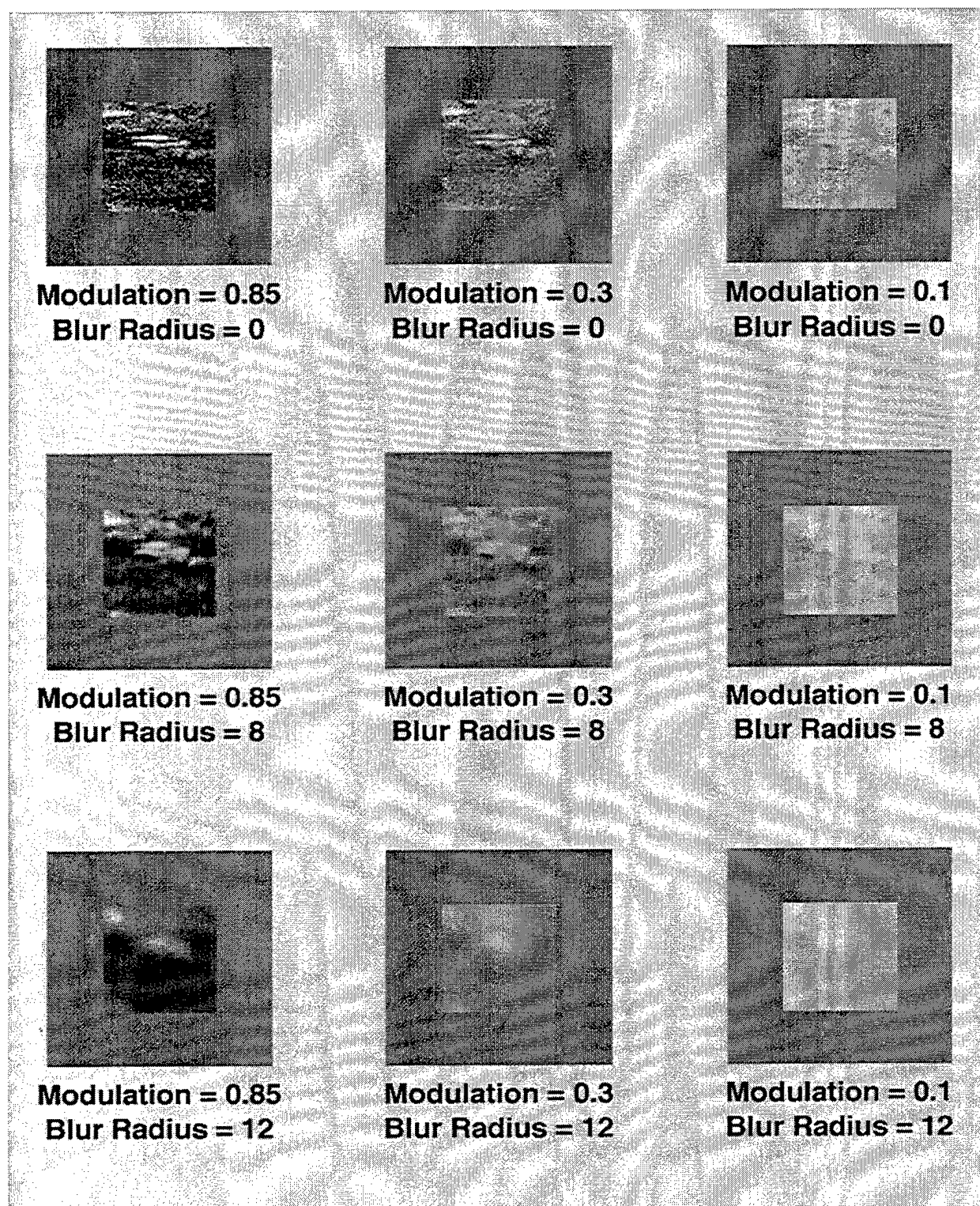
Figure 14. M-1 tank at all combinations of modulation and blur; range = 4500 meters.

At the beginning of the session, a medium green screen of the same average luminance as the images (104 candelas/m^2) was displayed with the word "READY" in the center. The subject initiated the presentation of the first image by moving the trackball slightly. The image appeared immediately and remained on the display for one second. The image was always displayed in the center of the medium green screen of the same average luminance as the image. This was followed by a medium green screen (104 candelas/m^2) with the word "RESPOND" in the center. At this time the subject would press one of six buttons on the response box to indicate whether or not he believed that a target was present in the image. The button responses were as follows:

Target **definitely** present.   Target **definitely** NOT present.

Target **probably** present.   Target **probably** NOT present.

Target **possibly** present.   Target **possibly** NOT present.

A diagram was provided above the control panel to remind the subject of which button was associated with each possible response. Only one button could be pressed for each image. There was no time limit for responding; however the response time was recorded. Subjects were instructed that accuracy was more critical than speed.

After the subject had pressed one of the response buttons, the "READY" screen appeared for the next image and the above procedure was repeated for each image. In each block, all "targets" were presented at both contrast conditions and at all ranges and all blur conditions (resolution) as were the corresponding "no target" images. Image presentation within each block was completely randomized for each subject. The order of block presentation for each subject was determined by Latin Square (Fisher and Yates, 1957).

<u>Results</u>

Figures 15 and 16 show the percentages of Hits and False Alarms respectively, for the images in which targets had no internal contrast. These percentages are presented as a function of modulation and blur for each of the four target ranges (1500, 2500, 3500 and 4500 meters). Figures 17 and 18 show the same data for images in which targets had internal contrast.
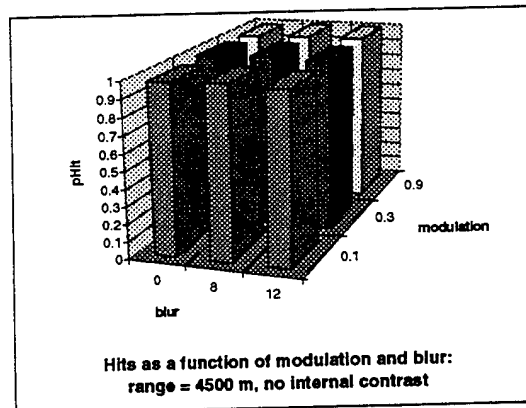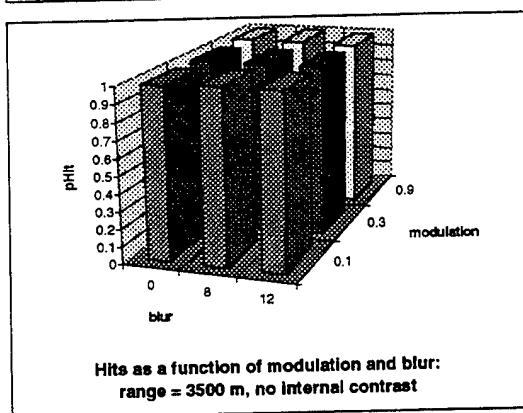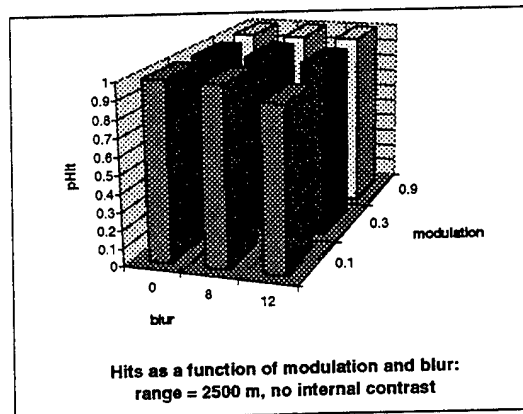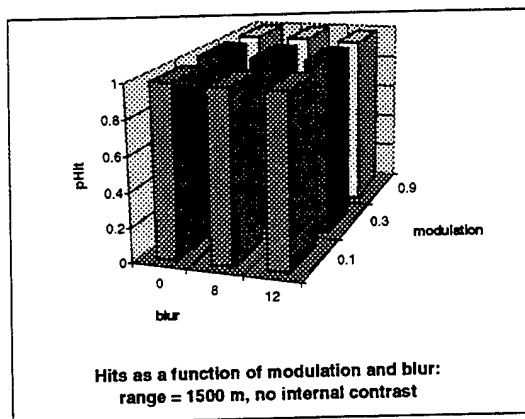
Figure 15. Hits as a function of modulation and blur; no internal contrast images.
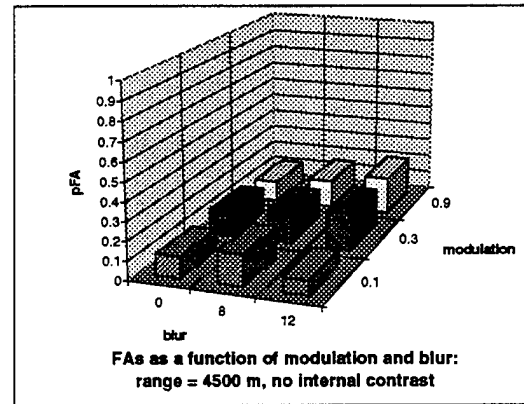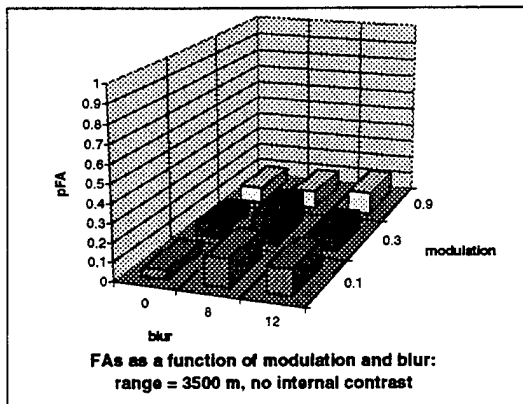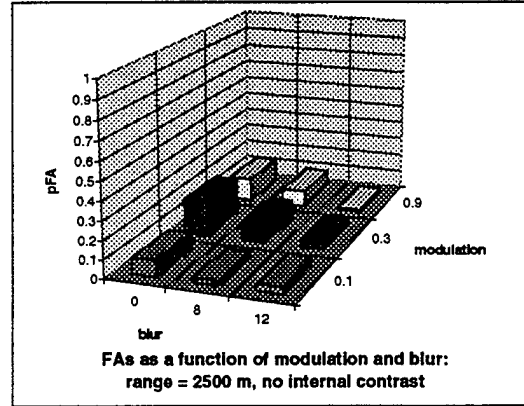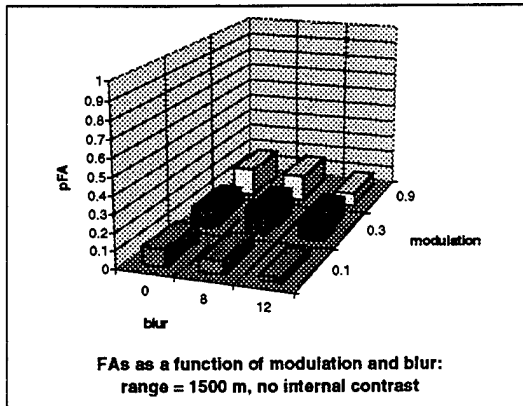
Figure 16. False alarms as a function of modulation and blur; no internal contrast images.
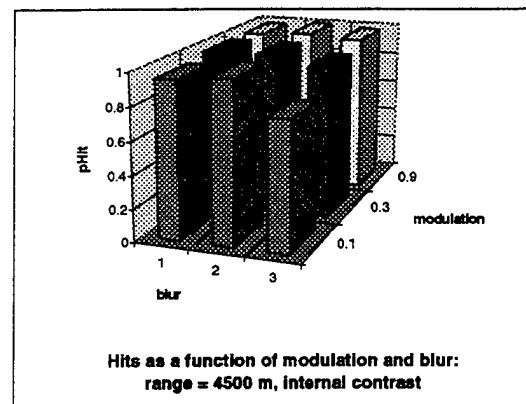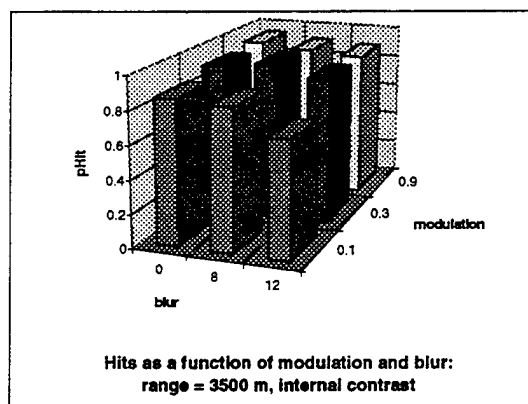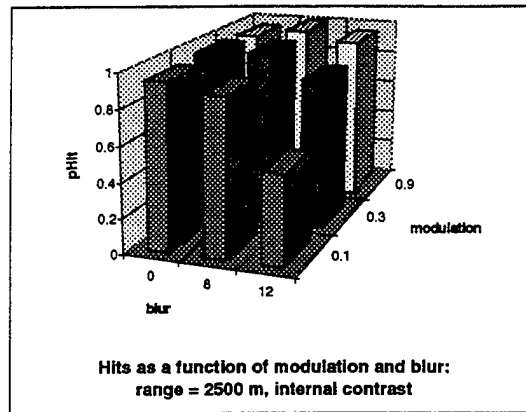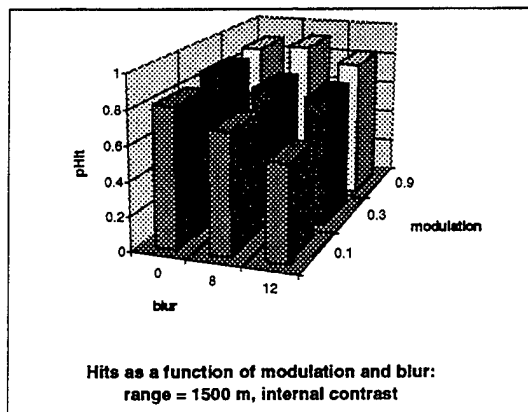
Figure 17. Hits as a function of modulation and blur; internal contrast images.
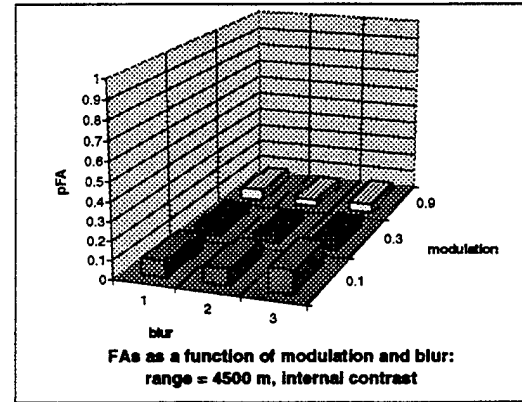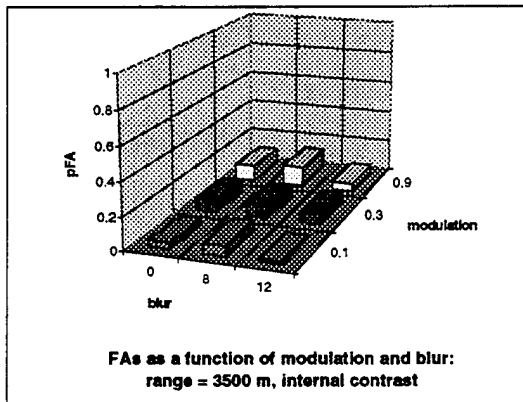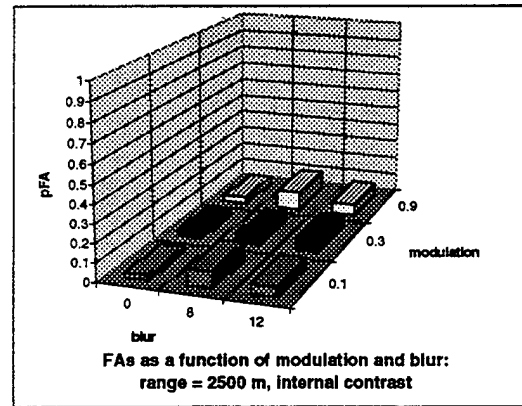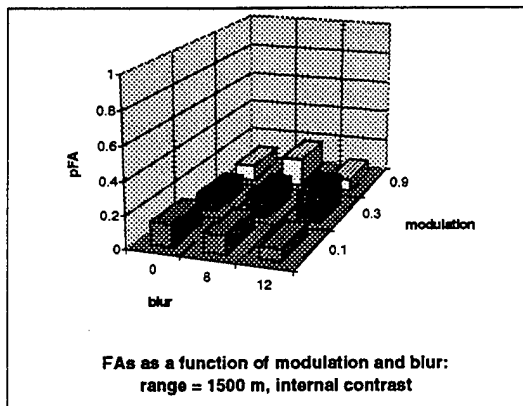
Figure 18. False alarms as a function of modulation and blur; internal contrast images.

Two five-way, full factorial, within subjects, fixed effects analyses of variance (ANOVAs) were performed using subject, target range, contrast treatment, modulation and blur as main effects and Hits Rate and false alarm rate as the dependent variables. The SAS (1982) data analysis software was utilized for these analyses. Tables 2 and 3 summarize the results of the ANOVAs.

Column one of the tables lists the experimental parameters and their interactions which may contribute to the variance in operator target detection performance. Interaction refers to the fact that scores associated with one experimental parameter may vary differently in the presence of different values of a second experimental parameter. Column two gives the degrees of freedom (df) associated with each experimental parameter. Degrees of freedom can be defined as the number of scores in a set that are free to vary; they are not fixed by some restriction placed on them. This is usually the number of scores in a set minus one.

The third column gives the sum of squares associated with each parameter. The sum of squares is a ratio of the sum of squared deviations of individual scores from a mean to the number of scores. The total sum of squares of an ANOVA model is made up of two component sums of squares. These are the sum of squares based on the variability of subjects treated alike and the sum of squares based on the variability of the treatment means. When calculating variances the sums of squares are adjusted by dividing them by the number of deviations associated with each; this is the degrees of freedom. This average sum of squares defines a variance, called a mean square.

The fourth column gives the F ratio which is formed by taking an estimate of treatment variability (mean square for the treatment) and dividing it by an estimate of the variability of subjects treated alike (mean square for subjects within the same treatment group). The latter term is called the error term of the F ratio. It provides an estimate of the experimental error influencing the differences among the treatment means. An F value of 1.0 would indicate no treatment effects. Values greater than 1.0 indicate that a treatment effect does exist. However, values greater than 1.0 can occur by chance even when no treatment effect exists. Therefore, the obtained F value is compared to a sampling distribution of F constructed by simulated experimentation in which there are no treatment effects. This sampling distribution gives the frequency with which each value of F may occur by chance. The experimenter selects a critical value of F (usually a value which has only five percent probability of occurring by chance). If the calculated value of F is greater than the critical value, then differences in scores due to experimental effects are said to be statistically significant.

The fifth column, designated as p, gives the probability that the calculated F value for that parameter might have occurred by chance when there was no real treatment effect.

The last column, designated as r^2 gives the portion of total variance in the scores that is accounted for by a particular parameter. This value is obtained by dividing the total sum of squares by the sum of squares for the parameter of interest.

36

Table 2
Detection Experiment: ANOVA Summary for Hits

Source	df	SS	F	p	r^2
Subjects (Sub)	9	9.4620			
Range (Ran)	3	4.6908	21.13	0.0001	0.0128
Sub x Ran	27	1.9984			
Treatment (Tr)	1	19.2516	46.07	0.0001	0.0526
Sub x Tr	9	3.7606			
Modulation (Mod)	2	6.4667	24.27	0.0001	0.0197
Sub x Mod	18	2.3979			
Blur (Blur)	2	5.0094	31.34	0.0001	0.0137
Sub x Blur	18	1.4385			
Ran x Tr	3	5.1644	22.19	0.0001	0.0141
Sub x Ran x Tr	27	2.0943			
Ran x Mod	6	0.7139	3.12	0.0107	0.0019
Sub x Ran x Mod	54	2.0604			
Tr x Mod	2	4.0625	28.23	0.0001	0.0111
Sub x Tr x Mod	18	1.2951			
Ran x Blur	6	1.1212	4.27	0.0014	0.0031
Sub x Ran x Blur	54	2.3615			
Tr x Blur	2	3.4406	49.52	0.0001	0.0094
Sub x Tr x Blur	18	0.6253			
Mod x Blur	4	3.0646	16.47	0.0001	0.0084
Sub x Mod x Blur	36	1.6750			
Ran x Tr x Mod	6	0.5736	2.23	0.0543	
Sub x Ran x Tr x Mod	54	2.3188			
Ran x Tr x Blur	6	0.3372	2.67	0.0244	0.0009
Sub x Ran x Tr x Blur	54	1.1385			
Ran x Mod x Blur	12	1.4007	2.79	0.0023	0.0038
Sub x Ran x Mod x Blur	108	4.5125			
Tr x Mod x Blur	4	2.1688	10.56	0.0001	0.0059
Sub x Tr x Mod x Blur	36	1.8486			
Ran x Tr x Mod x Blur	12	0.4326	0.68	0.7679	
Sub x Ran x Tr x Mod x Blur	108	3.9250			
				Σr^2	0.1573

Table 3
Detection Experiment: ANOVA Summary for False Alarms

Source	df	SS	F	p	r^2
Subjects (Sub)	9	26.1729			
Range (Ran)	3	1.8035	3.81	0.0213	0.0037
Sub x Ran	27	4.2590			
Treatment (Tr)	1	1.5340	7.31	0.0243	0.0031
Sub x Tr	9	1.8896			
Modulation (Mod)	2	0.4691	0.32	0.7337	
Sub x Mod	18	13.3990			
Blur (Blur)	2	0.5128	2.75	0.0907	
Sub x Blur	18	1.6781			
Ran x Tr	3	1.6396	3.56	0.0273	0.0034
Sub x Ran x Tr	27	4.1451			
Ran x Mod	6	0.3392	0.78	0.5856	
Sub x Ran x Mod	54	3.8899			
Tr x Mod	2	0.3983	3.27	0.0613	
Sub x Tr x Mod	18	1.0948			
Ran x Blur	6	0.8580	1.76	0.1244	
Sub x Ran x Blur	54	4.3816			
Tr x Blur	2	0.0753	0.45	0.6416	
Sub x Tr x Blur	18	1.4906			
Mod x Blur	4	0.1486	0.32	0.8644	
Sub x Mod x Blur	36	4.2125			
Ran x Tr x Mod	6	1.0323	2.77	0.0201	0.0021
Sub x Ran x Tr x Mod	54	1.0323			
Ran x Tr x Blur	6	1.7094	3.47	0.0057	0.0035
Sub x Ran x Tr x Blur	54	1.7094			
Ran x Mod x Blur	12	1.1181	1.32	0.2186	
Sub x Ran x Mod x Blur	108	1.1181			
Tr x Mod x Blur	4	0.2361	0.79	0.5389	
Sub x Tr x Mod x Blur	36	0.2361			
Ran x Tr x Mod x Blur	12	0.8500	0.94	0.5101	
Sub x Ran x Tr x Mod x Blur	108	8.5597			
				Σr^2	0.0158

The significant interaction, for both hit rate and false alarm rate, between target range and target contrast treatment, the two variables inherent to the imagery, was further examined by performing separate four-way ANOVAs for each target contrast treatment. The results of these ANOVAs are summarized in Tables 4 and 5 for the internal contrast condition and in Tables 6 and 7 for the no-internal-contrast condition.

Table 4
Detection Experiment: ANOVA Summary for Hits (Internal Contrast Images only)

Source	df	SS	F	p	r^2
Subjects (Sub)	9	12.4656			
Range (Ran)	3	9.8260	22.28	0.0001	0.0318
Sub x Ran	27	3.9691			
Modulation (Mod)	2	10.3896	28.00	0.0001	0.0328
Sub x Mod	18	3.3396			
Blur (Blur)	2	8.3688	40.48	0.0001	0.0264
Sub x Blur	18	1.8604			
Ran x Mod	6	1.1854	2.76	0.0205	0.0038
Sub x Ran x Mod	54	3.8632			
Ran x Blur	6	1.3313	4.04	0.0021	0.0042
Sub x Ran x Blur	54	2.9674			
Mod x Blur	4	5.1917	14.49	0.0001	0.0164
Sub x Mod x Blur	36	3.2250			
Ran x Mod x Blur	12	1.6417	1.97	0.0338	0.0052
Sub x Ran x Mod x Blur	108	7.4972			
				Σr^2	0.1206

Table 5
Detection Experiment: ANOVA Summary for False Alarms (Internal Contrast Images only)

Source	df	SS	F	p	r^2
Subjects (Sub)	9	8.5681			
Range (Ran)	3	1.7625	3.19	0.0396	0.0086
Sub x Ran	27	4.9736			
Modulation (Mod)	2	0.0250	0.04	0.9624	
Sub x Mod	18	5.8569			
Blur (Blur)	2	0.2250	1.38	0.2774	
Sub x Blur	18	1.4694			
Ran x Mod	6	.8833	2.74	0.0213	0.0043
Sub x Ran x Mod	54	2.9014			
Ran x Blur	6	0.4583	1.23	0.3045	
Sub x Ran x Blur	54	3.3472			
Mod x Blur	4	0.3562	0.96	0.4388	
Sub x Mod x Blur	36	3.3243			
Ran x Mod x Blur	12	0.5771	0.81	0.6392	
Sub x Ran x Mod x Blur	108	6.4090			
				Σr^2	0.0129

Table 6
Detection Experiment: ANOVA Summary for Hits (No Internal Contrast Images only)

Source	df	SS	F	p	r^2
Subjects (Sub)	9	0.7569			
Range (Ran)	3	0.0292	2.12	0.1206	
Sub x Ran	27	0.1236			
Modulation (Mod)	2	0.1396	3.55	0.0500	0.0049
Sub x Mod	18	0.3535			
Blur (Blur)	2	0.0813	3.59	0.0486	0.0027
Sub x Blur	18	0.2034			
Ran x Mod	6	0.1021	1.78	0.1205	
Sub x Ran x Mod	54	0.5160			
Ran x Blur	6	0.1271	2.15	0.0626	
Sub x Ran x Blur	54	0.5326			
Mod x Blur	4	0.0417	1.26	0.3052	
Sub x Mod x Blur	36	0.2986			
Ran x Mod x Blur	12	0.1917	1.83	0.0513	
Sub x Ran x Mod x Blur	108	0.9403			
				Σr^2	0.0076

Table 7
Detection Experiment: ANOVA Summary for False Alarms (No Internal Contrast Images only)

Source	df	SS	F	p	r^2
Subjects (Sub)	9	19.4944			
Range (Ran)	3	1.6806	4.41	0.0120	0.0060
Sub x Ran	27	3.4306			
Modulation (Mod)	2	0.8424	0.88	0.4328	
Sub x Mod	18	8.6368			
Blur (Blur)	2	0.3632	1.92	0.1749	
Sub x Blur	18	1.6993			
Ran x Mod	6	0.4882	1.01	0.4268	0.0017
Sub x Ran x Mod	54	4.3382			
Ran x Blur	6	2.1090	3.47	0.0057	0.0075
Sub x Ran x Blur	54	5.4674			
Mod x Blur	4	0.0285	0.07	0.9902	
Sub x Mod x Blur	36	3.5757			
Ran x Mod x Blur	12	1.3910	1.28	0.2410	
Sub x Ran x Mod x Blur	108	9.7826			
				Σr^2	0.0150
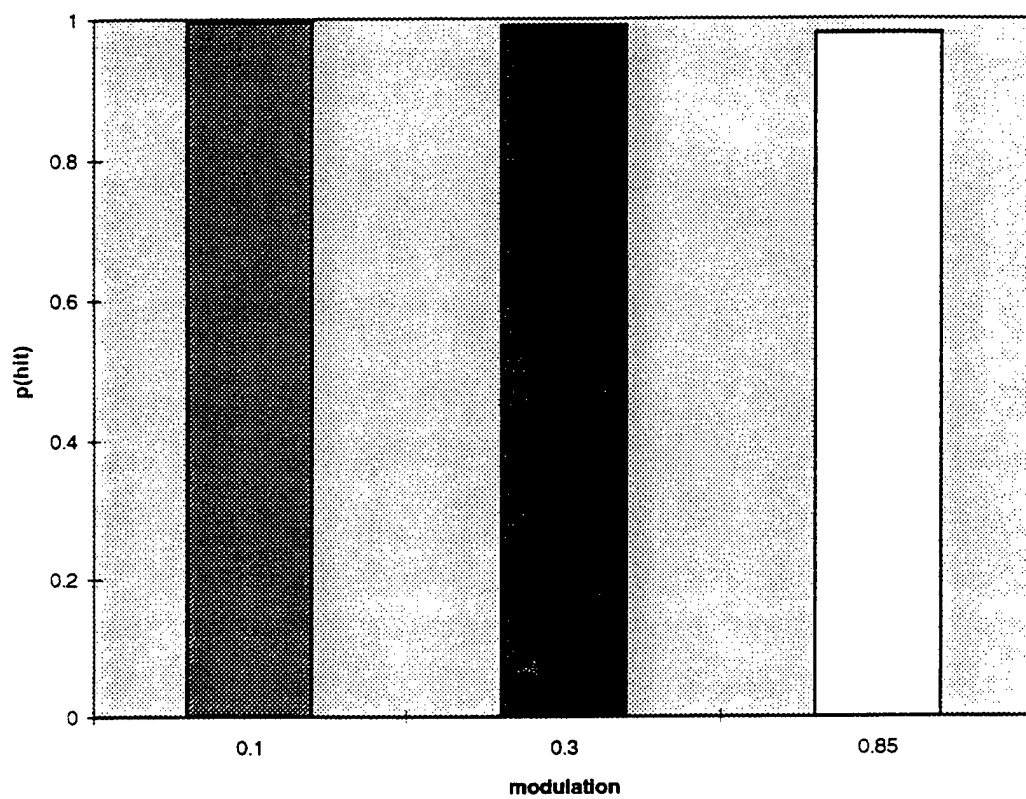
Figure 19. Effects of modulation upon hit rate; no internal contrast condition.
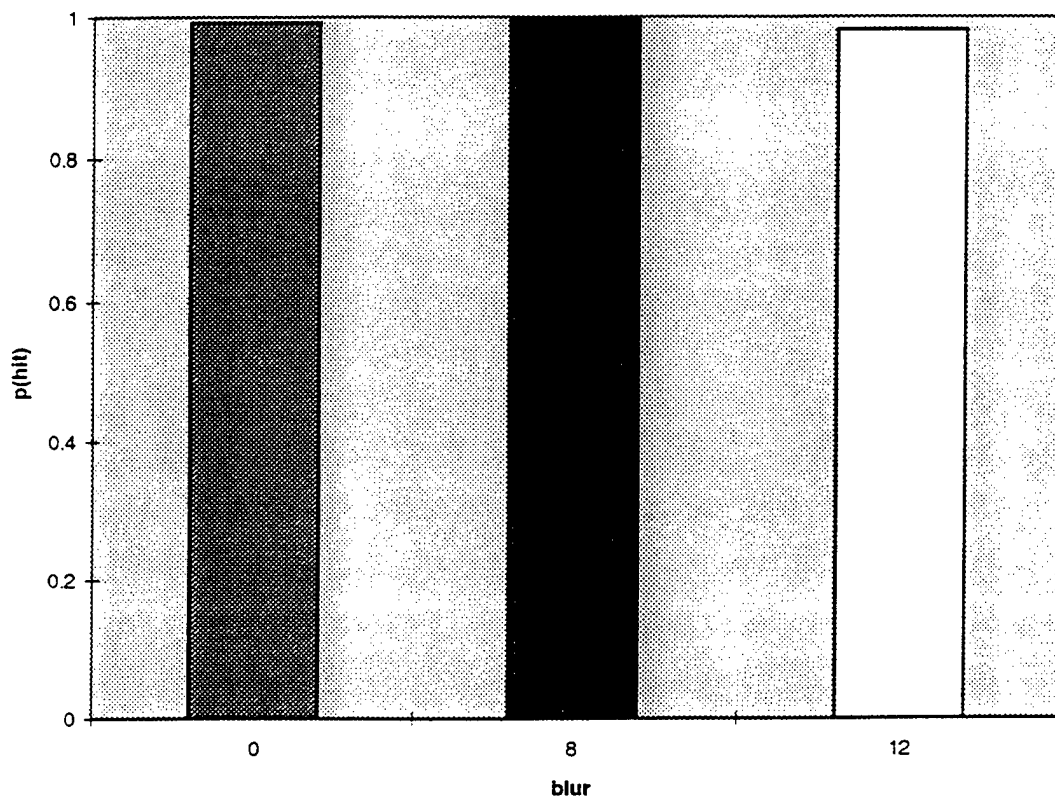
Figure 20. Effects of blur upon hit rate; no internal contrast condition.

For the no-internal-contrast treatment, target range did not have a significant effect upon hit rate. The mean hit rate across all target ranges was 0.99. The manipulations of modulation and blur were found to affect hit rate independently; there was no significant interaction between these variables. Figure 19 shows the effects of the modulation manipulations upon hit rate for this contrast condition. The mean hit rates are 0.996, 0.991, and 0.980 for the 0.85, 0.3, and 0.1 modulation conditions, respectively. Only the hit rates for the 0.85 and 0.1 modulation conditions were significantly different from one another. Figure 20 shows the effects of blur upon hit rate for this contrast condition. The mean hit rates were 0.992, 0.995 and 0.982 for the blur radius 0, 8, and 12, respectively. Only the hit rates for the blur radii 8 and 12 were significantly different from one another.

False alarm rate, however, was significantly affected by target range. In addition there were significant interactions between target range and blur. Therefore, a three-way ANOVA was performed for each range to examine the effects of the manipulations of blur for each level of target range. At the 1500 meter range and the 4500 meter range, false alarm rate was not affected by blur. The mean false alarm rates were 0.107 and 0.146 for 1500 meter and 4500 meters, respectively. At the 2500 meter and 3500 meter ranges, false alarm rate was significantly affected by blur. At the 2500 meter range only the false alarm rates for the no blur and the blur radius 12 conditions differed significantly from one another. At the 3500 meter range, only the no blur and blur radius eight conditions resulted in false alarm rates which differed significantly from one another.

For the internal contrast treatment, target range was found to interact significantly with modulation and blur in their effects upon hit rate. Therefore, separate three-way ANOVAs were performed for each target range. The results of these ANOVAs are summarized in Tables 8 - 15. Both modulation and blur were found to significantly affect hit rate at all ranges and were found to interact significantly at all ranges except 3500 meters. Blur was found to have a significant effect only at the lower modulations with fewer hits with increased blur. Modulation was found to have a significant effect only in the presence of blur. For all target ranges modulation was found to have no significant effect upon hit rate for the no blur condition. A greater effect of modulation was found to occur with increased blur. Whether the 0.3 modulation was significantly different from the 0.1 modulation seemed to vary somewhat with target range.

Although the ANOVA for false alarm rate revealed a significant interaction between target range and modulation, there are no significant effects of modulation at any of the four target ranges. The range by modulation interaction is due to the mediation of the range effect by modulation. Although significantly more False Alarms were found at the 1500 meter range that at the other ranges, this resulted only at the 0.3 and 0.85 modulations. At the 0.3 modulation, false alarm rates differed significantly for 1500 versus 2500 meters and for 1500 versus 4500 meters. At the 0.85 modulation, only the 1500 and 4500 meter ranges differed significantly in false alarm rate.

43

Table 8
Detection Experiment, Range = 1500m: ANOVA Summary for Hits
(Internal Contrast Images only)

Source	df	SS	F	p	r^2
Subjects (Sub)	9	6.2847			
Modulation (Mod)	2	3.8694	12.57	0.0004	0.0318
Sub x Mod	18	2.7694			
Blur (Blur)	2	2.1778	12.04	0.0005	0.0179
Sub x Blur	18	1.6278			
Mod x Blur	4	1.0722	3.01	0.0306	0.0088
Sub x Mod x Blur	36	3.2056			
				Σr^2	0.0585

Table 9
Detection Experiment, Range = 1500m: ANOVA Summary for False Alarms
(Internal Contrast Images only)

Source	df	SS	F	p	r^2
Subjects (Sub)	9	9.1167			
Modulation (Mod)	2	0.0778	0.21	0.8100	
Sub x Mod	18	3.2833			
Blur (Blur)	2	0.1194	0.68	0.5179	
Sub x Blur	18	1.5750			
Mod x Blur	4	0.7056	1.55	0.2090	
Sub x Mod x Blur	36				
				Σr^2	0.0000

Table 10
Detection Experiment, Range = 2500m: ANOVA Summary for Hits
(Internal Contrast Images only)

Source	df	SS	F	p	r^2
Subjects (Sub)	9	2.4944			
Modulation (Mod)	2	4.7250	21.29	0.0001	0.0680
Sub x Mod	18	1.9972			
Blur (Blur)	2	5.2583	27.61	0.0001	0.0956
Sub x Blur	18	1.7139			
Mod x Blur	4	4.2667	14.8	0.0001	0.0614
Sub x Mod x Blur	36	2.5944			
				Σr^2	0.2250

44

Table 11
Detection Experiment, Range = 2500m: ANOVA Summary for False Alarms
(Internal Contrast Images only)

Source	df	SS	F	p	r^2
Subjects (Sub)	9	0.8736			
Modulation (Mod)	2	0.0361	0.34	0.7182	
Sub x Mod	18	0.9639			
Blur (Blur)	2	0.2528	1.95	0.1705	
Sub x Blur	18	1.1639			
Mod x Blur	4	0.0889	0.30	0.8756	
Sub x Mod x Blur	36				
				Σr^2	0.0000

Table 12
Detection Experiment, Range = 3500m: ANOVA Summary for Hits
(Internal Contrast Images only)

Source	df	SS	F	p	r^2
Subjects (Sub)	9	4.6888			
Modulation (Mod)	2	2.1028	11.11	0.0007	0.0272
Sub x Mod	18	1.7028			
Blur (Blur)	2	1.1194	23.10	0.0001	0.0140
Sub x Blur	18	0.4361			
Mod x Blur	4	0.5722	1.96	0.1210	
Sub x Mod x Blur	36				
				Σr^2	0.0412

Table 13
Detection Experiment, Range = 3500m: ANOVA Summary for False Alarms
(Internal Contrast Images only)

Source	df	SS	F	p	r^2
Subjects (Sub)	9	2.0222			
Modulation (Mod)	2	0.3583	2.03	0.1599	
Sub x Mod	18	1.5861			
Blur (Blur)	2	0.2583	3.02	0.0739	
Sub x Blur	18	0.7694			
Mod x Blur	4	0.0833	0.44	0.7821	
Sub x Mod x Blur	36	1.7222			
				Σr^2	0.0000

Table 14
Detection Experiment, Range = 4500m: ANOVA Summary for Hits
(Internal Contrast Images only)

Source	df	SS	F	p	r^2
Subjects (Sub)	9	2.9667			
Modulation (Mod)	2	0.8777	10.77	0.0008	0.0245
Sub x Mod	18	0.7333			
Blur (Blur)	2	1.1444	9.81	0.0013	0.0317
Sub x Blur	18	1.0500			
Mod x Blur	4	0.9222	3.61	0.0142	0.0256
Sub x Mod x Blur	36			Σr^2	0.0818

Table 15
Detection Experiment, Range = 4500m: ANOVA Summary for False Alarms
(Internal Contrast Images only)

Source	df	SS	F	p	r^2
Subjects (Sub)	9	1.5292			
Modulation (Mod)	2	0.4361	1.34	0.2863	
Sub x Mod	18	2.9250			
Blur (Blur)	2	0.0528	0.36	0.7005	
Sub x Blur	18	1.3083			
Mod x Blur	4	0.0556	0.40	0.8073	
				Σr^2	0.0000

Discussion

The primary purpose of the detection experiment was to estimate reasonable levels of modulation and blur for the recognition study. Also of interest was the question of whether the effects of manipulation of these variables were more or less pronounced as a function of the target internal contrast condition and target range, variables inherent in the imagery.

The mean hit rate for the no-internal-contrast condition was 0.99 with a high of 1.0 and a low of 0.965 while the mean false alarm rate was 0.110 with a high of 0.158 and a low of 0.029. The mean hit rate for the internal contrast condition was 0.87 with a high of 1.0 and a low of 0.51 while the mean false alarm rate was 0.077 with a high of 0.175 and a low of 0.0125.

Surprisingly, the lowest hit rate occurred at the 1500 meter target range and the highest at the 4500 meter range for the target internal contrast condition. The lack of a significant target range effect upon hit rate for the no-internal-contrast condition was not surprising, as the target appeared as a black silhouette against the background and was easily detectable at all ranges.

The effects of modulation and blur upon hit rate were significant at all target ranges for both target contrast conditions. The effects of at least the highest and lowest conditions of modulation and blur were significantly different for all target ranges at both contrast conditions.

Few significant effects upon false alarm rate were found. The primary effect was that of target range with the fewest false alarms at the 2500 meter range for both target contrast conditions and the significantly higher false alarm rate for the 4500 meter distance in the no-internal-contrast condition. Discussions with the subjects after all studies had been run, revealed that when in doubt, subjects tended to take a conservative stance and give the "Target possibly **not** present" response rather than the "Target possibly present" response.

The narrow range of hit rate and false alarm rate variation for the no-internal-contrast condition, while statistically significant, would probably not be of much interest operationally. Also, the no-internal-contrast condition would, in most real world scenarios, be unrealistic. For these reasons, it was decided to drop the no-internal-contrast condition from further study.

Recognition Pilot Experiment

The purpose of the recognition pilot study was to examine the effects of the experimental parameters upon target recognition. Target recognition is here defined as the ability to determine that a vehicle belongs to a particular class; in this case, tanks versus armored personnel carriers versus wheeled vehicle versus artillery. Due to the large number of data points required for application of theory of signal detection to the analysis of the experimental data, it was desirable to first ascertain that the experimental parameters and the range of values selected for each were indeed appropriate. Also of interest was whether the effects of manipulation of these variables were more or less pronounced as a function of target range, a variable inherent to the imagery.

Method

Subjects: The subjects were eight of the ten trained observers who participated in the detection study.

Stimuli: The stimuli used in this study were the 32 internal contrast target image chips from the detection study. Again the images were of eight targets in four classes. All targets were imaged at the 45 degree aspect angle in the Medium background clutter condition. All four ranges were included. Only the target chips were included in this study. No background-only image chips were included. Every image displayed to the subjects contained a military vehicle.

As was done for the detection study, the images were further processed to produce three levels of image blur (image resolution) by applying gaussian filters of radii 8 and 12 in addition to the non-filtered condition. This resulted in 96 images.

At the time of presentation, each of the resultant 96 images was further processed to achieve one of three levels of image modulation (dynamic range). The three levels of modulation were 0.1, 0.3 and 0.85 as defined by the formula for Michelson Contrast. This resulted in 288 images (72 per target class, 36 per target.)

Equipment: This study was also conducted in the VIPER laboratory using the same equipment as described for the detection study.

Training: Prior to participation in the study, each subject was shown a one or two page written description of each of the eight vehicles. This description included at least one drawing or photograph of the vehicle. Also included with this material was a photograph of the image of the vehicle at each of the four ranges. These images were at the highest contrast condition with no blur. The subject was asked to read the written descriptions and briefly study the drawings and photographs.

The subject was then given a training session in the VIPER laboratory. The same 32 high contrast, no blur images were used for training. The subject was seated in the subject booth with the Electrohome display at the 76.2 (30 inch) viewing distance. As for the detection study, the medium green screen with the word "READY" was displayed. When ready to view the first practice image, the subject was instructed to move the trackball on the control panel. At this time one of the 32 images was selected at random and displayed for five seconds. This was followed by the medium green screen with the word "RESPOND" in the center. At this time the subject would press one of four buttons on the control panel to indicate to which of the four classes (Tanks, APCs, Wheeled Vehicles, Artillery) the vehicle in the image belonged. A diagram was provided above the control panel to remind the subject of which button was associated with each possible response. There was no time limit for responding. The subject was required to respond before he could go on to the next image. The image was then displayed again along with the class to which the vehicle belonged and the word "CORRECT" or "INCORRECT" to give the subject feedback on his performance. This screen was displayed for five seconds and was then followed by the "READY" screen for the next image. Any images which were classified incorrectly were flagged and shown to the subject again after all images had been shown the first time. This process continued until the subject was able to correctly classify each image. The software kept score of the percent correct on each pass. However, only the first pass was considered in determining whether training should be repeated. Subjects were required to train until they were able to complete two out of three successive practice runs with a score of 90 percent or greater on the first pass.

Immediately before beginning each experimental session, the subjects were required to do at least three practice runs with the criterion that they achieve a score or 90 percent or greater on at least two of the runs. If they failed to do so, they continued to repeat the practice until they had achieved the score of 90 percent or greater on two out of three successive runs.

Procedure: Each subject ran four sessions. For each session one of the four classes of vehicles was designated as the "target" class. The other three classes were designated as "nontargets." For a given session, all possible combinations of range, blur and modulation were presented once for each of the two vehicles in the designated "target" class, resulting in a total of 72 "target images." In addition, 72 images were presented from the three "nontarget" classes. The various conditions of range, blur and modulation were equally represented in the "nontarget" images. This resulted in 144 images per session. The order of presentation of the selected "target" class was varied for each subject by using a 4 x 4 Latin Square (Fisher and Yates, 1957) which was repeated twice for a total of eight subjects.

At the beginning of the session one of the two vehicles from the selected target class was displayed with the word "target" below the image. This image continued to be displayed until the subject pushed the "Definitely a target" button on the control box. Then the other vehicle from the target class was displayed with the word "target" until the subject again pressed the "Definitely a target" button. This was followed by each of the six vehicles from the three "nontarget" classes with the word "nontarget" displayed below the image. In this case, each image was displayed until the subject pressed the "Definitely **not** a target" button. All images were presented at the closest range, at the highest modulation and with no blur.

After the targets and nontargets had been reviewed by the subject, the data collection was begun. The procedure was the same as that employed in the detection study, except that each image was displayed for three seconds. In each block, all "targets" were presented at all ranges and at all modulation levels and all blur conditions (resolution) as were the corresponding "no target" images. Image presentation within each block was completely randomized for each subject.

Results

Two four-way, full factorial, within subjects, fixed effects analyses of variance (ANOVAs) were performed using subject, target range, modulation and blur as main effects and hit rate and false alarm rate as the dependent variables. The SAS(1982) data analysis software was utilized for these analyses. Tables 16 and 17 summarize the results of the ANOVAs.

Target range was found to have a significant effect upon both hit rate and false alarm rate. In addition, target range was found to interact with blur in their effects upon hit rate and to interact with both modulation and blur in their effects upon false alarm rate. The hit and false alarm rates for the four target ranges are given in Table 18. Only the hit rate for the 2500 meter target range is significantly different from the others. In the case of false alarm rate, only those of the 3500 and 4500 meter ranges are significantly different from one another.

Table 16
Recognition Pilot Experiment:
ANOVA Summary for Hits

Source	df	SS	F	p	r^2
Subjects (Sub)	7	11.6806			
Range (Ran)	3	2.0174	3.33	0.0392	0.0066
Sub x Ran	21	4.2396			
Modulation (Mod)	2	28.4436	49.59	0.0001	0.0928
Sub x Mod	14	4.0148			
Blur (Blur)	2	18.2405	51.74	0.0001	0.0595
Sub x Blur	14	2.4679			
Ran x Mod	6	0.5321	0.85	0.5413	
Sub x Ran x Mod	42	4.3984			
Ran x Blur	6	2.1519	4.27	0.0019	0.0070
Sub x Ran x Blur	42	3.5286			
Mod x Blur	4	8.8715	12.36	0.0001	0.0289
Sub x Mod x Blur	28	5.0243			
Ran x Mod x Blur	12	0.7674	0.64	0.8003	
Sub x Ran x Mod x Blur	84	8.3646			
				Σr^2	0.1940

Table 17
Recognition Pilot Experiment:
ANOVA Summary for False Alarms

Source	df	SS	F	p	r^2
Subjects (Sub)	7	5.0271			
Range (Ran)	3	1.3316	5.04	0.0087	0.0108
Sub x Ran	21	1.8504			
Modulation (Mod)	2	1.3250	6.35	0.0109	0.0108
Sub x Mod	14	1.4599			
Blur (Blur)	2	0.6381	4.41	0.0326	0.0052
Sub x Blur	14	1.0119			
Ran x Mod	6	0.1223	0.45	0.8396	
Sub x Ran x Mod	42	1.8966			
Ran x Blur	6	0.1933	0.55	0.7688	
Sub x Ran x Blur	42	2.4702			
Mod x Blur	4	0.5225	2.99	0.0358	0.0042
Sub x Mod x Blur	28	1.2243			
Ran x Mod x Blur	12	1.2000	2.37	0.0109	0.0098
Sub x Ran x Mod x Blur	84	3.5254			
				Σr^2	0.0408

Table 18
Hit and False Alarm Rates as a Function of Target Range

Target Range	1500m	2500m	3500m	4500m
Hit Rate	0.87	0.79	0.86	0.85
False Alarm Rate	0.041	0.072	0.025	0.085

Table 19
Recognition Pilot Experiment, Range = 1500m: ANOVA Summary for Hits

Source	df	SS	F	p	r^2
Subjects (Sub)	7	2.6649			
Modulation (Mod)	2	7.2535	29.07	0.0001	0.1089
Sub x Mod	14	1.7465			
Blur (Blur)	2	4.3368	30.46	0.0001	0.0651
Sub x Blur	14	0.9965			
Mod x Blur	4	3.4444	9.14	0.0001	0.0516
Sub x Mod x Blur	28	2.6389			
				Σr^2	0..2256

Table 20
Recognition Pilot Experiment, Range = 1500m: ANOVA Summary for False Alarms

Source	df	SS	F	p	r^2
Subjects (Sub)	7	1.2232			
Modulation (Mod)	2	0.4072	5.86	0.0142	0.0178
Sub x Mod	14	0.4863			
Blur (Blur)	2	0.2180	1.36	0.2889	
Sub x Blur	14	1.1232			
Mod x Blur	4	0.2782	1.93	0.1337	
Sub x Mod x Blur	28	1.0107			
				Σr^2	0.0178

Table 21
Recognition Pilot Experiment, Range = 2500m: ANOVA Summary for Hits

Source	df	SS	F	p	r^2
Subjects (Sub)	7	5.7778			
Modulation (Mod)	2	7.5313	15.70	0.0003	0.0793
Sub x Mod	14	3.3576			
Blur (Blur)	2	10.7188	26.45	0.0001	0.1128
Sub x Blur	14	2.8368			
Mod x Blur	4	1.5625	1.76	0.1651	
Sub x Mod x Blur	28	6.2153			
				Σr^2	0.1921

51

Table 22
Recognition Pilot Experiment, Range = 2500m:
ANOVA Summary for False Alarms

Source	df	SS	F	p	r^2
Subjects (Sub)	7	1.6380			
Modulation (Mod)	2	0.4621	5.90	0.0138	0.0118
Sub x Mod	14	0.5482			
Blur (Blur)	2	0.2005	1.88	0.1899	
Sub x Blur	14	0.7487			
Mod x Blur	4	1.0948	4.81	0.0044	0.0280
Sub x Mod x Blur	28	1.5936			
				Σr^2	0.0398

Table 23
Recognition Pilot Experiment, Range = 3500m:
ANOVA Summary for Hits

Source	df	SS	F	p	r^2
Subjects (Sub)	7	4.4288			
Modulation (Mod)	2	9.1250	29.29	0.0001	0.1311
Sub x Mod	14	2.1806			
Blur (Blur)	2	2.0417	11.31	0.0012	0.0293
Sub x Blur	14	1.2639			
Mod x Blur	4	1.8021	6.67	0.0007	0.0259
Sub x Mod x Blur	28	1.8924			
				Σr^2	0.1863

Table 24
Recognition Pilot Experiment, Range = 3500m:
ANOVA Summary for False Alarms

Source	df	SS	F	p	r^2
Subjects (Sub)	7	0.3376			
Modulation (Mod)	2	0.2093	2.16	0.1527	
Sub x Mod	14	0.6794			
Blur (Blur)	2	0.1529	3.27	0.0685	
Sub x Blur	14	0.3278			
Mod x Blur	4	0.1622	1.04	0.4042	
Sub x Mod x Blur	28	1.0916			
				Σr^2	0.0000

Table 25
Recognition Pilot Experiment, Range = 4500m:
ANOVA Summary for Hits

Source	df	SS	F	p	r^2
Subjects (Sub)	7	3.0486			
Modulation (Mod)	2	5.0660	31.42	0.0001	0.0693
Sub x Mod	14	1.1285			
Blur (Blur)	2	3.2951	25.65	0.0001	0.0451
Sub x Blur	14	0.8993			
Mod x Blur	4	2.8299	7.50	0.0003	0.0389
Sub x Mod x Blur	28	2.6424			
				Σr^2	0.1531

Table 26
Recognition Pilot Experiment, Range = 4500m:
ANOVA Summary for False Alarms

Source	df	SS	F	p	r^2
Subjects (Sub)	7	0.3376			
Modulation (Mod)	2	0.2093	2.16	0.1527	
Sub x Mod	14	0.6794			
Blur (Blur)	2	0.1529	3.27	0.0685	
Sub x Blur	14	0.3278			
Mod x Blur	4	0.1622	1.04	0.4042	
Sub x Mod x Blur	28	1.0916			
				Σr^2	0.0000

To further examine the interactions of target range with the other variables, separate three-way ANOVAs were performed for each target range for both hit rate and false alarm rate. Tables 19, 21, 23 and 25 summarize the ANOVA results for hit rate while Tables 20, 22, 24 and 26 summarize the results for false alarm rate.

Both modulation and blur were found to significantly affect hit rate at all target ranges. In addition, modulation and blur were found to interact significantly in their effects upon hit rate for all ranges except 2500 meters. Figure 21 shows the effects of modulation and blur and their interaction as a function of target range.

At the 1500 meter range, as blur was increased, the effect of modulation upon hit rate became greater. For the no blur condition, modulation had no significant effect. The mean hit rate across all modulations was 0.958. For the blur radius 8 condition, the 0.1 and 0.85 modulations differed significantly in their effects upon hit rate. The 0.1 modulation was found to differ from both 0.3 and 0.85 for the blur radius 12 condition. At this range, the effect of blur was significant only at the lowest modulation, where the no blur and the blur radius 8 conditions both differed from the blur radius 12 condition in their effects upon hit rate.
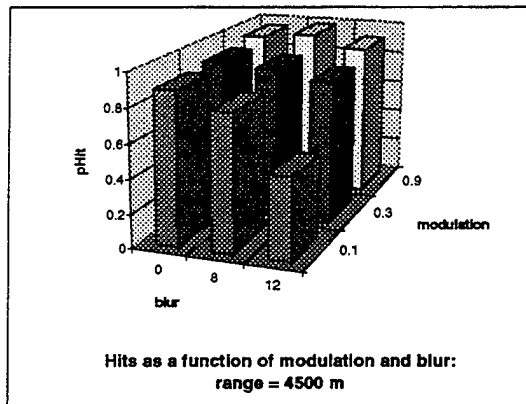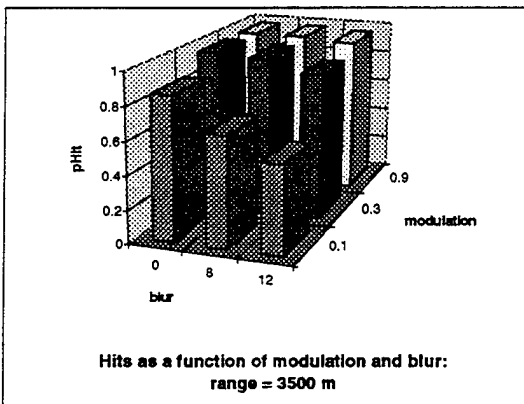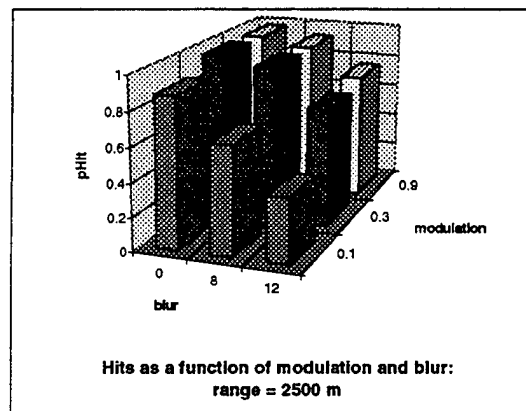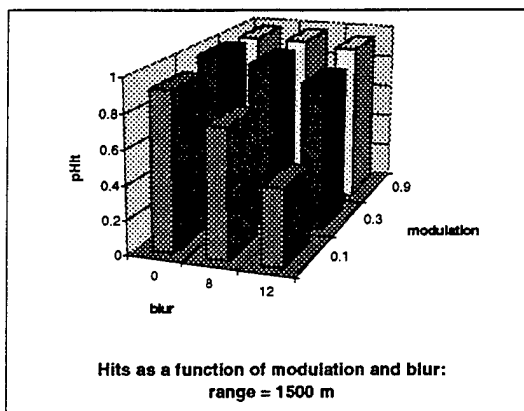
Figure 21. Effects of modulation and blur upon hit rate at each target range.

At the 2500 meter range, where modulation and blur did not interact, the 0.1 modulation differed significantly in its effects upon hit rate from both the 0.3 and the 0.85 modulations. The no blur and the blur radius 8 conditions both differed significantly from the blur radius 12 condition.

At the 3500 meter range, the effect of modulation became greater with increasing blur. The 0.1 modulation differed from 0.3 and 0.85 at all levels of blur. Conversely, the effect of blur was found to be greatest at the lowest modulation, where the no blur condition differed significantly from either of the blur conditions in its effects upon hit rate. At 0.3 modulation, the no blur condition differed only from the blur radius 12 condition; and at the 0.85 modulation, there was no effect of blur at all.

The same interaction pattern is evident at the 4500 meter range. As blur was increased, the effect of modulation became greater. Modulation had no significant effect upon hit rate at the no blur condition. At the blur radius 8, 0.1 modulation differed from 0.85. At blur radius 12, 0.1 modulation differed from both 0.3 and 0.85. Blur had a significant effect upon hit rate only at the lowest modulation where the no blur condition differed from both of the blur conditions.

For false alarm rate, modulation was found to have a significant effect at the 1500 meter range, and both modulation and the interaction of modulation and blur were found to have significant effects at the 2500 meter range. Neither modulation nor blur were found to significantly affect false alarm rate at the 3500 and the 4500 target ranges.

At the 1500 meter range, false alarm rates were 0.077, 0.031 and 0.015 for the 0.1, 0.3 and 0.85 modulations, respectively. Only the 0.1 modulation differed from 0.85 in their effects upon false alarm rate.

At the 2500 meter range, the effect of modulation was found only with blur; modulation had no effect upon false alarm rate for the no blur condition. Blur was found to have a significant effect only at the highest modulation where more false alarms occurred for blur radius 12 than for blur radius 8.

Discussion

The mean hit rate for the 2500 meter target range was significantly lower (0.79) than that of the other three target ranges (0.87, 0.86 and 0.85 for 1500, 3500 and 4500 meters, respectively). However, this was due to the low hit rates at the more difficult conditions of modulation and blur (0.375 vs 0.453, 0.531 and 0.484). The hit rate at the less difficult conditions differed little from that at other target ranges (0.968 vs 0.984, 0.968 and 0.984).

The modulation by blur interaction effect upon hit rate at the 1500, 3500 and 4500 meter ranges was not surprising. At all ranges, the effect of modulation was greater with increased blur. Conversely, the effect of blur was greater with decreased modulation. The same trend was evident at the 2500 meter range, although the interaction was not

55

statistically significant. This may be due to the more pronounced effect of blur at all modulations.

As was the case for the detection experiment, there were few significant effects upon false alarm rate. In fact, at the 3500 and 4500 meter target ranges, there were no significant effects for modulation or blur. The mean false alarm rates for these two target ranges differed significantly from each other. As there were no other significant effects at these ranges, the difference must be attributed to target range itself. There were no other significant differences among the mean false alarm rates at the four target ranges. The widest range of false alarm rates again occurred at the 2500 meter target range (0 to 0.176) and seems to be purely an effect of modulation.

Due to the paucity of interesting effects as a function of target range, it was decided to carry only one target range into the primary recognition experiment. The 3500 and 4500 meter ranges were eliminated due to the lack of significant effects for false alarm rate. The 2500 meter target range was selected for further experimentation, because the effects of modulation and blur upon both hit rate and false alarm rate were somewhat more pronounced at this range than at the 1500 meter range.

Recognition Experiment

The purpose of the recognition study was to apply theory of signal detection methods in evaluating the effects of modulation, blur and noise upon the target recognition task. These methods allow operator hit rates and false alarm rates to be combined into a single measure of perceptual sensitivity, d'. In addition, Receiver Operating Characteristic curves are generated which show graphically the effects of operator decision criterion upon target recognition performance. A thorough understanding of the interaction of the effects of blur, modulation and noise upon operator target recognition performance provides information for system design trade-offs.

Method

Subjects: The subjects were the same eight trained observers who had participated in the previous studies.

Stimuli: The stimuli used for this experiment were the eight internal contrast, range = 2500 meters, stimuli from the recognition pilot experiment. Again, the images were of eight targets in four classes. All targets were imaged at the 45 degree aspect angle and the Medium background clutter condition. Every image contained a military vehicle; no background-only image chips were included.

The same three levels of image blur were used as for the two pilot studies. This resulted in 24 images.

At the time of presentation, each of the resultant 24 images was further processed to achieve one of nine combinations of three levels of modulation and three static noise conditions. The three levels of modulation were again 0.1, 0.3 and 0.85 as defined by the formula for Michelson Contrast. In addition to a no-noise condition, two levels of static noise were created. Gaussian noise distributions of 512^2 pixels, having the same mean as the image and standard deviations of 6.0 and 10.87, were created in a separate image channel. At the time of image presentation, a single pixel of the noise distribution was selected at random to correspond with the upper left corner of the image. One half of each noise pixel intensity value was then added to one half of the corresponding image pixel intensity value to produce the "noisy" image. This resulted in 216 images (54 per target class, 27 per target). Figures 22 and 23 show the M-1 tank at all combinations of modulation and blur with the low and high levels of noise respectively. (The no noise condition is shown in Figure 12.)

The normalized least squares error (NLSE) was used as a measure of the difference between the no noise image and the corresponding noisy images. The NLSE is defined by Pratt (1991) as

$$NLSE = \frac{\sum_{j=1}^{J} \sum_{k=1}^{K} |F(j,k) - G(j,k)|^2}{\sum_{j=1}^{J} \sum_{k=1}^{K} |F(j,k)|^2}$$

where:

$F(j, k)$ is the no noise image

$G(j, k)$ is the noisy image.

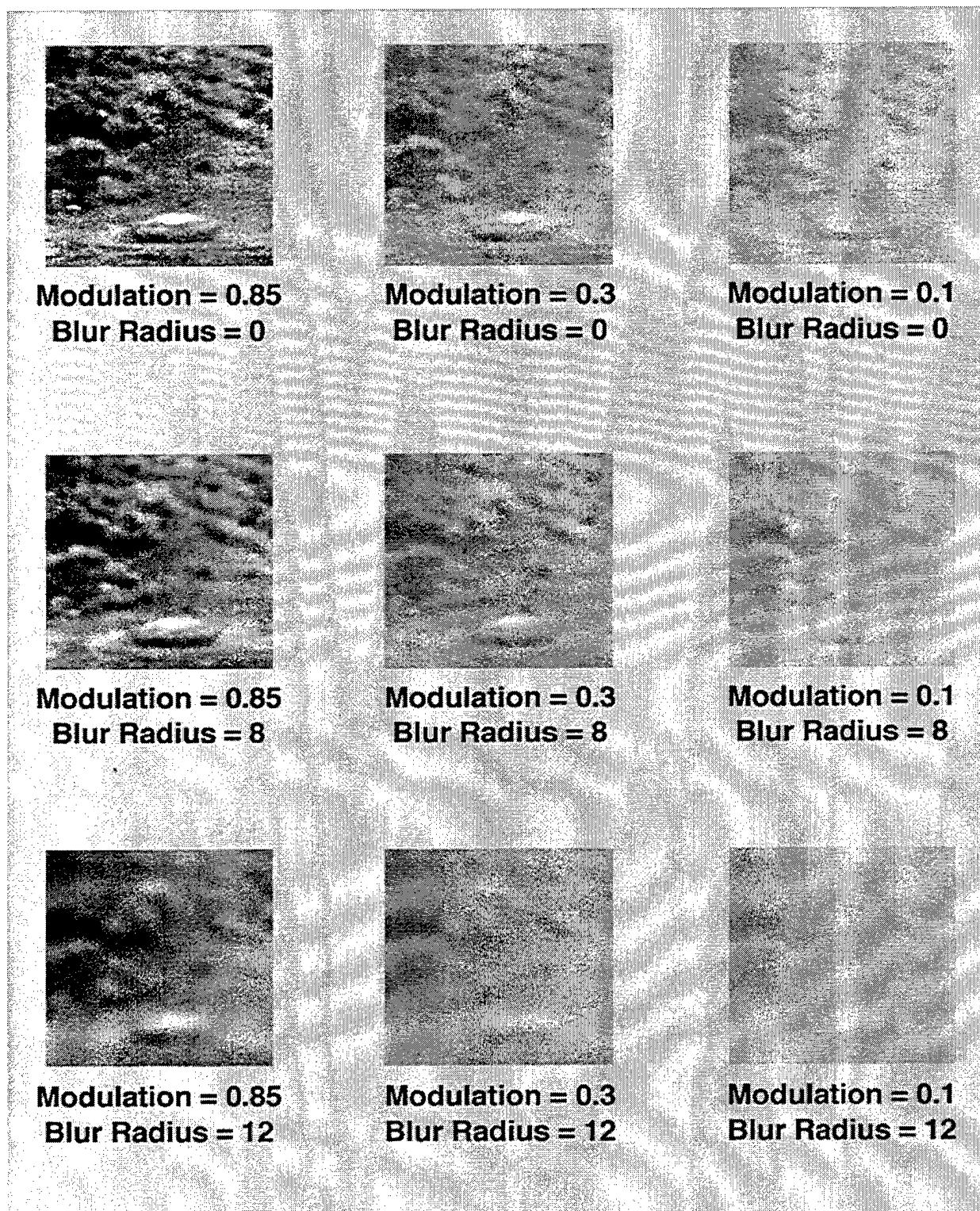The average NLSE for the low noise images was 0.014, while that for the high noise images was 0.445.

Figure 22. M-1 tank at all combinations of modulation and blur. Range = 2500 meters; low noise.
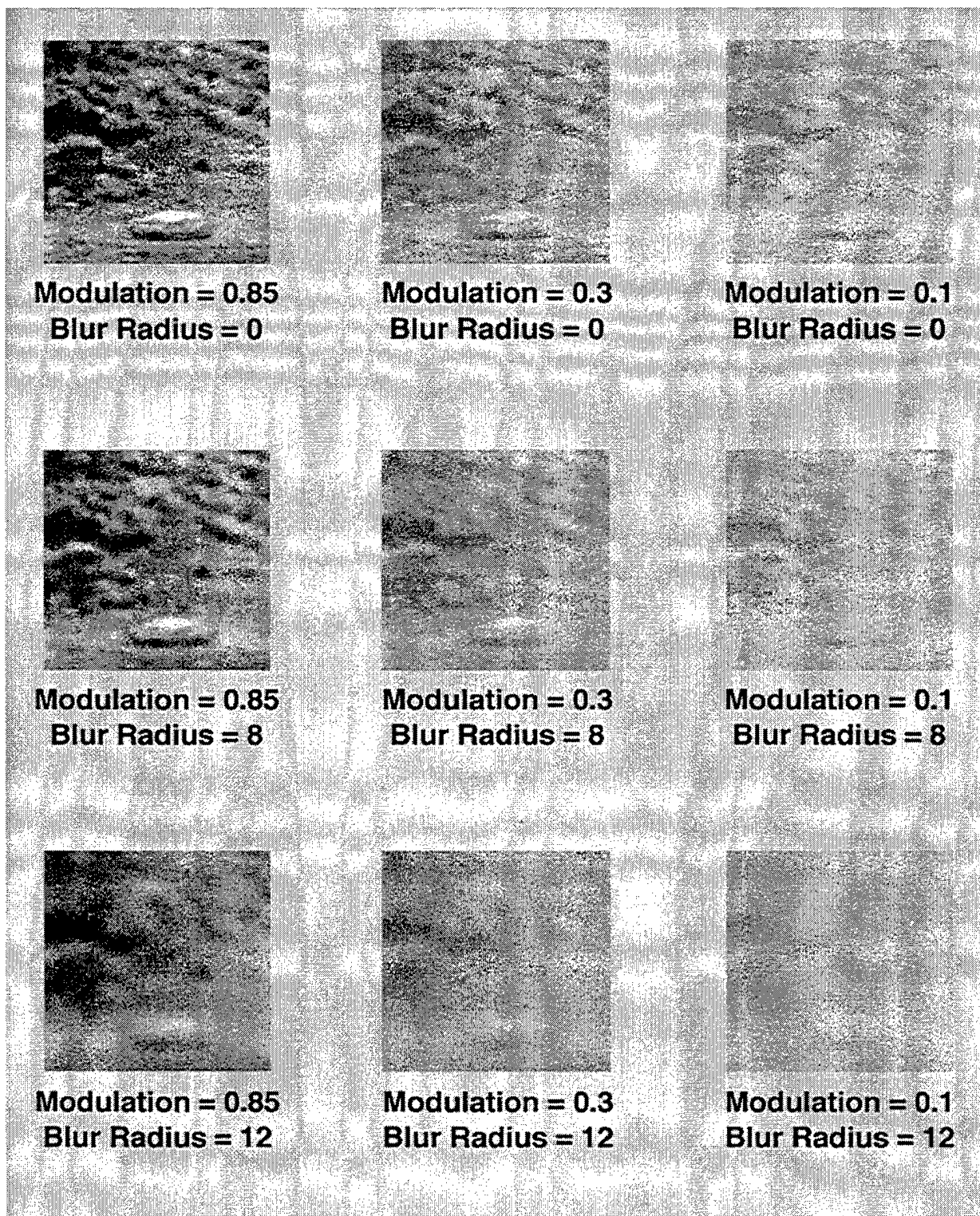
Figure 23. M-1 tank at all combinations of modulation and blur. Range = 2500 meters; high noise.

Equipment: This experiment was conducted in the VIPER laboratory using the same equipment as described for the pilot experiments.

Training: Training was the same as the recognition pilot experiment with the exception that subjects trained on only the 2500 meter target range images. A practice run consisted of 32 images; each of the eight target images was repeated four times at the 2500 meter target range. The training criterion remained the same as the pilot experiment; two out of three successive practice runs with a score of 90 percent or greater on the first pass.

Immediately before beginning each experimental session, the subjects were required to do at least one practice run with the criterion score of 90 percent or greater on the first pass. If they failed to do so, they continued to repeat the practice until they had achieved the score of 90 percent or greater on two out of three successive runs.

Procedure: Each subject ran eight two-part sessions. For each session one of the four classes of vehicles was designated as the "target" class. The other three classes were designated as "nontargets." For a given session, all possible combinations of noise, blur and modulation were presented four times for each of the two vehicles in the designated "target" class, resulting in a total of 216 "target images." In addition, 216 images were presented from the three "nontarget" classes. The various conditions of noise, blur and modulation were equally represented in the "nontarget" images. This resulted in 432 images per session. The order of presentation of the selected "target" class was varied for each subject by using paired 4 x 4 Latin Square (Fisher and Yates, 1957) which were repeated twice for a total of eight subjects.

The experimental procedure was the same as for the recognition pilot experiment. Each subject viewed each combination of noise, blur and modulation 64 times for target images and 64 times for nontarget images. Each individual vehicle was viewed eight times as a target and eight times as a nontarget by each of the eight subjects at all 27 combinations of noise, modulation and blur. This resulted in a total of 27,648 stimulus presentations (3456 per subject).

Results

Due to an error in the software for applying the static noise to images, it was necessary to discard the data for all conditions including noise. The entire study was rerun with the corrected noise conditions. The results from all images associated with the "no noise" condition were retained. This resulted in 128 observations per subject for all conditions not including noise and 64 data points per subject for all conditions including noise. Therefore the data were analyzed using the SAS (1982) general linear models (GLM) procedure for analysis of variance (ANOVA). The GLM procedure adjusts for unequal numbers of observations among conditions being compared.

Two four-way, within subjects, fixed effects ANOVAs were performed using subject, modulation, blur and noise as main effects and hit rate and false alarm rate as the dependent variables. Tables 27 and 28 summarize the results of the ANOVAs.

Noise, modulation and blur were each found to have significant effects upon both hit rate and false alarm rate. They were also found to interact with one another significantly in their effects upon hit rate and false alarm rate. These interactions are depicted graphically in Figures 24 and 25. Further one-way ANOVAs were performed to examine the interaction of the three variables. Post hoc analyses revealed that at no noise or low noise and modulation of 0.1, hit rate differed significantly at all levels of blur. For all other combinations of noise and modulation, the no blur condition and the blur radius 8 condition did not differ significantly from one another in their effects upon hit rate. However the blur radius 12 condition resulted in significantly lower hit rate than either of the other blur conditions. Only at the low or high noise condition coupled with blur radius 12 did all levels of modulation have significantly distinct effects upon hit rate. Otherwise, with no noise or less blur, the 0.3 and 0.85 modulations did not differ significantly in their effects upon hit rate. Finally, for all levels of blur: (1) the three levels of noise had significantly different effects upon hit rate at the lowest modulation, (2) the no noise and low noise conditions did not differ significantly at modulation = 0.3, and (3) none of the noise levels were significantly different from one another at the highest modulation. Noise was found to have little or no effect upon false alarm rate at very low modulation or in the presence of increased blur.

For each subject and each experimental condition, the theory of signal detection measure of sensitivity, d', and measure of decision criterion, Beta, were calculated. Two additional ANOVAs were then performed using subject, modulation, blur and noise as main effects and d' and Beta as the dependent variables. The results of these ANOVAs are summarized in Tables 29 and 30.

As was the case for hits and false alarms, noise, modulation and blur each had significant effects on d' and the three variables interacted with one another in their effects upon d'. This interaction is depicted graphically in Figure 26. Further one-way ANOVAs were performed to examine the interaction of the three variables. The effects of the modulation by blur by noise interaction upon d' closely follow those for hit rate. That is, the modulation by blur interaction becomes more pronounced in the presence of increased noise.

Beta was found to be affected significantly only by the interaction between modulation and blur. Figure 27 shows Beta as a function of modulation and blur. Further examination of this interaction revealed that of the nine combinations of modulation and blur, only the modulation = 0.1 with no blur and the modulation = 0.3 and blur radius 12 conditions resulted in Beta values which were significantly higher than some (but not all) of the other conditions.

Table 27
Recognition Experiment: ANOVA Summary for Hits

Source	df	SS	F	p	r^2
Subjects (Sub)	7	37.6675			
Noise (Noi)	2	162.9819	46.10	0.0004	0.0555
Sub x Noi	14	24.7459			
Modulation (Mod)	2	682.7816	125.86	0.0001	0.2324
Sub x Mod	14	29.9561			
Blur (Blur)	2	153.1540	242.48	0.0001	0.0521
Sub x Blur	14	5.0039			
Noi x Mod	4	131.6090	46.58	0.0001	0.0448
Sub x Noi x Mod	28	19.7790			
Noi x Blur	4	0.9238	1.35	0.2770	
Sub x Noi x Blur	28	4.7975			
Mod x Blur	4	39.5106	47.92	0.0001	0.0135
Sub x Mod x Blur	28	4.1064			
Noi x Mod x Blur	8	34.4417	18.75	0.0001	0.0117
Sub x Noi x Mod x Blur	56	12.8577			
				Σr^2	0.4100

Table 28
Recognition Experiment: ANOVA Summary for False Alarms

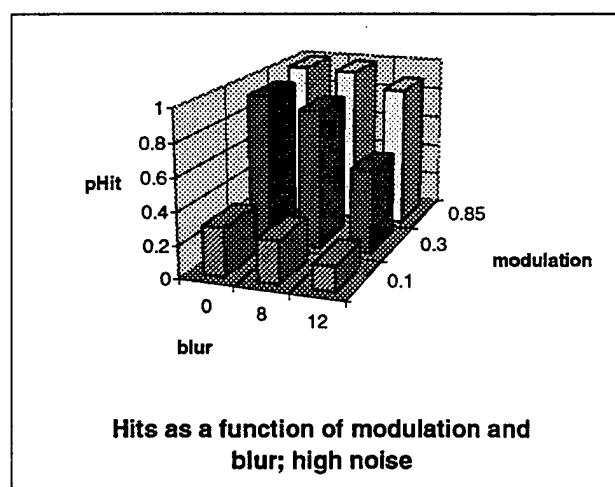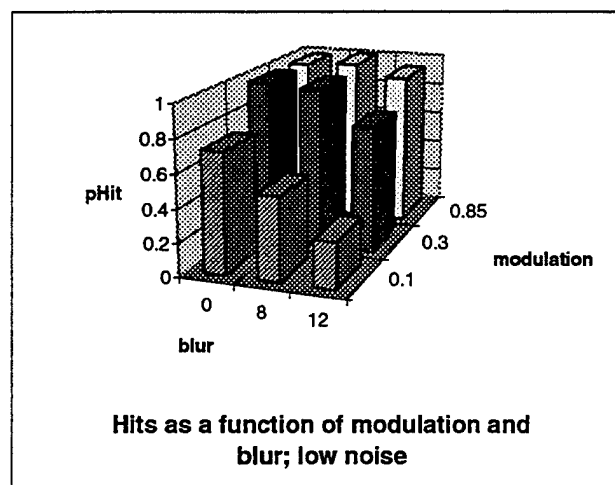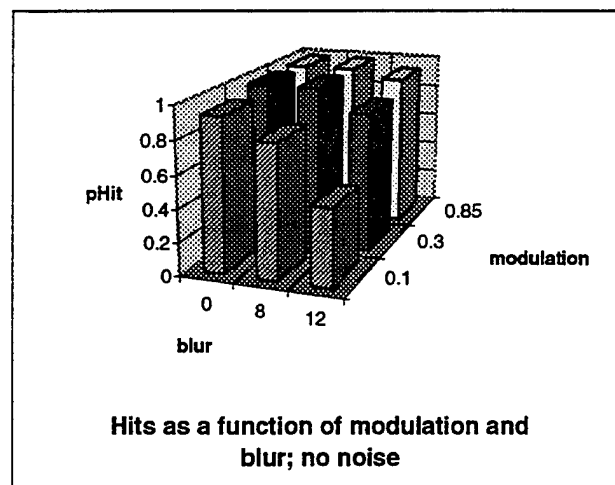| Source	df	SS	F	p	r^2
Subjects (Sub)	7	4.7396			
Noise (Noi)	2	3.9819	6.04	0.0129	0.0045
Sub x Noi	14	4.7530			
Modulation (Mod)	2	15.9333	30.73	0.0001	0.0156
Sub x Mod	14	2.5424			
Blur (Blur)	2	6.3033	34.43	0.0001	0.0071
Sub x Blur	14	1.3684			
Noi x Mod	4	1.1975	2.55	0.0613	
Sub x Noi x Mod	28	3.1896			
Noi x Blur	4	0.2150	0.97	0.4374	
Sub x Noi x Blur	28	1.5164			
Mod x Blur	4	0.8612	2.39	0.0749	
Sub x Mod x Blur	28	3.1482			
Noi x Mod x Blur	8	2.4998	4.54	0.0003	0.0028
Sub x Noi x Mod x Blur	56	3.8529			
				Σr^2	0.0300

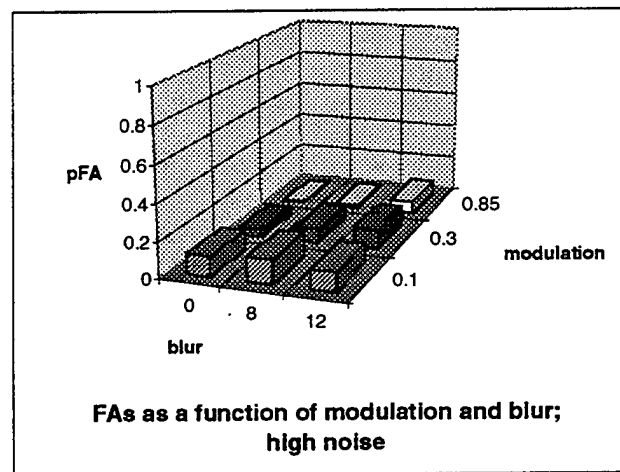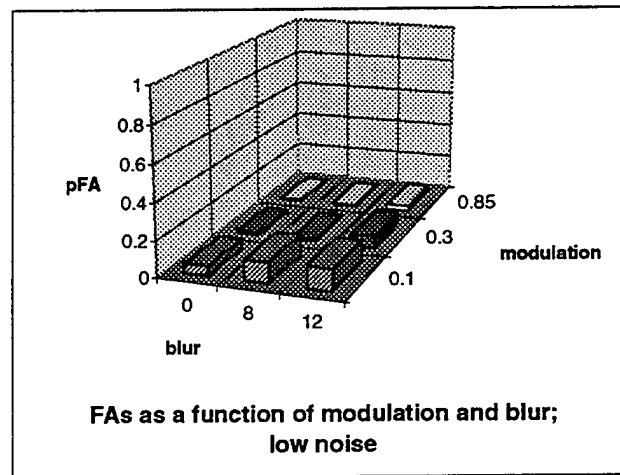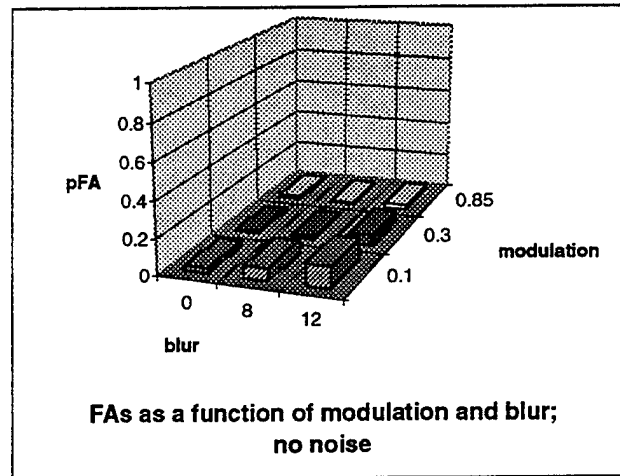Figure 24. Hit rate as a function of noise, modulation and blur.

Figure 25. False alarm rate as a function of noise, modulation and blur

Table 29

Recognition Experiment: ANOVA Summary for d'

Source	df	SS	F	p	r^2
Subjects (Sub)	7	11.6269			
Noise (Noi)	2	57.6332	55.75	0.0001	0.1391
Sub x Noi	14	7.2360			
Modulation (Mod)	2	269.1533	401.13	0.0001	0.5204
Sub x Mod	14	4.6969			
Blur (Blur)	2	98.7733	317.46	0.0001	0.1672
Sub x Blur	14	2.1779			
Noi x Mod	4	19.3949	41.30	0.0001	0.0491
Sub x Noi x Mod	28	3.2875			
Noi x Blur	4	0.8847	1.79	0.1590	
Sub x Noi x Blur	28	3.4608			
Mod x Blur	4	8.0809	13.75	0.0001	0.0143
Sub x Mod x Blur	28	4.1154			
Noi x Mod x Blur	8	10.6063	9.05	0.0001	0.0274
Sub x Noi x Mod x Blur	56	8.2003			
				Σr^2	0.9195

Table 30
Recognition Experiment: ANOVA Summary for Beta

| Source	df	SS	F	p	r^2
Subjects (Sub)	7	77.9409			
Noise (Noi)	2	2.7741	0.44	0.6515	
Sub x Noi	14	43.9417			
Modulation (Mod)	2	8.6473	3.73	0.0504	
Sub x Mod	14	16.2466			
Blur (Blur)	2	4.5190	0.91	0.4263	
Sub x Blur	14	34.8923			
Noi x Mod	4	11.8279	1.76	0.1655	
Sub x Noi x Mod	28	47.0995			
Noi x Blur	4	3.0249	1.05	0.4017	
Sub x Noi x Blur	28	20.2585			
Mod x Blur	4	29.5606	3.89	0.0123	0.0424
Sub x Mod x Blur	28	53.1492			
Noi x Mod x Blur	8	16.4593	1.10	0.3762	
Sub x Noi x Mod x Blur	56	104.6039			
				Σr^2	0.0424
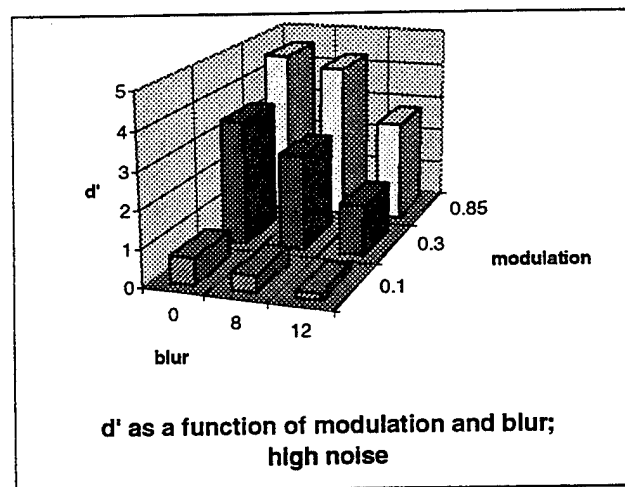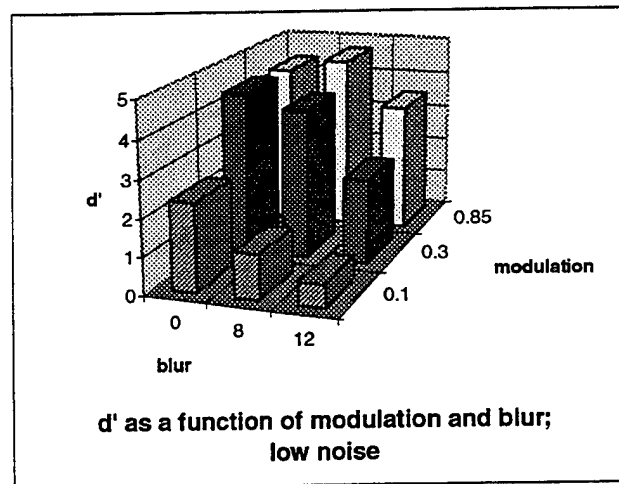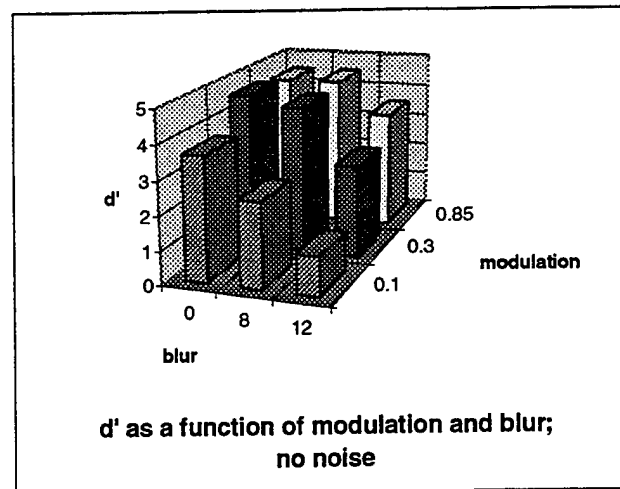
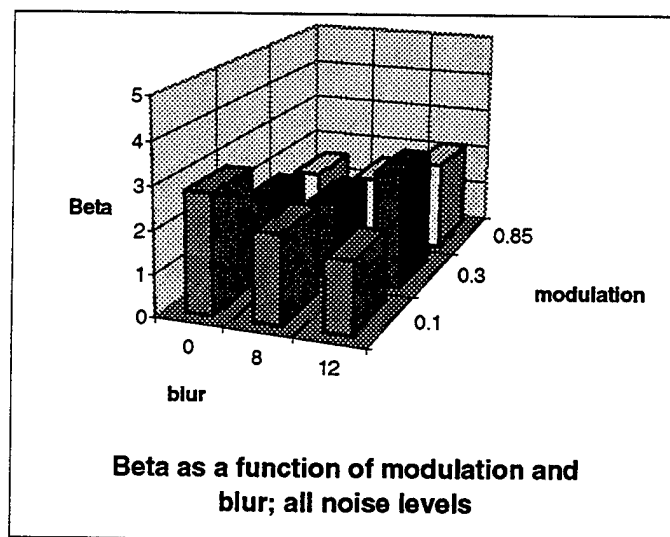Figure 26. d' as a function of noise, modulation and blur.

Figure 27. Beta as a function of modulation and blur.

Discussion

While modulation, blur and noise each has its individual effects upon hit and false alarm rates and d', the interactions between the three variables in their effects upon hit and false alarm rates is the really interesting and useful finding of this study. These results indicate that in system design, there are trade-offs which can be made.

The paucity of significant effects for Beta indicates that subjects were able to maintain a constant decision criterion across all experimental conditions. Only the interaction between blur and modulation had the effect of causing subjects to shift their decision criterion somewhat. Only for the two cases of very low modulation with no blur and moderate modulation with high blur did they adopt a somewhat more stringent decision criterion. For all other cases the decision criterion remained constant.

The implications for system design are even more evident when one views the Receiver Operating Characteristic (ROC) curves which were generated as a result of the confidence rating procedure employed in this study. Figures 28 thru 30 present the ROC curves for all combinations of modulation, noise and blur investigated in this study.

The ROC curves show the probability of hits (vertical axis) and false alarms (horizontal axis) at five different confidence levels. The first point to the right of the 0,0 anchor indicates the probability of hits versus false alarms if only those target presentations for which the subject responded "Definitely a target" were treated as hits and all others treated as correct rejections (if nontargets) or false alarms (if targets). The next point to the right indicates the probabilities of hits and false alarms if all targets for which the subject responded either "Definitely a target" or "Probably a target" were treated as hits and all others treated as correct rejections or false alarms. The third, or center, point indicates the probabilities of hits and false alarms is all targets for which the subject responded "Definitely a target," "Probably a target" or "Possibly a target" were treated as hits and those for which the subject responded "Possibly not a target," "Probably not a target" or "Definitely not a target" are treated as correct rejections or false alarms. The fourth point to the right of the 0,0 anchor indicates the probabilities of hits versus false alarms if all targets for which the subject responded "Definitely a target," "Probably a target" or "Possibly a target" and "Possibly not a target" were treated as hits and all others treated as correct rejections or false alarms. The fifth point to the right indicates the probabilities of hits versus false alarms if all targets except those for which the subject responded "Definitely not a target" are treated as hits.

Clearly, as we move from left to right on the ROC curve we observe the effects of changing decision criterion. The first point shows the effect of a very strict decision criterion where the observer must be able to say "Definitely a target" in order for a hit to be declared. Each successive point to the right allows for a more lax decision criterion until, finally, anything which the observer cannot declare to be "Definitely not a target" is treated as a target declaration.
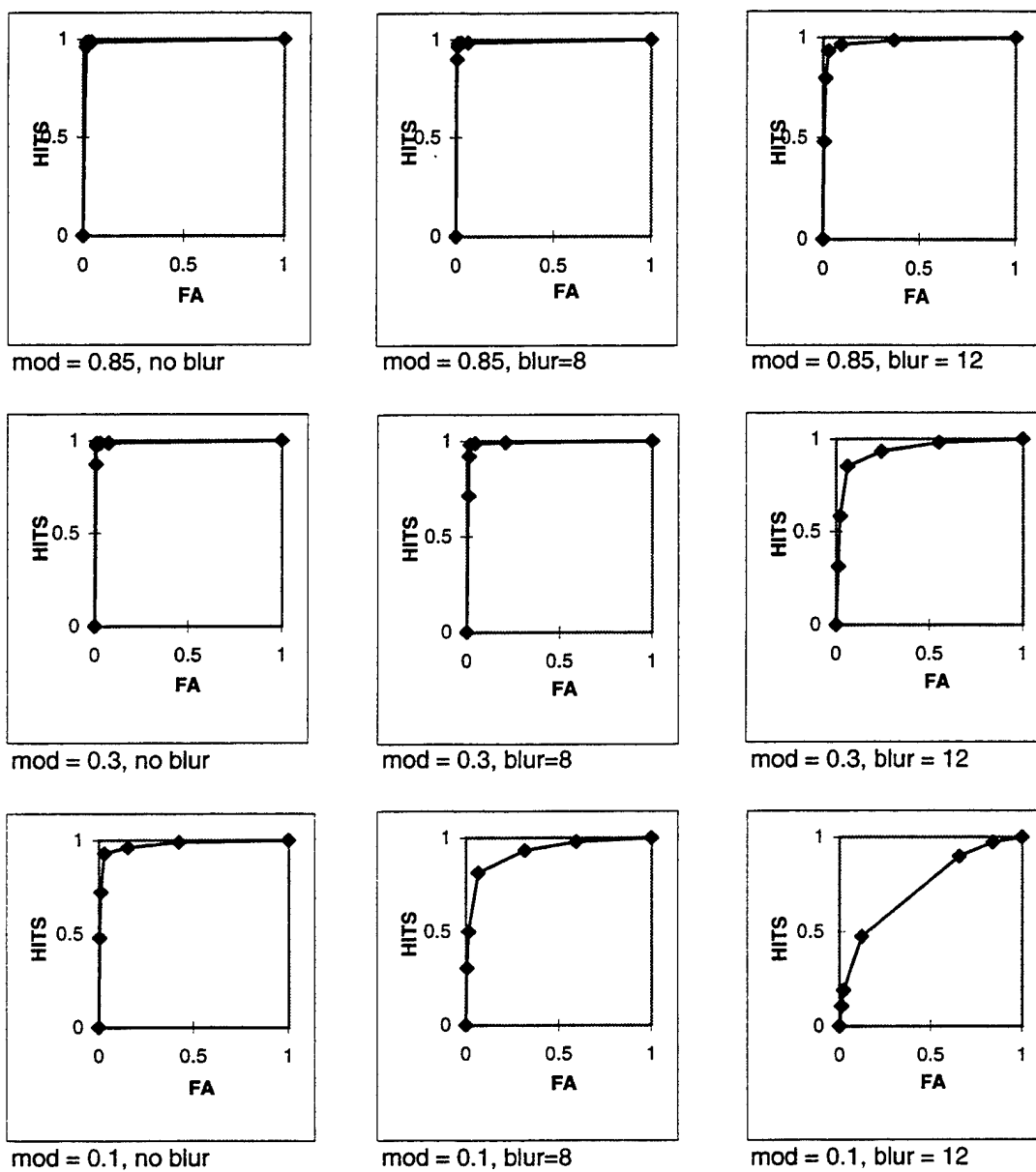
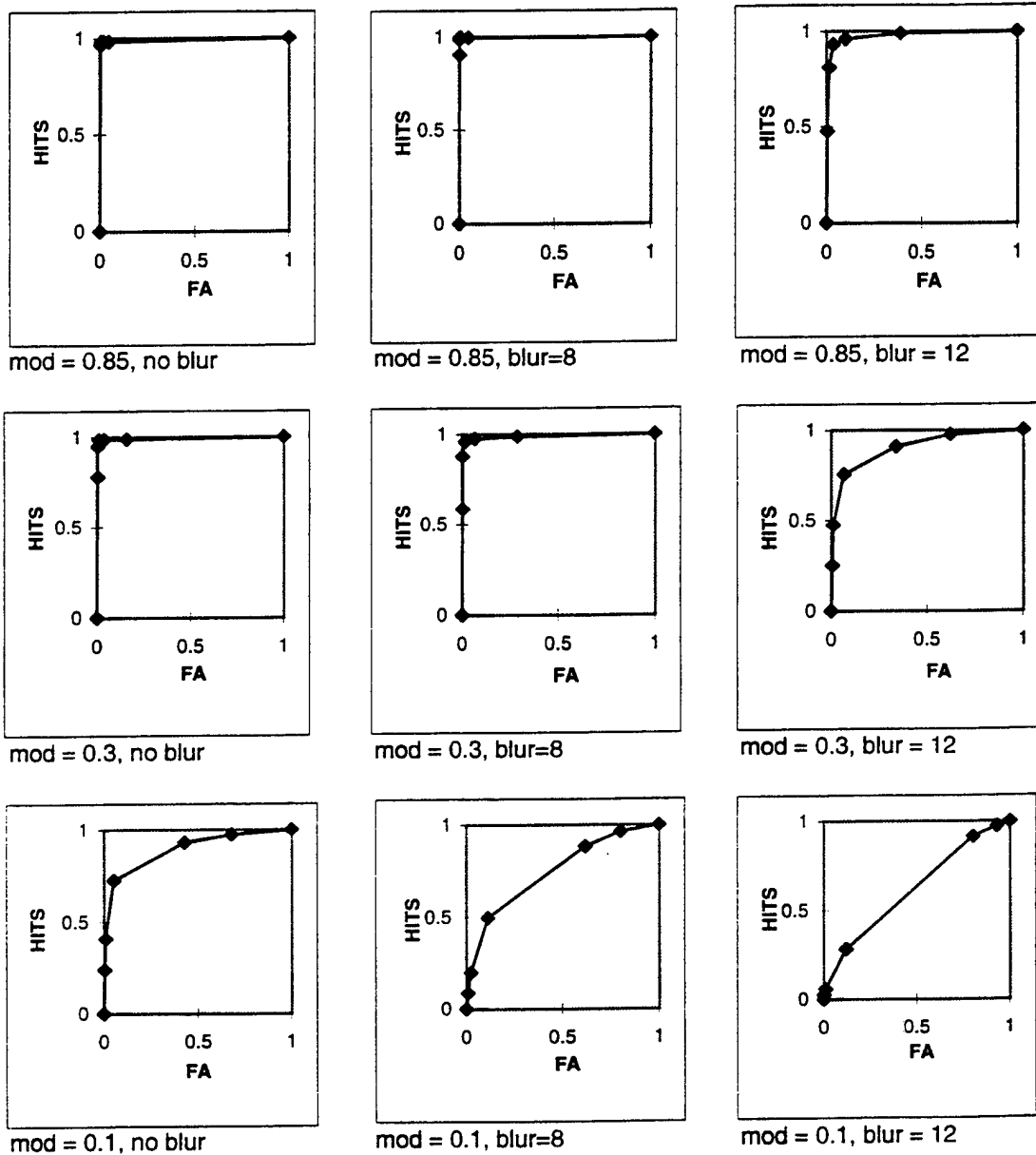Figure 28. ROC curves as a function of modulation and blur; no noise.

69

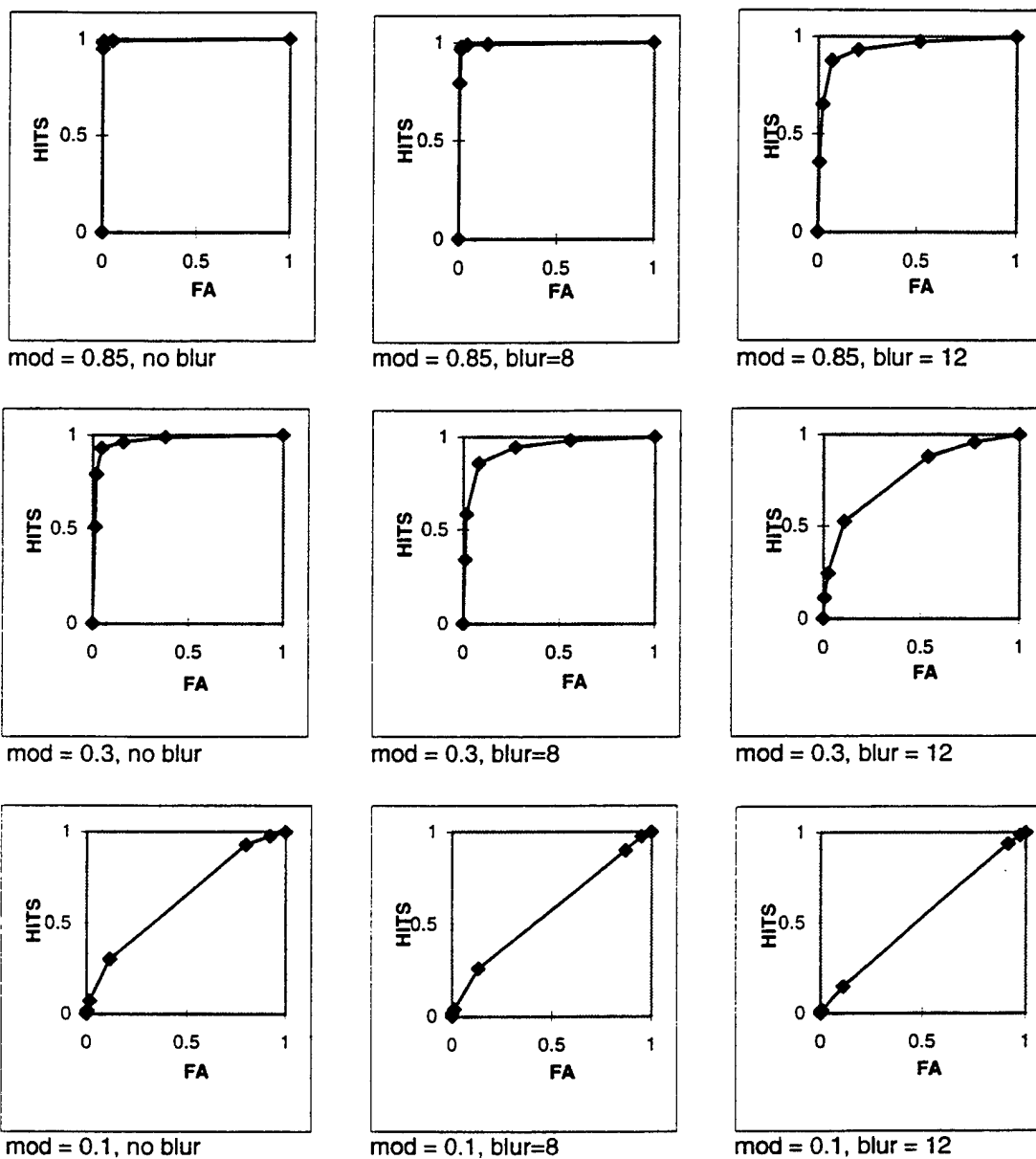Figure 29. ROC curves as a function of modulation and blur; low noise.

Figure 30. ROC curves as a function of modulation and blur; high noise

Another approach to predicting operator performance as a function of modulation, image blur and noise is through regression analysis. The SAS Institute (1982) RSREG procedure was utilized which fits the parameters of a complete quadratic response surface. The R^2 value for the d' regression was 0.87, indicating that 87 percent of the total variance in the data was accounted for by the model. The predictive equation for d' is as follows:

$$d' = 2.03 - 5.74N + 12.41M + .07B + 1.48N^2 + 4.67NM - 10.79M^2 + .05NB + .07MB - .02B^2$$

where N = noise, M = modulation and B = blur radius.

The equation for predicting the probability of a hit is similar:

$$p(hit) = .61 - 1.22N + 2.37M + .005B + .44N^2 + 1.23NM - 2.29M^2 - .0004NB + .03MB - .003B^2$$

having an R^2 value of 0.84.

The R^2 value for the regression to predict probability of false alarm was quite low at only 0.48. This is not surprising, as the false alarm rates for all conditions studied were quite low and varied very little. Beta also varied very little, indicating that subjects maintained a nearly constant decision criterion across all experimental conditions. The R^2 value for Beta was 0.06.

The above equations can be used to predict operator target recognition performance in terms of d' and probability of hit for any combination of modulation, blur and noise within the ranges studied in this experiment. Although the regressions did not yield useful predictive equations for probability of false alarm and Beta, the values of these parameters wound not be expected to differ significantly from those measured in the experiment.

CHAPTER 4

SUMMARY

Three target acquisition experiments were conducted using simulated infrared imagery of eight military vehicles. The first, a target detection study, required subjects to declare whether or not a military vehicle was present in an image. The succeeding studies were recognition studies which required the subject to determine whether the vehicle present in an image belonged to one of four classes.

Variables of interest in the detection study were target internal contrast, target range, scene modulation and blur. Only slight effects of modulation and blur were evident for the no-internal-contrast target condition, so this condition was dropped from further study. Although target range was found to have significant effects upon hit and false alarm rates, these effects were not explainable in terms of ground resolved distance. Although the effects of modulation and blur were significant at all target ranges, and their interaction was significant at all ranges except 3500 meters, these effects were somewhat more pronounced at the 2500 meter range. In all cases of the modulation by blur interaction, the effects of modulation were greatest in the presence of blur, and the effects of blur were greatest at the lower modulations. There were no significant effects upon false alarm rate at any of the four target ranges.

The recognition pilot study employed the same levels of target range and scene modulation and blur as did the detection study. Only targets having internal contrast were used in the recognition studies. As with the detection study, target range significantly affected hit rate, but not in such a way as to be explainable in terms of ground resolved distance. (The 2500 meter range resulted in the lowest hit rate.) The same is true for the effects of target range upon false alarm rate. Modulation and blur significantly affected hit rate at all target ranges, as did their interaction at all ranges except 2500 meters. Modulation significantly affected false alarm rate at the 1500 and 2500 meter ranges, as did the modulation by blur interaction at the 2500 meter range. There were no significant effects upon false alarm rate at the 3500 and 4500 meter ranges.

The modulation by blur interaction in all cases behaved as it had for the detection study. That is, the effects of modulation were greater in the presence of blur, and the effects of blur were greater at the lower modulations.

The effects of modulation and blur were most pronounced at the 2500 meter range for both hit rate and false alarm rate. Therefore, the 2500 meter target range images were selected for the next recognition study.

The final study examined the effects of scene modulation, blur and noise upon target recognition performance and applied the theory of signal detection in the analysis of the data. Modulation and blur were found to interact significantly with noise in their effects upon both hit rate and false alarm rate. The interaction of modulation and blur followed

the same pattern as described for the two previous studies. With the addition of noise in the current study, the interaction of modulation and noise became more pronounced with increased noise.

ROC curves were produced from the theory of signal detection rating scale procedure which allow one to examine target recognition performance at any combination of modulation, blur and noise. In addition, these curves allow one to examine these effects at various levels of operator confidence in the target recognition decision.

Regression analyses were utilized to derive equations which can be used to predict operator target recognition performance. These equations can be used to predict d' and probability of hit for any combination of modulation, blur and noise within the ranges studied in this experiment.

CHAPTER 5

DISCUSSION AND FUTURE DIRECTIONS

The interaction of modulation, blur and noise in their effects upon target recognition performance has important implications for trade-offs that may be possible in system design. The interaction of modulation, blur and noise in their effects upon target acquisition performance indicates that moderate amounts of blur and/or noise do not hinder performance greatly if modulation is sufficiently high. Data from the recognition experiment indicates that observers were able to achieve hit rates of greater than 90 percent with very low false alarm rates when the worst-case noise and blur conditions were applied to the images with modulation of 0.85. When modulation was dropped to 0.1 with the same conditions of noise and blur, performance was no better than could have been achieved by chance. The effects of blur and noise together is more detrimental to performance than the effect of either alone. Conversely, when blur and noise were kept to a minimum, the observer was able to perform the target acquisition tasks almost without error at the 0.1 modulation level. The ROC curves in Figures 28 through 30 provide a means for rapidly assessing the effects of the various levels of the three variables studied. This data would allow system designers to assess effects of various system design changes and select those changes which are most advantageous in terms of both feasibility and cost as well as improved system performance.

Application of the theory of signal detection to the study of human target recognition performance allows for the separation of perceptual sensitivity and operator decision criterion. The ROC curves in Figures 28 through 30 indicate observer target recognition performance at six different levels of observer confidence. The payoff for correctly classified targets and the costs for false alarms and misses play an important role in determining how well the entire system must perform.

Highly trained observers are able to maintain a relatively constant decision criterion across a wide range of image quality conditions. The analysis of Beta from the recognition experiment indicate that for only two of the nine combinations of modulation, blur and noise studied, did observers shift their decision criterion somewhat.

One must keep in mind that there may be differences between statistical significance and operational significance. While an increase in probability of a hit from 0.86 to 0.92 as a result of increasing modulation may be statistically significant, it may or may not be worth the increased cost of building a system which delivers the higher modulation.

The target acquisition studies described here employed a limited target set at only one aspect angle. A larger target set presented at various aspect angles would add to the realism of the task and might greatly influence both operator target acquisition performance and operator confidence.

Scene clutter was not included as a variable in these studies. While a moderate amount of scene clutter was present in all images, it was constant with respect to the targets. Varying the amount of clutter may introduce spatial frequencies similar to those within the targets and increase confusibility of terrain features with the targets. This is a possible explanation for lower hit rates at the 2500 meter target range in the recognition pilot experiment. Also the targets in the studies were not at all obstructed from view by scene clutter. Varying amounts of target obstruction may affect target acquisition performance and operator confidence. Spatial frequencies of clutter similar to spatial frequencies inherent in the targets would be expected to cause the most difficulty.

Clearly, the variables studied do not operate in isolation in their effects upon target acquisition. Care should be taken to examine their interactions with any new variables which might be introduced in further studies.

APPENDIX A

Consent Form and Instructions to Subjects

INFORMATION PROTECTED BY THE PRIVACY ACT OF 1974

CONSENT FORM

TITLE: TRIM2 TARGET RECOGNITION

1. Models of human visual perception are being evaluated for their utility in predicting target detection and recognition capabilities of human observers. This experiment, a target recognition study, will consist of nine blocks of 20 to 30 minutes each. The first block will be a training session and will also include visual acuity and contrast sensitivity tests. Each of the succeeding eight blocks will consist of two sessions of 10-12 minutes each. The experiment utilizes simulated Forward-Looking Infrared (FLIR) imagery.

2. If I decide to participate, all necessary procedures will be explained. I will have the opportunity to ask questions and to rehearse the procedures. The experiment will be conducted in the Crew-Aiding and Information Warfare Analysis Laboratory (CIWAL) at the Human Engineering Division of the Armstrong Laboratory at Wright-Patterson Air Force Base, OH. During the experiment, I will be asked to perform the following tasks: 1) classify targets as one of four types and 2) provide confidence ratings of my responses.

3. The test environment does not represent any unusual or risky procedures or equipment. There are no drugs or medical procedures involved in this demonstration. Data collected in this study will be treated so as to protect my privacy. Data presented or published will not identify individual subjects. Results of this study will be available to me upon request.

4. Participation in this study will afford me an opportunity to assist in the further development and enhancement models of human vision.

5. There are no alternative methods for obtaining these data. I should incur no personal risk as a result of my participation.

Subject's Signature   **Date**

PLEASE CAREFULLY READ AND FILL IN THE FOLLOWING SECTION

6. I, _____, am participating because I want to. The decision to participate in this research study is completely voluntary on my part. No one has coerced or intimidated me into participating in this program.

_____ has adequately answered any and all questions I have asked about this study, my participation, and the procedures involved, which are set forth in this Agreement. I understand that the Principal Investigator or his designee will be available to answer any questions concerning procedures throughout this study. I understand that if significant new findings develop during the course of this research which may relate to my decision to continue participation, I will be informed. I further understand that I may withdraw this consent at any time and discontinue further participation in this study without prejudice to my entitlements. I also understand that the Medical Consultant for this study may terminate my participation in this study if he/she feels this to be in my best interest. I may be required to undergo certain further examinations, if in the opinion of the Medical Consultant, such examinations are necessary for my health or well being.

7. **Minimal Risk.** Minimal risk means that the risk of harm in the proposed research is no greater, considering the hazard probability and severity, than the risk encountered in daily life or during the performance of routine physical or psychological examinations or tests.

8. I understand that my entitlement to medical care or compensation in the event of injury are governed by federal laws and regulations, and that if I desire further information I may contact the Principal Investigator.

I understand that I will not be paid for my participation in this experiment.

I understand that my participation in this study may be photographed, filmed, or audio/videotaped. I consent to the use of these media for training purposes and understand that any release of records of my participation in this study may only be disclosed according to federal law, including the Federal Privacy Act, 5 U.S.C. 522a, and its implementing regulations. This means personal information will not be released to an unauthorized source without my permission.

I FULLY UNDERSTAND THAT I AM MAKING A DECISION WHETHER OR NOT TO PARTICIPATE. MY SIGNATURE INDICATES THAT I HAVE DECIDED TO PARTICIPATE HAVING READ THE INFORMATION PROVIDED ABOVE.

VOLUNTEER SIGNATURE	SSAN	DATE	TIME

PRINCIPAL/ASSOCIATE INVESTIGATOR	DATE	TIME

WITNESS SIGNATURE	DATE	TIME

INFORMATION PROTECTED BY THE PRIVACY ACT OF 1974

Authority: 10 U.S.C. 8012, Secretary of the Air Force; powers and duties; delegation by; implemented by DOI 12-1, Officer Locator.
Purpose: is to request consent for participation in approved medical research studies. Disclosure is voluntary.
Routine Use: Information may be disclosed for any of the blanket routine uses published by the Air Force and reprinted in AFP 12-36 and in Federal Register 52 FR 16431.

TARGET DETECTION STUDY

INSTRUCTIONS TO SUBJECTS

During each session of this study, a series of images will be presented. Approximately half of the images will contain targets like those shown in the accompanying photographs. The other half of the images will be empty background scenes (that is, scenes containing no targets). The images are of scenes at four different ranges from the sensor (1500, 2500, 3500, and 4500 meters). Therefore the targets will not always appear to be the same size on the display. Examples of how the targets will look at the four ranges are shown in the photographs.

Your task in this study is to indicate whether or not you believe that a target was presented in each of the presented images. The study procedure will be as follows.

You will be seated in the VIPER subject booth approximately 30 inches from the display. While no head restraint will be used, you are requested to keep your chair and head touching the back wall of the subject booth. This is so that we can maintain the 30-inch viewing distance. **PLEASE DO NOT LEAN FORWARD OR MOVE THE CHAIR FORWARD.**

At the beginning of the session, a medium gray screen will come up on the display with the word **READY** in the center. When you are ready to view the first image, move the trackball slightly. **The image will appear immediately and will remain on the display for one second.** This will be followed by a medium gray screen with the word **RESPOND** in the center. At this time you will press one of six buttons on the control panel to indicate whether or not you believe a target was present in the image. The button responses are as follows:

Target **definitely** present.	Target **definitely NOT** present.
Target **probably** present.	Target **probably NOT** present.
Target **possibly** present.	Target **possibly NOT** present.

A diagram is provided above the control panel to remind you of which button is associated with each possible response. Please press only one button for each image.

After you press one of the buttons to make your response, the READY screen will appear for the next image. Repeat the above procedure for each image.

Each session consists of a total of 384 images. While it is estimated that you will finish a session in 15 minutes or less, time is not so critical as accuracy. **Once you press a response button, you cannot change your response. So please respond carefully to each image.** If you should make a mistake, simply continue with the session.

Note: The images in the photographs are of high contrast. They have not had noise added. They have not been blurred. During the course of the experiment, the amount of contrast in the images will be varied. Noise may be present in the images. Images may be blurred.

Remember: We are not testing your individual ability to detect targets. We are testing the utility of models for predicting human target detection performance. Your target detection data is needed, along with that of several other subjects, to evaluate the ability of the models to make predictions. So please answer as carefully and honestly as possible in indicating your level of confidence.

THANK YOU FOR TAKING PART IN THIS STUDY.

TARGET RECOGNITION STUDY

INSTRUCTIONS TO SUBJECTS

During each session of this study, a series of images will be presented. Each image will contain a military vehicle from one of the four classes (tank, APC, wheeled vehicle, or artillery). **For each session, only one class of vehicles will be considered as targets while those of other classes will be considered non-targets. The target class will change for each session.** You will be told at the beginning of each session which class of vehicles are targets for that session. Approximately half of the images will contain vehicles from the target class. The other half of the images will contain vehicles from the non-target classes. The vehicles were imaged at a range of 2500 meters from the sensor, the same as the practice images. Your task in this study is to indicate, for each presented image, whether or not you believe that a target vehicle was present. The study procedure will be as follows.

You will be seated in the VIPER subject booth approximately 30 inches from the display. While no head restraint will be used, you are requested to keep your chair and head touching the back wall of the subject booth. This is so that we can maintain the 30-inch viewing distance. **PLEASE DO NOT LEAN FORWARD OR MOVE THE CHAIR FORWARD.**

At the beginning of the session, the designated targets for that session will be displayed on the screen. These targets will be two vehicles from one of the four classes (tanks, APCs, wheeled vehicles, or artillery). All other vehicles, belonging to the other three classes, will be non-targets for that session. It is very important that you remember which class of vehicles are targets for that session. You may want to write it down, as it is easy to get confused when doing multiple sessions.

After you have viewed the targets and non-targets for that session, a medium gray screen will come up with the word **READY** in the center. When you are ready to view the first image, move the trackball slightly. **The image will appear immediately and will remain on the display for three seconds.** This will be followed by a medium gray screen with the word **RESPOND** in the center. At this time you will press one of six buttons on the control panel to indicate whether or not you believe the vehicle in the image belonged to the target class. The button responses are as follows:

Target **definitely** present.	Target **definitely NOT** present.
Target **probably** present.	Target **probably NOT** present.
Target **possibly** present.	Target **possibly NOT** present.

A diagram is provided above the control panel to remind you of which button is associated with each possible response. Please press only one button for each image.

After you press one of the buttons to make your response, the **READY** screen will appear for the next image. Repeat the above procedure for each image.

Each session consists of a total of 216 images. While it is estimated that you will finish a session in 15 minutes or less, time is not so critical as accuracy. **Once you press a response button, you cannot change your response. So please respond carefully to each image.** If you should make a mistake, simply continue with the session.

Note: The images that you saw in the practice sessions were of high contrast. They did not have added noise. They were not blurred. During the course of the experiment, the amount of contrast in the images will be varied. Noise may be present in the images. Images may be blurred. Some of the images may be very difficult. Do not be discouraged, but continue to do the best that you can.
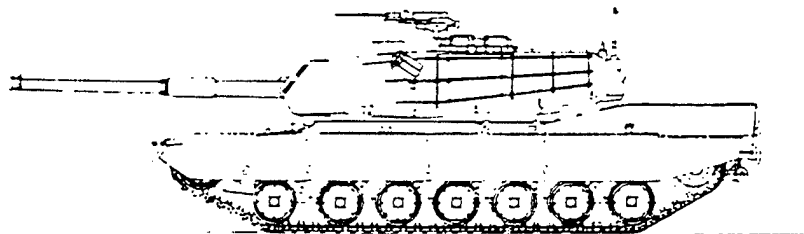
THANK YOU FOR TAKING PART IN THIS STUDY

APPENDIX B

Study Materials

TANK (M-1)
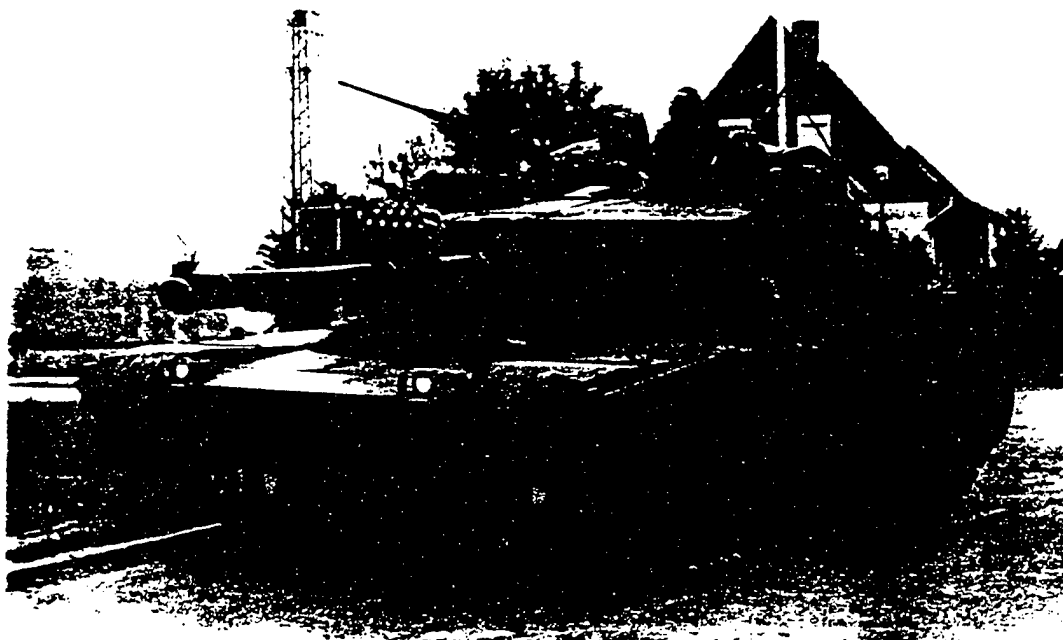
M1 MBT with 105 mm gun during exercises in West Germany (Michel C Klaver)

M1 MBT

83

TANK (M-1)

Description (M1A1)

The hull and turret of the M1 is of advanced armour construction similar to the Chobham armour developed in the United Kingdom and also used on the Challenger and Leopard 2 MBTs. This gives protection against ATGWs and other battlefield weapons.

The driver is seated at the front of the vehicle in the centre and operates the vehicle from a semi-reclining position when driving with the hatch closed. Steering is accomplished by rotating a motorcycle type T-bar which actuates the steering lever on the transmission to produce the steering speed bias of the track. At both ends of the T-bar are twist grip controls which serve as the throttle for the electronic fuel management system. The condition of fluid levels, filters, batteries, electrical connectors and circuit breakers are displayed on the driver's maintenance monitoring panel. The driver is provided with a single hatch opening to the right with three integral periscopes for observation when the hatch is closed. The centre periscope can be replaced by an image intensification periscope for night driving. The driver's has 120° field-of-view and his night driving periscope will fit into the loader's periscope housing for night time surveillance.

The commander and gunner are seated on the right of the turret and the loader on the left. The commander is provided with six periscopes which cover 360° as well as a sight with a magnification of ·3 for the ·2 7 mm machine gun mounted over his position and an optical extension of the gunner's primary sight. The gunner has a primary sight (GPS) with dual day optics with a magnification of ·0 (narrow field-of-view), magnification of 3 (wide field-of-view), close-in surveillance magnification of ·1 and an 18° field-of-view, thermal imaging night vision optics with a magnification of ·0 (narrow field-of-view), magnification of 3 (wide field-of-view), sight stabilisation in elevation and a Hughes laser rangefinder. The turret is stabilised in azimuth with a compensating graticule drive to keep the aim point on target in deflection.

The gunner's auxiliary sight (a Kollmorgen model 939) has a magnification of ·8 and an 8° field-of-view. The loader is provided with a periscope with a magnification of ·1 which can be traversed through 360°.

The fire control system includes the laser rangefinder, full solution solid-state digital computer and stabilised day/thermal night sight. The stabilisation system permits accurate firing-on-the-move and the gunner merely places his graticule on the target, uses the laser rangefinder (Neodymium YAG) to determine the range. The computer then determines and applies the weapon sight offset angles necessary to obtain a target hit and the gunner opens fire. The main armament is equipped with a muzzle reference system to measure the bend of the gun. Information from a wind sensor mounted on the turret roof and a pendulum static cant sensor at the turret roof centre is fed automatically to the computer together with inputs from the laser rangefinder and the lead angle. The following data is manually set battle sight range, ammunition type, barrel wear, muzzle reference compensation, barometric pressure and ammunition temperature.

The infra-red Thermal Imaging System (TIS) has been developed by the Hughes Aircraft Company and produces an image by sensing the small difference in heat radiated by the objects in view. The detected energy is converted into electrical signals which are displayed on a cathode ray tube, similar to a TV picture, and the image displayed is projected into the eyepiece of the gunner's sight. In addition, the sight displays target range information and indicates if the laser rangefinder has received more than one return. The operator can select which return to use if there is more than one displayed. Ready to fire indication and confirmation that the systems are working properly are also provided.

The thermal imaging system generates a graticule pattern boresighted to the day graticule and to the laser rangefinder. This allows the gunner to operate the TIS just as he would the day sight. The infra-red sight to operate the TIS just as he would the day sight. The infra-red sight is based on use of common modules, components standardised to specifications of the US Army Night Vision and Electro-Optics Center.

The digital fire control computer is produced in Canada by Computing Devices Company, a division of Control Data Canada Limited. The fire control computer hardware consists of an electronics unit and a separate data entry and test panel. The electronic unit contains the computing element, the power regulators and interfaces with other elements of the fire control system. The entry and test panel contains the keyboard, control switches and indicators, and a numeric display. The fire control computer carries out a continuous monitoring of its internal function and memory, and provides a visual display of any malfunction. A manually initiated self-test facility gives fault diagnosis in either unit of the system to the replaceable sub-assembly level.

Power for the electro-hydraulic gun and turret drive system is provided by an engine-driven pump through a slip ring in the turret/hull interface to a power valve in the manifold beneath the main armament.

The crew compartment is separated from the fuel tanks by armour bulkheads. Sliding armour doors and armour protected boxes isolate the crew from on-board main armament ammunition explosion. An automatic Halon fire-extinguishing system in the tank reacts to the outbreak of a fire in two milliseconds and extinguishes fires in less than 250 milliseconds. Ready-use ammunition is stowed in the turret bustle and in the event of penetration by a HEAT projectile, the explosion would blow off the top panels with the crew being protected by the access doors which are normally kept in the closed position. The loader holds the switch closed to keep the doors open. The doors close automatically when the pressure switch is relieved. In addition to venting upwards, the turret bustle magazine vents to the rear.

The M1 is powered by a Lycoming Textron AGT 1500 gas turbine. The engine operates primarily on diesel or kerosene-based fuel, but can operate on petrol during emergencies. Approximately 70 per cent of the engine accessories and components can be removed without removing the powerpack from the tank. The complete powerpack can be removed and replaced in less than an hour compared with four hours for the current M60 series. The gas turbine delivers more horsepower to the sprocket than a comparable diesel engine because of the low cooling requirement. The exhaust for the gas turbine is at the rear of the hull with the air inlet on the hull top.

The engine is coupled to a Detroit Diesel X-1100-3B fully automatic transmission with four forward and two reverse speeds. The transmission also provides integral brakes, variable hydrostatic steering and pivot steering.
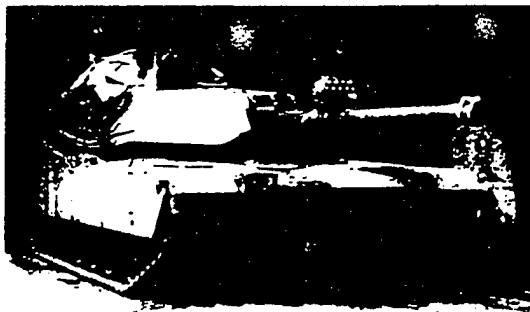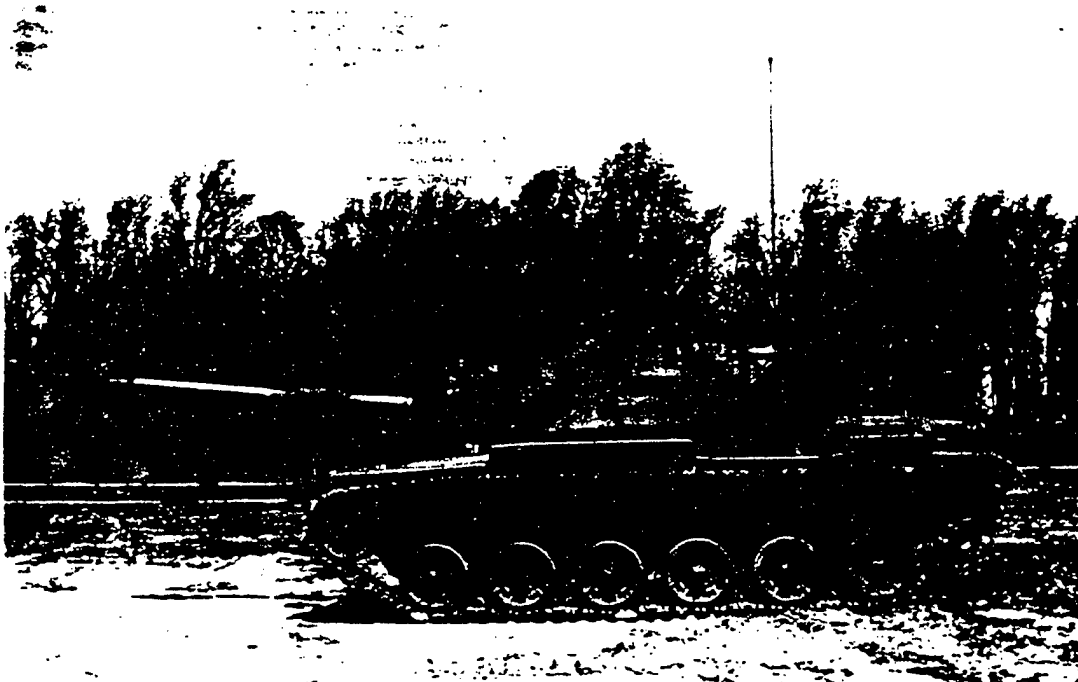

M1 MBT showing commander's 12.7 mm M2 HB machine gun and weapon effects simulator over 105 mm main gun (Pierre Touzin)
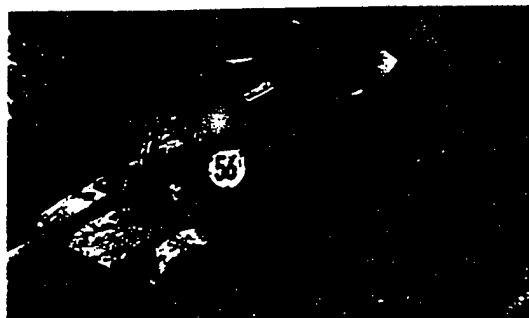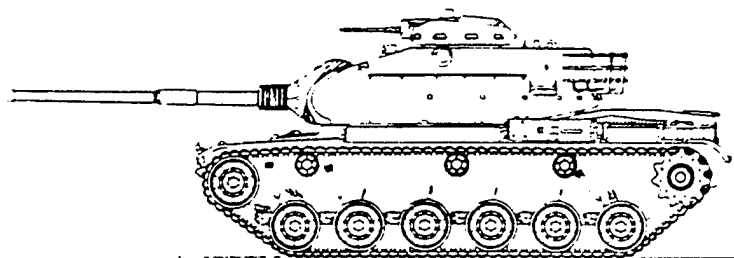

M1 Abrams MBT on exercise in West Germany showing extensive stowage of kit on turret and with commander's, loader's and driver's hatches open (US Army)

TANK (M-60)

General Dynamics Land Systems Division-built M60A3 MBT with thermal sleeve for 105 mm M68 tank gun and British-supplied smoke dischargers on turret side

M60A1 MBT armed with 105 mm gun

TANK (M-60)

Description (M60A1)

The hull of the M60A1 is made of cast sections and forged floor plates welded together. It is divided into three compartments: driver's at the front, fighting in the centre and the engine and transmission at the rear.

The driver is seated at the front of the vehicle and is provided with a single piece hatch cover that opens to the right. Three M27 periscopes are mounted forward of his hatch and an M24 infra-red periscope can be installed in a mount in the centre of his hatch cover for driving at night. The M24 is now being replaced by the AN/VVS-2 night viewer, which is of the passive rather than infra-red type. A hull escape hatch is provided near the driver's position.

The all-cast turret is in the centre of the vehicle with the loader on the left and the commander and gunner on the right. There is an external stowage basket at the rear of the turret. The loader is provided with a single hatch cover that opens to the rear with an integral M37 periscope that can be traversed through 360°

The commander has a cupola that can be traversed through 360° by hand, a single piece hatch cover that opens and swings to the rear, an M28C sight in the forward part and eight vision blocks for all-round observation. The M28C can be replaced by an M36 infra-red periscope or an M36E1 passive periscope for night vision. The gunner is seated in front of and below the commander and is provided with an M31 periscope with a magnification of ·8 and an M105D telescope with a magnification of ·8 and a 7.5° field-of-view. The M31 periscope can be replaced by an M32 infra-red periscope or an M35E1 passive periscope for night engagement of targets. The M17A1 or M17C rangefinder has a magnification of ·10, a 4° field-of-view and a range of between 500 and 4400 m

The engine compartment at the rear of the hull is separated from the fighting compartment by a fireproof bulkhead, and is equipped with a fire-extinguishing system

The torsion bar suspension system consists of six dual rubber-tyred road wheels with the idler at the front, drive sprocket at the rear and three track return rollers. The first, second and sixth road wheel stations are provided with a hydraulic shock absorber

The NBC system of the M60 is of the central air filtration type which pipes fresh air to each crew member via a tube. A full range of night vision equipment is fitted as standard including an infra-red searchlight over the main armament. The latter is either the AN/VSS-1 or the more recent AN/VSS-3A. The former is a 2.2 kW Xenon unit that provides a narrow or wide beam of high-intensity visible or infra-red light. A 50 per cent increase in light intensity can be temporarily provided for 15 to 20 seconds by overriding the searchlight. It has a narrow beam width of 0.5 to 0.75° and a wide beam width of 15°. The AN/VSS-3A can be used in both the visible or infra-red modes with three types of beam, compact, spread or variable width

The crew compartment is provided with a heater and a RADIAC NBC detector can be fitted if required. The tank can ford to a depth of 1.219 m without preparation and with preparation to a depth of 2.438 m. The tank can also be fitted with an M9 bulldozer blade on the front of the hull for preparing fire positions and clearing obstacles.

Main armament of the M60, M60A1 and M60A3 tanks is a 105 mm M68 rifled tank gun with a bore evacuator. A well-trained crew can fire between six and eight rds/min. Of the 63 rounds of ammunition carried, 26 are carried in the forward part of the hull, to the left and right of the driver's

position, 13 in the turret for ready use, 21 in the turret bustle and the remaining three under the gun.

The 105 mm gun can fire the following types of fixed ammunition: APDS-T (M728), APFSDS-T (M735/M735A1), APFSDS-T (M774), APDS-T (M392A2), APERS-T (M494), HEAT-T (M456 series), TP-T (M467), TP-T (M490), TPDS-T (M724), TPDS (M737), HEP-T (M393A1/M393A2), Dummy (M457), TP-T (M393A1), and Smoke WP-T(M416). The US Army is expected to start funding of the new 105 mm XM900E1 APFSDS round for the M60 series in FY89.

Mounted in the commander's cupola is an M85 12.7 mm (0.50) machine gun with an elevation of -60° and a depression of -15°. Mounted coaxially to the left of the main armament is a 7.62 mm M73 machine gun, currently being replaced by the M240 weapon which is the Belgian MAG-58.

A number of M60A1s are being updated with the RISE engine, main armament fully stabilised in both elevation and traverse, top-loading air cleaner fitted, new T142 tracks and improved night vision equipment. Additional details of this programme are given in the entry for the M60A3.

M60A2

This model, fully described in *Jane's Armour and Artillery 1981-82* pages 93-94, has now been phased out of service with the US Army. A total of 526 M60A2s were built and most have been sent back to the Anniston Army Depot where they will be converted to other uses such as AVLB, M728 Combat Engineer Vehicles or Counter Obstacle Vehicles.

M60A3

The M60A3 (development designation M60A1E3) is a product-improved M60A1 and some of the improvements in the tank, for example the add-on-stabilisation system, RISE engine, and the smoke grenade launchers were first fitted to the M60A1 some years ago.
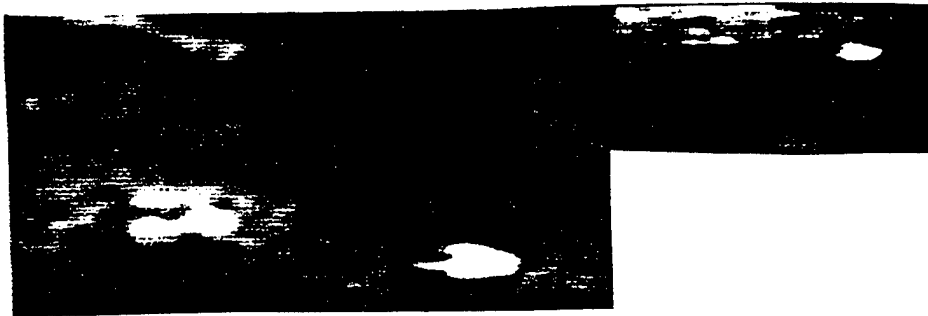

M60A3 MBT from rear, clearly showing rear stowage basket and commander's cupola on right side of turret
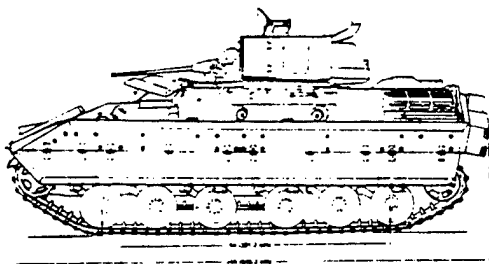

M60A3 MBT showing thermal sleeve for 105 mm M68 series tank gun and bank of smoke dischargers either side of turret
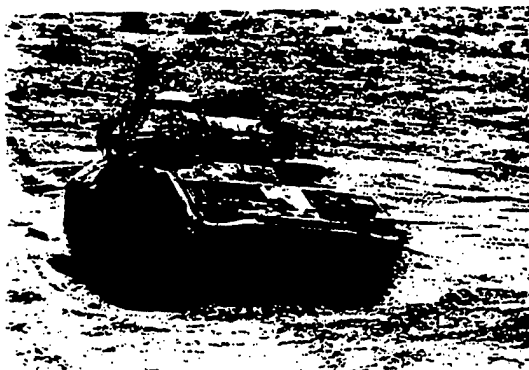
APC (M-2)

M3 Bradley CFV clearly showing covered firing ports in hull sides and with turret traversed to left (Pierre Touzin)
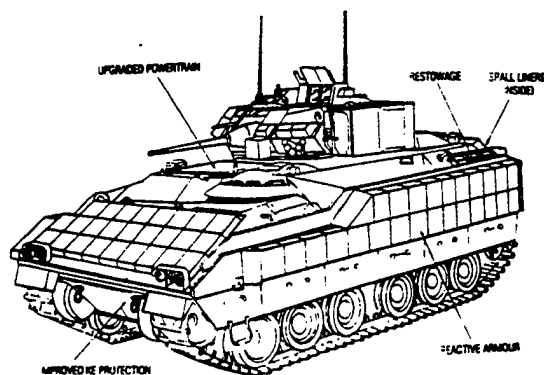

M2 Bradley infantry Fighting Vehicle with TOW launcher retracted and hatches propped (not to 1/76th scale)

APC (M-2)

M2 Bradley infantry fighting vehicle with driver's hatch in open position (Michael Green/US Army)

Drawing of FMC M2A2 Bradley IFV showing main improvements over earlier M2A1 vehicle (not to 1/76th scale)

Description

The hull of the M2 Infantry Fighting Vehicle is made of all-welded aluminium armour with spaced laminate armour fitted to the hull, sides and rear. According to FMC the armour of the M2 can defeat 95 per cent of all of the types of ballistic attack encountered on the battlefield under IFV/CFV doctrine. Latest production M2A2/M3A2 Bradleys have an additional layer of applique steel armour plus explosive reactive armour for increased battlefield survivability.

The driver sits at the front of the vehicle on the left and has a single piece hatch cover that opens to the rear and four periscopes, three to the front and one to the left side. The centre front periscope can be replaced by an AN/VVS-2 passive night periscope.

The engine compartment is to the right of the driver. The engine is coupled to a General Electric HMPT-500 hydro-mechanical transmission. The transmission design incorporates two hydraulic pump/motor assemblies that utilise radial ball pistons and a unique gearing arrangement to provide both steer and propulsion ratios. There are three speed ranges with overall transmission ratios infinitely variable in all ranges. There is a 3.2 kg Halon fixed fire extinguisher in the engine compartment and two 2.3 kg ones in the personnel compartment. In addition there is also a 1.2 kg portable Halon fire extinguisher.

The turret, which is of welded steel and aluminium armour construction, is mounted in the centre of the vehicle on the right side with the gunner seated on the left and the commander on the right. Each crew member is provided with a single piece hatch cover that opens to the rear. The gunner has a combined day/thermal sight with an optical relay for the commander with magnifications of ×4 and ×12, and both crew members have periscopes for front and side observation. In addition, production vehicles are fitted with a fixed power, daylight back-up sight which will allow the gunner or commander secondary sighting capability in the event of primary sight failure.

Main armament consists of a McDonnell Douglas Helicopter Company M242 25 mm Chain Gun with a 7.62 mm M240C machine gun mounted coaxially to the right of the main armament. The 25 mm cannon has dual feed and the gunner can select single shots, 100 or 200 rpm rates of fire. The cannon will fire both Oerlikon 25 mm and American M790 series of ammunition including M791 APDS-T, M792 HEI-T and M793 TP-T. The M791 will defeat the Soviet BMP-1 at a range of 2500 m. The empty cartridge cases are automatically ejected outside the turret. Currently under development is the XM919 APFSDS-T round which will have greatly increased penetration characteristics compared with the current APDS-T M791 round.

The turret has 360° electric traverse and the weapons can be elevated from −10 to +60°. The General Electric turret drive and stabilisation system allows the armament to be laid and fired while moving across rough country. The system consists of a traverse drive assembly for positioning and holding the turret, gun elevation drive assembly for positioning and holding the weapon, TOW elevation drive assembly for positioning and holding the TOW missile launcher, a TOW lift mechanism for raising and lowering the TOW launcher, electronic control assembly, three gyro blocks, gunner's handstation, commander's handstation and cabling.

The TOW weapon subsystem has been developed by the Hughes Aircraft Corporation under a contract worth $16.5 million. When travelling the twin tube TOW launcher is retracted and lies along the left side of the turret. The TOW system enables the M2/M3 vehicles to engage enemy armour out to a maximum range of 3750 m. The TOW missile launcher has an elevation of −30° and a depression of −20°.

Two M257 electrically-operated smoke dischargers, with four smoke grenades in each, are mounted on the forward part of the turret, one on either side of the main armament. In addition production vehicles are fitted with an engine smoke-generating system similar to that on most Soviet vehicles.

The M2 carries seven infantrymen: one sits forward of the turret on the left side facing the rear, one to the left of the turret facing the front, one at the left rear of the vehicle facing inwards, two sit at the right rear facing the back and two sit to the back of the turret facing the front. The commander also dismounts with infantry. The M2A2 only carries a six man squad and the seat to the rear of the driver's position has been eliminated.

The infantrymen enter and leave the vehicle via a large hydraulically-operated ramp at the rear of the hull, which has an integral door in the left side. A single piece hatch cover that opens to the rear is provided over the top of the troop compartment. Six firing ports, two in each side of the hull and two at the rear, each with a periscope over it, enable the infantrymen to fire their M231 5.56 mm weapons from inside the vehicle. The M2A2 has no side firing ports but the ones in the ramp are retained.

The suspension system includes torsion bars, and on each side there are six dual rubber-tyred road wheels with the drive sprocket at the front and the idler at the rear. There are two track return rollers that support the inside of the track only, and one double roller. Hydraulic shock absorbers are fitted to the first, second, third and sixth road wheel stations.
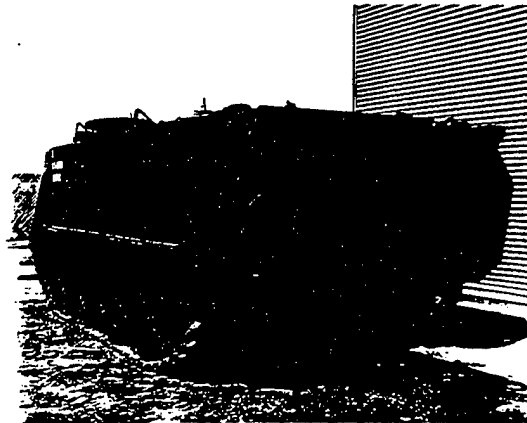
APC (M-113)
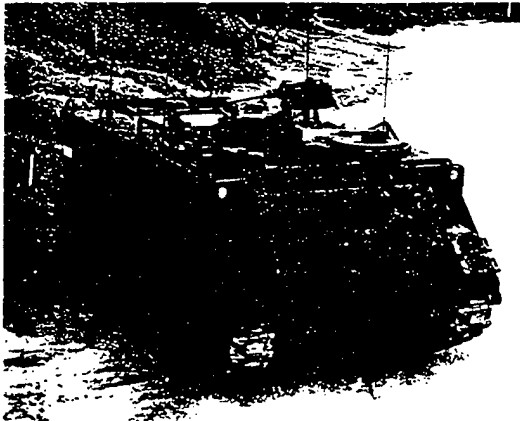
Basic M113A2 APC with 12.7 mm M2 HB machine gun

M113A3 with add-on armour kit for increased protection, smoke dischargers and armoured cupola with 12.7 mm M2 MG
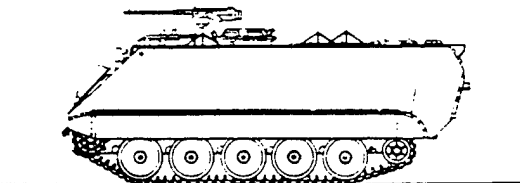
M113A3 APC showing fuel tanks at hull rear
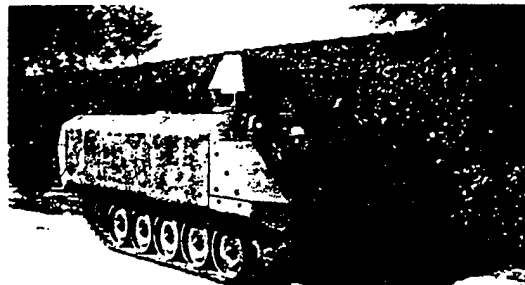
M113A3 with external fuel cells at rear of hull

M113 series APC leaving a river during exercises in West Germany with trim vane erected at the front of the hull (US Army)

M113A1 armoured personnel carrier armed with 12.7 mm (0.50) M2 HB machine gun

APC (M-113)

M113 Armoured Personnel Carrier Family

Development

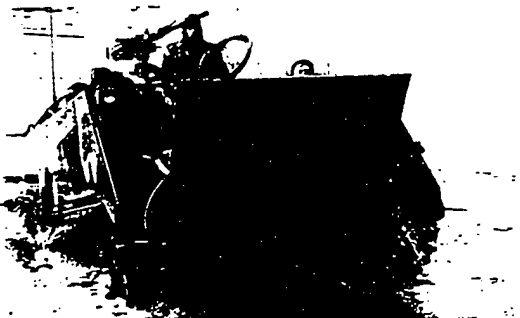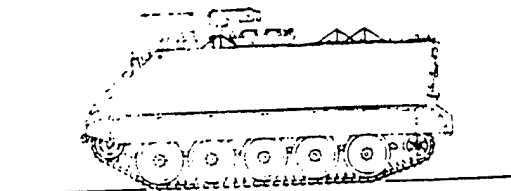In January 1956 development began of an air-transportable, armoured, multi-purpose vehicle family, to provide a lightweight, armored personnel carrier for armour and infantry units capable of amphibious and air-drop operation, superior cross-country mobility and adaptation to multiple functions through applications of kits and/or modifications of its superstructure.

Prototypes of both aluminium (T113) and steel (T117) were built and tested but development of the T117 was cancelled in favour of further development of the T113. This became the T113E1 which was standardised as the M113 in 1960 and entered production at FMC's San Jose facility in early 1960. Trials of a diesel-engined model called the T113E2 showed a substantial improvement in operating range (from 321 to 483 km) as well as a reduction in fire risk. This model was standardised as the Carrier, Personnel, Full-Tracked, Armored, M113A1, in May 1963. After standardisation 10 pre-production vehicles were built and the M113A1 replaced the M113 in production from September 1964.

Description

The all-welded aluminium hull of the M113 protects the crew from small arms fire and shell splinters.

The driver sits at the front of the hull on the left side and has a single piece hatch cover that opens to the rear. To his front and left side are four M17 periscopes and there is also an M19 intra-red periscope in his roof hatch.

The engine compartment to the right of the driver's position is fitted with a fire-extinguishing system that can be operated by the driver or from outside the vehicle. The air-inlet and air-outlet louvres and the exhaust pipe outlet are in the roof and there is an engine access door in the front of the hull that hinges forwards.

The power train consists of the power plant (engine, transfer gear case and transmission), steering control differential, pivot steer, final drive and associated drive shafts and universal joints.

The commander sits to the rear of the engine compartment and has a cupola that can be traversed through a full 360°, five M17 periscopes and a single piece hatch cover. Pintle-mounted on the forward part of the commander's cupola is a 12.7 mm (0.50) Browning M2 HB machine gun with an elevation of -53°, a depression of -21° and a total traverse of 360°. One hundred rounds of ready-use ammunition are carried for this weapon.

The infantrymen enter and leave the M113 via a power-operated ramp in the rear of the hull that opens downwards and has a door in the left side. Behind the commander's cupola is an oblong hatch cover that opens to the rear, behind which is a domed ventilator. The infantrymen travel on seats down each side of the hull, which can be folded up to enable the vehicle to be used as an ambulance or to carry cargo.

The torsion bar suspension either side consists of five dual rubber-tyred road wheels with the drive sprocket at the front and the idler at the rear. There are no track return rollers and the first and last road wheel stations are fitted with a hydraulic shock absorber. A rubber track shroud on each side of the hull controls the flow of water over the tracks when the vehicle is afloat. The M113 is fully amphibious being propelled in the water by its tracks. Steering when afloat is the same as on land. Before entering the water the two bilge pumps are switched on and the trim vane, which folds back onto the glacis plate when not in use, is extended at the front of the hull.

The following kits are available for members of the M113 family: anti-mine armour bolted on front half of vehicle bottom (includes buoyancy aids), anchor kit (set of two for use with capstans for self-recovery), buoyant side pods, combination bulldozer/snow plough, NBC detector and automatic alarm, full width buoyant trim vane, gun shields, heater for personnel and cargo areas, heater for engine coolant and battery, stretcher kit which provides support for four stretchers when the vehicle is being used as an ambulance. M8A3 gas-particulate unit (includes M2A2 air purifier with flexible hoses to fit M14A1 tank gas masks of driver and commander and up to two others) non-skid ramp plate kit and windscreen for driving with hatch open.

M113A2 (formerly Product Improved M113A1)

Following successful trials with prototype vehicles the United States Army in 1978 decided to carry out a product improvement programme on its fleet of M113 (5300) and M113A1 (12 700) APCs, all of which are to be brought up to the new standard by 1989. The conversions are being carried out at the Red River Army Depot Texas, Daewo Industries in South Korea and Mainz Army Depot. West Germany. The Army plan to have 21 323 Product Improved M113A1s in service by the end of fisc year 1989. The US Army also ordered an initial batch of 2660 M113A2s at a cost of $154 million, the first of which were completed at FMC's San Jose facility in July 1979. These improvements can be summarised as follows:

Improved engine cooling design that reverses the position of the fan and radiator and incorporates a new radiator and surge tank and a new cooling fan. This new cooling system draws in ambient air through the radiator providing increased cooling efficiency for both the engine and transmission, reduces oil film and dust build-up on the core of the radiator, provides a negative pressure engine compartment which reduces the possibility of exhaust fumes leaking into the crew compartment and finally provides a longer engine life and greater tractive effort at reduced temperatures.

The improved suspension system incorporates high-strength steel torsion bars that provide 228 mm of roadwheel travel, improved shock absorbers on the first, second and fifth road wheel stations, stronger rear idler assembly which has also been raised to reduce the chance of ground impact and finally increased ground clearance to minimise sprocket ground contact on rough terrain.

Other M113A2 variants such as the M577A2 and the M125A2 are currently available. The M548 cargo carrier with A2 improvements has been redesignated the M548A1 and first production vehicles were completed in 1982.

Rear-mounted, armoured fuel cells are a current production option and many non-United States orders are calling for their installation. This option provides more interior space and reduces the danger of fire. M113A1 vehicles have now been phased out of production. A 200 A generating system is available and is being phased into production on some vehicle models. A kit is also available.

M113A3

In mid 1980 a Development-in-Process Review consisting of Army Material Command, TRADOC and Logistics Evaluation Agency members recommended to the Department of the Army that the improve M113A1E1, developed by TACOM at Warren, Michigan should be type classified for US Army use. M113A3 production commenced in early 1987 and US Army units started receiving these vehicles in the summer of 1987.

The M113A3 incorporates the cooling and suspension improvements of the M113A2 but also has better performance and reliability. Major improvements include the replacement of the 6V-53 (212 hp) diesel engine by the turbo-charged Detroit Diesel 6V-53T (275 hp) and the replacement of the present TX100-1 transmission, transfer gearcase, steering, differential and pivot steer with the X-200-4 Allison transmission which provides four forward speeds instead of the present three, hydrostatic steering to provide smoother turning with less effort and reduced shock loading on the suspension system and greater cover efficiency which results in more horsepower and fuel savings.

The driver's controls have also been changed and the conventional sticks have been replaced by a steering wheel and brake pedal.

The US Army refers to this improvement as the RISE power train (Reliability Improvement of Selected Equipment). During development tests, a significant improvement for the M113A1E1 over the M113A1 was achieved including acceleration of 0 to 32 km/h in 8.1 seconds compared with 11.7 seconds, braking from a speed of 32 km/h in 7.3 compared with 10 m cross-country speed of 33.7 km/h compared with 26 km/h. For 48 270 km of development tests the M113A1E1 went 3047 km between failures as opposed to 1298 km for the standard M113A1. At a speed of 35.4 km/h the vehicle used 22 per cent less fuel than the M113A1. The M113A3 has a 200 A generating system, four batteries and improved electrical diagnostic capabilities to replace the 100 A system with two batteries in the M113A2. It also has armoured external fuel tanks and internal spall protection liners. The three improvements (RISE, AEFT and spall liners) will be applied to the M901A1 and M981 vehicles which will become the M901A2 and M981A1. The first M113 family variant to be converted to the RISE power train were M730 Chaparral carriers. The entire US fleet of 495 vehicles will be converted to the M730A2 betwe 1987 and 1989.

WHEELED VEHICLE (HMMWV)

HMMWV M998 Series
Multipurpose Wheeled Vehicles

Development

Based on the draft specification for the High Mobility Multipurpose Wheeled Vehicle (HMMWV) issued by the US Army in mid-1979 AM General Corporation designed and built a prototype in the weapons carrier configuration

The first prototype was completed in August 1980 and was sent to the Nevada Automotive Test Center for extensive trials and by February 1981 the prototype had accumulated 21 000 km of instrumented and dynamic testing

AM General became one of three contenders awarded a US Army contract for the design and construction of 11 prototype HMMWVs (six weapons carriers and five utility) which were delivered in May 1982 In March 1983 AM General was awarded a $59.8 million contract by the US Army Tank Automotive Command (TACOM) for 2334 HMMWVs which were then designated the M998 Series (unofficially HUMMER). This was the first increment in a five-year contract for 54 973 vehicles worth approximately $1.2 billion. Of these some 39 000 were for the US Army and the remainder were divided between the US Air Force, Navy and the Marine Corps (initially 31231) Production commenced at Mishawaka, Indiana, early in 1985. Contract options for a further 15 000 were exercised to bring the total production by mid-1991 to over 72 000 vehicles, including overseas sales

In August 1989 the US Army awarded AM General a further multi-year contract worth approximately $1 billion. The contract calls for a further 33 331 vehicles until 1993, with two further option years. Production under the new contract began in January 1990 and production for the US Armed Forces will continue until March 1995, by which time the US Armed Forces will have approximately 100 000 HMMWVs. A further 10 000 units have been ordered by 30 foreign governments, including 2300 units purchased by Saudi Arabia in mid-1991 at a cost of $123 million

In service the M998 Series HMMWVs replaced some M151 Jeeps, the M274 Mule (830 in service), the M561/ M792 Gama Goat (11 000 in service) and the M880 series (40 000 in service) with 20 per cent of the fleet of M151s and many of the M880s being replaced by the Commercial Utility Cargo Vehicle (CUCV)

Description

The HMMWV has 2 + 2 seating on each side of the drive train which is in a midship position allowing the front differential to be raised. This together with the geared hubs, provides a ground clearance of 0.41 m. The location of the crew on each side of the drive train also allows a low centre of gravity. The windshield frame is strong enough to serve as a roll bar and support for various equipment kits. Other pillars also make the ballistically protected weapon station inherently strong and a steady location on which to mount a variety of weapons such as TOW, 7.62 and 12.7 mm machine guns and the MK19 MOD3 40 mm grenade launcher. At the rear the

cargo bed is large enough to accommodate an S.250 similar shelter without overhang; it also accommodates the Standard Integrated Command Post System (SICPS) shelter with a 15-in (381 mm) overhang

Production versions of the HMMWV can be converted into numerous variants by changing the basic configuration. These configurations are:
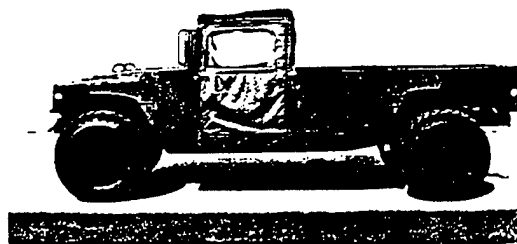M998 Cargo/troop Carrier without winch
M1038 Cargo/troop Carrier with winch
M966 TOW Missile Carrier, basic armour, without winch
M1036 TOW Missile Carrier, basic armour, with winch
M1045 TOW Missile Carrier, supplemental armour, without winch
M1046 TOW Missile Carrier, supplemental armour, with winch
M1025 Armament Carrier, basic armour, without winch
M1026 Armament Carrier, basic armour, with winch
M1043 Armament Carrier, supplemental armour, without winch
M1044 Armament Carrier, supplemental armour, with winch
M997 Maxi-ambulance 4-litter, basic armour
M1035 Soft-top Ambulance, 2-litter
M1037 Shelter Carrier, without winch
M1042 Shelter Carrier, with winch

In addition to the above selected application kits produced as follows:
Cargo/troop Carrier soft-top enclosure (2-door cab) M998
Cargo/troop Carrier soft-top enclosure (4-door cab) M998

HMMWV M997 Maxi-ambulance with deep water fording kit

HMMWV M998 cargo/troop carrier

WHEELED VEHICLE (HMMWV)

Cargo/troop Carrier soft-top enclosure (2-door cab, troop seats) for M1038

Cargo/troop Carrier soft-top enclosure (2-door cab, troop/cargo) for M1038

Cargo/troop Carrier, soft-top enclosure (4-door cab, cargo) for M1038

Armament Carrier, basic armour with M60 7.62 mm machine gun for M1026

Armament Carrier, supplemental armour with M2 0.50/12.7 mm machine gun for M1044

Armament Carrier, supplemental armour with MK19 MOD3 grenade launcher for M1043

Retrofitable weapon station kit for the M998/M1038 (weight 114 kg).

The HMMWV has been adapted for use as a missile launch vehicle. Launch vehicles produced to date include the following:

Pedestal-Mounted Stinger (PMS) carrying eight Stinger surface-to-air missiles and one 12.7 mm machine gun. This became operational with the US Army in 1989-90 and the total requirement is for 273 over a five-year period. For full details refer to *Jane's Land-based Air Defence 1993-94* pages 156 to 158

LTV Crossbow Pedestal-Mounted Weapon System carrying a variety of air defence or anti-tank systems. For details of this private venture refer to *Jane's Land-based Air Defence 1992-93* pages 153 and 154.

Fibre Optic Guided Missile (FOG-M) System. The HMMWV was selected as the launch vehicle for the Non-Line-of-Sight (NLOS) component of the FOG-M which was cancelled in December 1990. For details refer to *Jane's Land-based Air Defence 1993-94* pages 159 and 160.

An HMMWV was used for firing trials involving the Hellfire anti-tank guided weapon in a surface-to-surface role.

An HMMWV has been adapted to carry an M40A2 106 mm recoilless rifle for overseas sales.

At least one HMMWV has been used by Alliant Techsystems for trials involving a Light Volcano version of the M139 Volcano multiple delivery mine system - see under *Minelaying equipment* for details.

To reduce life cycle and initial procurement costs, standard automotive components are used wherever possible, as in the engine, transmission, transfer case, brakes and steering.

The independent suspension front and rear, gives good manoeuvrability, ease of handling and part commonality. The geared hubs give 0.41 m ground clearance incorporating raised axles for high speed operations on road and across country. They also provide a 1.92:1 torque output multiplication at the ground.

The suspension carrier front and rear axles are identical, have differentials and are mounted high directly in the chassis frame. The front propeller shaft has double cardan joints and the rear propeller shaft has single cardan joints which, according to AM General, give minimal motion, improved torque characteristics and higher reliability with resultant lower support costs. Vehicle handling is enhanced by the front stabiliser bar being attached to the lower control arms and pivot bracket reducing shock from the lower A-frame member to the chassis.

Acceleration of the HMMWV is such that it can move from a standstill to 48 km/h in 8 seconds and from a standstill to 80 km/h in 24 seconds.

In addition to the above-mentioned variants, AM General has also produced the M1097 'Heavy Hummer variant (HHV) to increase the GVW to 4536 kg - all existing HMMWV versions can be produced to this level, known as the Heavy Weapons Carrier or Heavy Armament Carrier. The 'heavy' chassis permits a payload increase to 1996 kg in the case of the M1097 - GVW is 4536 kg. The M1097 chassis incorporates improved front and rear differentials, a new transfer case, new front and rear propshafts, an improved frame mounting for the steering gear, variable rate rear springs and new lower ball joints. The heavier chassis allows the use of an up-armoured ballistic panel protection kit with 5.56 and 7.62 mm NATO ball protection and permits the carriage of heavy weapons such as the McDonnell Douglas Helicopters 30 mm ASP-30 cannon. Production commenced in September 1992.

Modification kits developed by and available directly from AM General include: a selective up-armour kit; a brushguard, spare tyre and jerrican carriers; a driveline skid protection kit; a central tyre inflation system (CTIS) and a special desert operations package including secondary oil and fuel filtration; sealed dipsticks; a constant drive fan and enhanced oil filtration. A retrofitable weapon station kit is an adaptation of that used on standard HMMWV weapon carriers (M998 and M1038 only) and weighs 114 kg.

The M1097 HHV was used as the basis for the Hummer Cab-Over-Engine (COE) (4 × 4) 2268 kg cargo truck - see following entry. Civilian and public utility versions of the HMMWV are available.

A high mobility trailer (HMT) for use with the HMMWV is under development and testing. It will provide improved mobility and payload capacity compared to currently fielded trailers. On March 22 1993 the US Army issued a procurement solicitation for a family of three trailers: a 680 kg cargo trailer, a 1134 kg cargo trailer and a 1134 kg chassis trailer. Under a five-year contract up to 23 000 trailers may be procured. The contract was expected to be awarded in September 1993 with first deliveries expected during 1994.

Three HMMWVs can be carried in a C-130 Hercules transport aircraft, six in a C-141B and 15 in a C-5A Galaxy.

M998A1 Series

In late 1993 AM General began producing the M998A1 series of HMMWV for the US Army. All A1 models incorporate the M1097 'Heavy Hummer' chassis components plus new front seats, an improved parking brake lever with safety release, a metal hood grill, improved slave receptacle, solid state glow plug controller, modified rifle mounts, and upgraded rear half-shafts. Using these common chassis components enhances HMMWV standardisation across all models, leading to improvements in logistic support, training and fleet durability. The introduction of the A1 series resulted in the elimination from new production of the M1037 and M1042 Shelter Carriers (replaced by the M1097A1) and the M1036 TOW Missile Carrier.

GVW for all A1 models, except the M1097A1, increases by approximately 81 kg although vehicles payloads and loads remain the same.

AM General offer a new front seat retrofit kit for the existing HMMWV fleet as part of the new series production.

Specifications (M1038 Cargo/troop Carrier w/winch)

Cab seating: 1 + 3
Configuration: 4 × 4
Weight:
  (kerb) 2416 kg
  (GVW) 3493 kg
Max load: 1077 kg
Max towed load: 1542 kg
Length: 4.72 m
Width: (mirrors folded) 2.18 m
Height: 1.83 m
Ground clearance: 0.41 m
Track: 1.82 m
Wheelbase: 3.3 m
Angle of approach/departure: 47°/45°
Max speed: 113 km/h
Range: 482 km
Fuel capacity: 94.6 l
Max gradient: 60%
Side slope: 40%
Fording: 0.76 m
  (with preparation) 1.52 m
Engine: V-8 6.2 l diesel developing 150 hp at 3600 rpm
Transmission: automatic with 3 forward and 1 reverse gears
Transfer box: 2-speed, full-time 4-wheel drive
Suspension: (front and rear) independent, double A-arm, coil spring
Steering: power-assisted
Turning radius: 7.62 m
Brakes: hydraulic disc front and rear
Tyres: 36 × 12.50 R 16.5 LT load range D
Electrical system: 24 V
Batteries: 2 × 12 V

Status

In production. In service with US Army, Air Force, Navy and Marine Corps. Some 10 000 vehicles have been sold to 30 friendly foreign countries. Known to be in service with Abu Dhabi (3), Djibouti (10), Luxembourg (29), the Philippines, Saudi Arabia (2300 ordered in 1991), Taiwan and Thailand (150). Civilianised versions have been sold to the Chinese Ministry of Petroleum Exploration, the US Border Patrol and other civilian agencies.
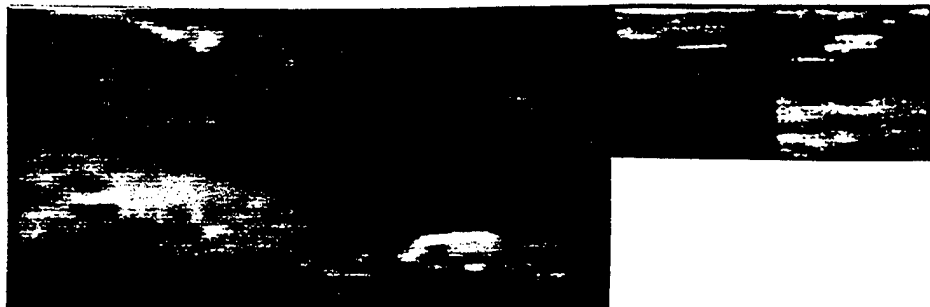
Manufacturer

AM General Corporation. One Michiana Square. Suite 150, 100 E Wayne Street, South Bend, Indiana 46601, USA.
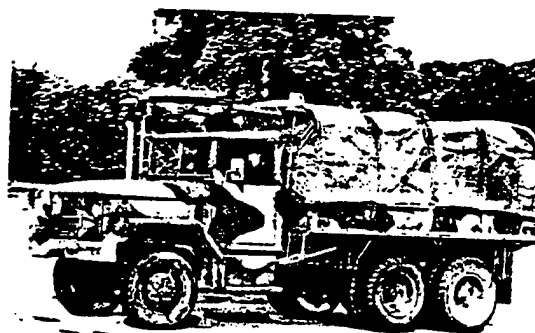Tel: (219) 284 2942/2911 Fax: (219) 284 2959/2814

WHEELED VEHICLE (M-35)

Specifications

Model	M35A2
Type	cargo
Cab seating	1 + 2
Configuration	6 × 6
Weight (empty)	5900 kg
(loaded, road)	10 400 kg
Weight on front axle (loaded)	2700 kg
Weight on rear axle (loaded)	7700 kg
Max load (road)	4535 kg
(cross-country)	2268 kg
Towed load (road)	4535 kg
(cross-country)	2721 kg
Load area	3.7 × 2.2 m
Length (without winch)	6 7 m
Width	2.4 m
Height (reduced)	2.1 m
(overall)	2 9 m
(load area)	1 32 m
Ground clearance (axles)	0.28 m
Track (front, rear)	1 721/1 778 m
Wheelbase	3.912 m
Angle of approach/departure	47°/40°
Max speed (road)	90 km/h
Range	480 km
Fuel capacity	189 l
Max gradient	60%
Fording (without preparation)	0 76 m
(with preparation)	1 98 m
Engine	LDT-465-1C 6-cylinder
Gearbox	all have a manual gea
Clutch	single dry plate is fitte
Transfer box	2-speed
Steering	all have cam and twin
Turning radius	11 m
Suspension (front/rear)	semi-elliptical springs
Tyres	9.00 × 20
Brakes (main)	

M35A2 2 -ton (6 × 6) cargo/personnel truck with machine gun mounting over cab

M35/M44A2 (6 × 6) 2½-ton Cargo Truck Series

Development

In the late 1940s Reo and the Truck and Bus Division of General Motors Corporation each developed a new 2½-ton (6 × 6) truck for the US Army to replace wartime vehicles. Reo was awarded the initial production contract for 5000 vehicles and delivered the first vehicle in 1950. Originally it was to have been only an interim solution pending large-scale production of the General Motors design, but as soon as the Korean War broke out it was apparent that Reo alone could not meet the requirements of the Army so the General Motors models were placed in immediate production. They were the M135 with single rear wheels and the M211 with dual rear wheels, but they were phased out of production after the end of the Korean War in favour of the Reo design which was also built by Studebaker and was commonly known as the Eager Beaver.

The first vehicles were powered by a Reo (model OA-331) or Continental (COA-331) petrol engine which developed 146 bhp at 3400 rpm, but later models with the suffix A1 (for example M35A1) were powered by a Continental LDS 427-2 multi-fuel engine. Current models (for example M35A2) have the Continental LD 465-1 multi-fuel engine which develops 140 bhp (gross) at 2600 rpm.

In 1964 the Kaiser Jeep Corporation bought the Studebaker facilities in South Bend, Indiana, and was awarded contracts to build both 2½-ton (6 × 6) and 5-ton (6 × 6) trucks for the US Army.

In 1967 Kaiser Jeep formed the Defense and Government Products Division to handle its government contracts, but in 1970 Kaiser Jeep was acquired by American Motors and the Defense and Government Products Division was named the General Products Division of the Jeep Corporation. In 1971 it was renamed the AM General Corporation, then a wholly owned subsidiary of American Motors Corporation.

By early 1980 AM General had produced over 150 000 M35/M44 series 6 × 6 trucks. A product improved prototype designated the M963 series was developed by the company under contract to the US Army but it did not enter production.

The M963 series was powered by a Caterpillar Model 3208 V-8 diesel developing 210 hp coupled to an Allison MT643 four-speed automatic transmission. New axles gave the vehicle a wider track and larger tyres improved soft soil mobility, allowing single instead of the usual dual rear wheels to be fitted. Other improvements included redesigned suspension, brakes and steering, a forward-tilting bonnet for easier maintenance and a wider three-man cab with a spring-mounted seat for the driver.

By 1988 M35/M44 production was being carried out by AM General Corporation. In that year an order for a further 399 M44A2s was placed for delivery by October 1988. In September 1988 it was announced that AM General would discontinue medium and heavy truck

93

ARTILLERY (M-730)
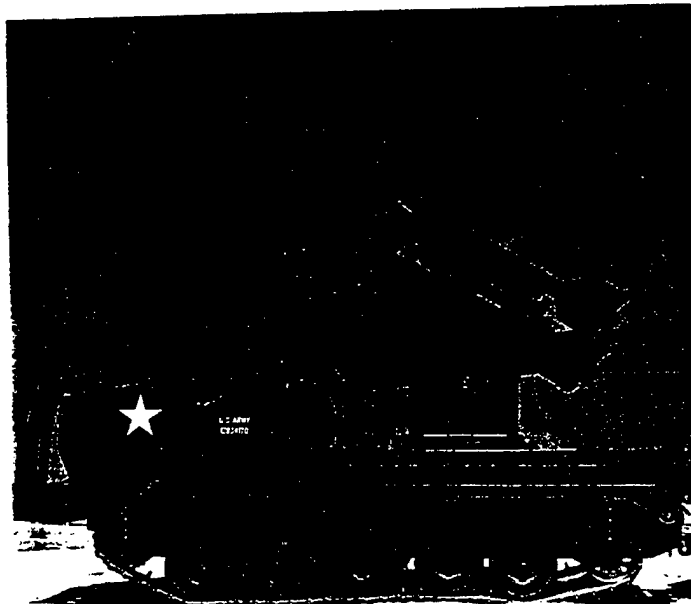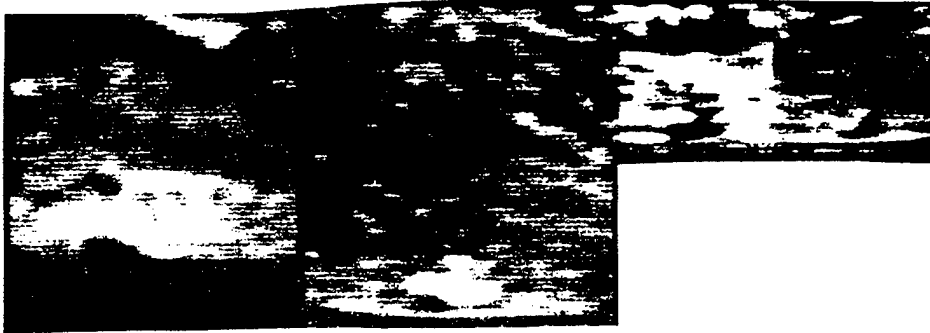
M730 series Chaparral surface-to-air missile launcher, based on the M548 tracked cargo carrier with four Chaparral surface-to-air missiles in ready to launch position

M730 Chaparral SAM launcher

This is based on a modified M548 series tracked cargo carrier and mounted over the rear area is a one man power operated turret with four Chaparral SAMs in the ready to launch position with a further eight missiles being carried in reserve. In addition to being used by the US Army, the Chaparral is also used by Egypt, Israel, Morocco, Portugal, Taiwan and Tunisia.

ARTILLERY (M-163)
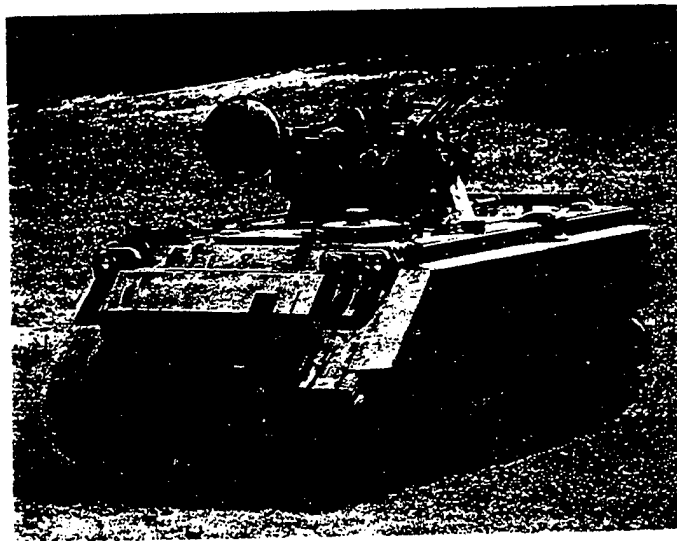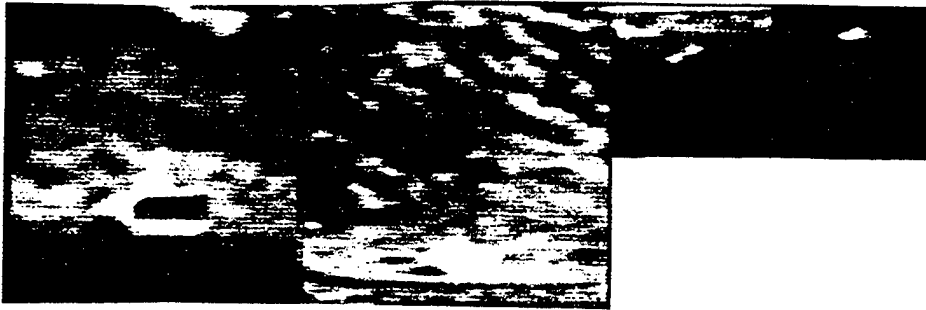
M163A1 20 mm Vulcan self-propelled anti-aircraft gun system of the US Army fitted with the Lockheed Electronics Company Product Improved Vulcan Air Defense System (PIVADS) kit

M163 Vulcan Self-propelled Anti-aircraft Gun

This is essentially an M113A1 chassis fitted with a one-man electrically-driven turret which is armed with a 20 mm M168 Vulcan gun. Navy Mk 20 Mod. A gyro lead-computing sight and a range-only radar are mounted on the right side of the turret. The chassis is designated the M741.

95

REFERENCES

Attneave, F. (1954). Some information aspects of visual perception. Psychological Review, 61, 452.

Bitterman, M. E., Krauskopf, J. and Hochberg, J. E. (1954). Threshold for visual form: A diffusion model. American Journal of Psychology, 67, 205.

Blackwell, H. R. (1946). Contrast thresholds of the human eye. Journal of the Optical Society of America, 36, 624.

Campbell F. W. and Green D. G. (1965). Optical and retinal factors affecting visual resolution. Journal of Physiology (London) 181, 576-593.

Casperson, R. C. (1950). The visual discrimination of geometric forms. Journal of Experimental Psychology, 40, 668.

Cornsweet, T. N. (1970). "Visual Perception." Academic Press, New York.

Engstrand, R. D. and Moeller, G. (1962). The relative legibility of ten simple geometric figures. American Psychologist, 17, 386.

Fisher, Ronald A. and Yates, Frank (1957). "Statistical Tables for Biological, Agricultural and Medical Research." Hafner Publishing Company Inc., New York.

Fox, W. R. (1957). Visual discrimination as a function of stimulus size, shape and edge gradient. In form discrimination as related to military problems, (J. W. Wulfech and J. H. Taylor, Eds.) National Academy of Science N. R. C., Washington D. C., 168.

Gescheider, George A. (1976). Psychophysics method and theory. Hillsdale, New Jersey: Lawrence Erlbaum Associates.

Ginsburg, A. P. (1971). Psychological correlates of a model of the human visual system. Masters thesis, Air Force Institute of Technology, Wright-Patterson AFB, Ohio 45433.

Green, David M. and Swets, John A. (1966). Signal detection theory and psychophysics. New York: John Wiley and Sons.

Guth, S. K. and McNelis, J. F. (1969). Threshold contrast as a function of target complexity. American Journal of Optometry, 46, 98.

Helson, H. and Fehrer, E. V. (1932). The role of form in perception. American Journal of Psychology, 44, 79.

Johnson, J. (1957). "Analysis of Image Forming Systems." Proceedings of the Image Intensifier Symposium.

Johnson, J. and Lawson, W. (1974). Performance Modeling Methods and Problems." Proceedings of the IRIS Imaging Systems Group, January, 1974.

Lamar, E. S., Hecht, S., Schaler, S. and Hendley, C. D. (1947). Size, shape and contrast in the detection of targets by daylight vision I. Data and Analytical description, Journal of the Optical Society of America, 37, 531.

Lin, Jae S. (1990). *Two Dimensional Signal and Image Processing.* Prentice Hall Signal Processing Series, Englewood Cliffs, New Jersey.

Moser, P. (1972). *Mathematical model of FLIR performance.* Memorandum No. NADC-20203:PMM, Naval Air Development Center.

Ogle, K. N. (1961). Foveal contrast thresholds with blurring of the retinal image and increasing size of test stimulus. Journal of the Optical Society of America, 51, 862.

O'Neill, George (1974). *The Quantification of image detail as a function of irradiance by empirical tests.* Memorandum No. NADC-200139:GJO, Naval Air Development Center.

Overington, Ian (1976). Vision and Acquisition. Pentech Press, London.

Saleh, Bahaa E. A. (1982). Optical information processing and the human visual system. In Stark, Henry (ed.) Applications of Optical Fourier Transforms. Academic Press, Inc., New York.

SAS Institute Inc. (1982). SAS User's Guide: Basics, 1982 Edition. Cary, NC: SAS Institute Inc., 923pp.

SAS Institute Inc. (1982). SAS User's Guide: Statistics, 1982 Edition. Cary, NC: SAS Institute Inc., 584pp.

Shumaker, David (1995). Target detection and recognition revisited. Spectral Reflections, Volume 25(3),

Stockham, Thomas G. Jr. (1975). "An overview of human observer characteristics and their effect on image transmission and display." SPIE vol. 66, pp2-4.

Swets, John A., Tanner, Wilson P. Jr., and Birdsall, Theodore G. (1964). Decision processes in perception. In John A Swets (ED) Signal detection and recognition by human observers. New York: John Wiley and Sons.